THE UNIVERSITY OF CHICAGO

SUPRAMOLECULAR PEPTIDE NANOFIBERS FOR ACTIVE IMMUNOTHERAPY

A DISSERTATION SUBMITTED TO

THE FACULTY OF THE DIVISION OF THE BIOLOGICAL SCIENCES

AND THE PRITZKER SCHOOL OF MEDICINE

IN CANDIDACY FOR THE DEGREE OF

DOCTOR OF PHILOSOPHY

DEPARTMENT OF PATHOLOGY

BY

CAROLINA MORA SOLANO

CHICAGO, ILLINOIS

AUGUST 2017

DEDICATION

This thesis is dedicated to my (soon 1-year-old) son, Maximilian.

"*Success is failure turned inside out-*

the silver tint of the clouds of doubt

and when you never can tell how close you are,

it may be near when it seems so far;

so stick to the fight when you're hardest hit-

it's when things seem worst that you must not quit"

by E. A. Guest

TABLE OF CONTENTS

LIST OF FIGURES ..... **V**

LIST OF TABLES ..... **VII**

ABBREVIATIONS ..... **VIII**

ACKNOWLEDGEMENTS ..... **X**

ABSTRACT ..... **XIV**

CHAPTER 1: INTRODUCTION **1**

1.1 SUMMARY 1
1.2 INTRODUCTION 2
1.3 BASIC BIOMATERIAL PROPERTIES FOR EXPLOITING ADAPTIVE IMMUNITY 4
Epitope content 7
Size 9
Multivalency 14
1.4 SELF-ASSEMBLING PEPTIDE MATERIALS 16
1.5 TUMOR NECROSIS FACTOR SIGNALING IN HEALTH AND DISEASE 23
1.6 OVERVIEW OF THIS THESIS 26

CHAPTER 2: MATERIALS AND METHODS **28**

2.1 PEPTIDE SYNTHESIS MATERIALS. 28
2.2 PEPTIDE SYNTHESIS. 29
2.3 PREPARATION OF VACCINE FORMULATIONS. 30
2.4 TRANSMISSION ELECTRON MICROSCOPY (TEM). 31
2.5 THIOFLAVIN T (THT) BINDING FLUORESCENCE ASSAY. 32
2.6 INTRINSIC PEPTIDE FLUORESCENCE ASSAY FOR IN VITRO T EPITOPE PEPTIDE TITRATION. 32
2.7 MICE AND IMMUNIZATIONS. 33
2.8 ANTI-TNF ANTIBODY ELISA 33
2.9 T CELL ELISPOT. 34
2.10 INTRAPERITONEAL LPS CHALLENGE. 35
2.11 LISTERIA INFECTION. 35
2.12 SURFACE PLASMON RESONANCE (SPR). 36
2.13 STATISTICAL ANALYSIS. 37

CHAPTER 3: ACTIVE IMMUNOTHERAPY FOR TNF-MEDIATED INFLAMMATION USING SELF-ASSEMBLED PEPTIDE NANOFIBERS **38**

3.1 SUMMARY 38
3.2 INTRODUCTION 39
3.3 RESULTS 43
Self-assembling nanofibers induce anti-TNF antibodies 43
Anti-TNF antibody responses were adjustable by titrating the T cell epitope content. 52
Cell-mediated immunity depended on T cell epitope concentration and was focused on the exogenous T cell epitopes, not the TNF component. 56
Vaccination protected from TNF-mediated inflammation in mice. 61
The ability to clear infections was not impaired by peptide nanofiber vaccination 71
3.4 DISCUSSION 73

CHAPTER 4: NANOFIBER SELF-ASSEMBLY OF T AND B CELL EPITOPE-BEARING PEPTIDE MIXTURES FOR ANTI-TNF ACTIVE IMMUNOTHERAPY. 76
4.1 SUMMARY 76
4.2 INTRODUCTION 76
4.3 RESULTS 78
Fibrillization of individual TNF (B) cell epitopes and foreign T cell epitopes is facilitated with Q11 sequence modification. 78
Binary mixtures of epitope-bearing Q11 peptides with unmodified Q11 adopt morphologies more typical of Q11. 81
Titration of T cell epitopes in Nanofiber Assemblies 83
4.4 DISCUSSION 87

CHAPTER 5: GENERAL DISCUSSION 88
FUTURE DIRECTIONS 97

CONCLUSIONS 100

APPENDIX 1: DETAILED PROTOCOLS FOR PEPTIDE SYNTHESIS, FORMULATION, IMMUNIZATION, AND IMMUNOLOGICAL ANALYSIS 102
SUMMARY 102
INTRODUCTION 103
PART 1: PEPTIDE DESIGN, SYNTHESIS, AND PREPARATION 104
PART 2: IMMUNIZATIONS: FORMULATION AND DELIVERY 110
PART 3: ASSESSMENT OF IMMUNE RESPONSE PHENOTYPES 116
NOTES 122

REFERENCES 128

LIST OF FIGURES

Figure 1.1 Canonical pathways for particles or materials to engage immune cells. ------- 5

Figure 1.2. Biomaterials enabling antibody responses via the multivalent surface display of antigens can span a range of sizes. ---------- 10

Figure 1.3 Antibody and tissue responses elicited by decellularized xenogeneic matrices and self-assembled peptide materials. ---------- 22

Figure 3.1 Co-assemblies of B cell and T epitopes form nanofibers by TEM. ---------- 46

Figure 3.2 Foreign T cell help is required to break B cell tolerance to mouse TNF------ 47

Figure 3.3 T-cell epitope-containing assemblies raised significant IgG responses against TNF peptide and TNF cytokine, with minimal antibody responses against the T-cell epitopes ---------- 49

Figure 3.4 Vaccination using mouse TNF-derived antigen raises antibodies that also react with human TNF cytokine ---------- 50

Figure 3.5 Serum polyclonal antibody binding measurements by SPR. ---------- 51

Figure 3.6 The strength and quality of anti-TNF antibody responses can be modulated by the amount of PADRE T cell epitope within nanofibers ---------- 53

Figure 3.7 The strength and quality of anti-TNF antibody responses was modulated by the amount of VAC T cell epitope within nanofibers ---------- 55

Figure 3.8 PADRE-containing co-assembled nanofibers elicited dose-dependent IL-4/Th2 dominated T-cell responses against the foreign T cell epitope PADRE, but not the endogenous TNF B-cell epitope ---------- 59

Figure 3.9 VAC-containing co-assembled nanofibers elicited dose-dependent, balanced Th1/Th2 responses focused against the foreign T cell epitope VAC, not the endogenous TNF B-cell epitope---------- 60

Figure 3.10 Immunization with PADREQ11/TNFQ11/Q11 peptide nanofibers protects mice from LPS-induced inflammation ---------- 64

Figure 3.11 Individual body temperature traces after LPS challenge of PADRE-immunized mice---------- 65

Figure 3.12 Individual weight traces after LPS challenge of PADRE-immunized mice. 66

Figure 3.13 Protection from LPS in VAC-containing nanofibers with and without CpG adjuvant, or with a scrambled TNF sequence ---------- 67

Figure 3.14 Individual body temperature traces after LPS challenge of VAC-immunized mice ---------- 68

Figure 3.15 Individual weight traces after LPS challenge of VAC-immunized mice. ---- 69

Figure 3.16 CpG adjuvantation of optimized peptide nanofibers resulted in a robust Th1 polarization of the T epitope-specific T cell cytokine response.---------- 70

Figure 3.17. Vaccination with peptide assemblies did not increase susceptibility to infection by *Listeria monocytogenes*---------- 72

Figure 4.1 Transmission Electron Microscopy (TEM) and Thioflavin T (ThT)-binding fluorescence of individual peptides---------- 79

Figure 4.2 TEM and ThT of VACQ11 in water revealed long and homogenous fibers - 81

Figure 4.3 TEM of binary peptide mixtures with Q11 ---------- 82

Figure 4.4 TEM micrographs of ternary complexes incorporating PADREQ11 T cell epitope peptide ---------- 84

Figure 4.5 TEM micrographs of ternary complexes incorporating varying concentrations of VACQ11 T cell epitope---------- 85

Figure 4.6 Co-assemblies with scrambled TNFQ11 peptide of optimized formulation for anti-TNF antibodies ---------- 86

Figure 5.1 Working model of immune recognition of co-assembled T and B epitope-containing nanofibers ---------- 96

LIST OF TABLES

Table 1. Summary of peptide sequences……30

ABBREVIATIONS

AD: Alzheimer's Disease

ANOVA: analysis of variance

APC: antigen presenting cell

BCR: B cell receptor

CFA: complete Freunds adjuvant

DAMPs: damage/danger-associated molecular patterns

DC: dendritic Cells

ELISA: enzyme-linked immunosorbent assay

ELISPOT: enzyme-linked immunospot assay

FRC: fibroblastic reticular conduits

IBD: inflammatory bowel disease

ICMV: interbilayer cross-linked multilamellar vesicles

IEDB: immune epitope database

IFA: incomplete Freund's adjuvant

IFNγ: interferon gamma

IL: Interleukin

IL-1β: interleukin-1 beta

IL-4: interleukin-4

JNK: Janus kinase

LPS: lipopolysaccharide

MHC: major histocompatibility complex

MPLA: monophosphoryl lipid A

MyD88: myeloid differentiation factor 88

NALP3: NOD-like receptor, also called NLRP3 or cryopyrin

OVA: ovalbumin-derived peptide

PADRE: pan-DR epitope

PAMPs: pathogen-associated molecular patterns

PRR: pathogen recognition receptors

RA: rheumatoid arthritis

SA: streptavidin

SIS: small intestinal submucosa

SPR: surface plasmon resonance

TACE: TNF alpha converting enzyme

TCR: T cell receptor

TEM: transmission electron microscopy

T_{FH}: T follicular helper cell

Th: CD4 T helper cell

TLR: toll-like receptor

TNF: tumor necrosis factor

Treg: T regulatory cell

VAC: vaccinia virus-derived T cell epitope $I1L_{7-21}$

VLP: virus-like particle

ACKNOWLEDGMENTS

I want to thank all my graduate school professors who supported my scientific career through the years as well as the Pathology department for accepting me into the PhD Program. To my committee members, Dr. Stephen Meredith, Dr. Anita Chong, and Dr. Tobin Sosnick, I want to thank you for your honest feedback and for your willingness to help me when I needed guidance and support during my training as a scientist. Most importantly, I want to thank my current PhD advisor, Dr. Joel Collier. Joel has been everything I could have asked in an advisor: he has been a mentor, a coach, a writing editor, a career counselor, a friend, and he has taken these various roles with the utmost respect and charisma. He has been an excellent example of an empathic leader. I feel very lucky to have had the opportunity to work on different projects under his guidance, to learn from him, and to be his colleague while we wrote together our manuscripts.

I would like to thank all of the past and present members of the Collier laboratory, especially Dr. Rebecca Pompano, Dr. Jianjun Chen, Dr. Gregory Hudalla, and Dr. Yi Wen. Each of them shared with me wisdom, taught me techniques, or contributed to the successful completion of this thesis after our laboratory move to Duke University in January of 2016. Our former technicians, Huifang Han and Tao Sun, thank you for your professionalism and lending some extra hands whenever we needed you. This work in particular could not have been completed without Fang's exceptional peptide synthesis. I want to thank Dr. Marisa Alegre and her laboratory (and Dr. Tom Gajewski's) for welcoming me back since my laboratory rotation in my first year in the PhD program,

and providing a collegial and professional environment in which I could finish my thesis dissertation and obtain feedback for my defense. I would like to thank Dr. Michelle Miller in particular for providing her time in assisting in Listeria and ELISPOT experiments, for the continuous scientific discussions, and most importantly, for her friendship throughout these past 6 years. I am thankful also to several University of Chicago technical staff: Yimei Chen and Joe Austin in the Advanced Electron Microscopy (TEM) facility, Elena Solomaha in the BioPhysics Core Facility, and the veterinary staff in the Carlson Animal Facility and the Animal Resources Center.

I am truly in awe and inspired by the commitment of professors to my academic and professional success. In this regard, I am especially grateful for mentors like Dr. Vicky Prince and Dr. Cathy Nagler, which showed me unrelenting support and kept checking that I was meeting my thesis deadlines and successfully finished what seemed the most difficult 1.5 years as an independent (lableless) graduate student. I am grateful for the Biological Science Division at large for providing useful resources and professional opportunities through the MyCHOICE seminars and the ARETE internship in science communication to find my passions and my career aspirations post-PhD. Thanks also to UChicagoGRAD, especially Michel Tessel and Brianna Konnick for their support with preparing me for the next step in my career. This doctorate could not happen without the support from the BSD administrative staff: Diane Hall, Melissa Lindberg, as well as the Biomed Cluster staff through the years: Kristin Reepmeyer,

Josephine Beaudreau, Chevette Young, Nadja Otikor, Emily Traw, Helen Polanski, and Lisa Abston-Leftridge.

I would not be here in the first place had it not being a result of my former mentors for their encouragement to pursue a career in science. Back in high school in Costa Rica, I could not have imagined having the honor to obtain the highest educational degree from one of the top universities in USA and the world. To my teachers, Arturo Rodríguez and Gloria Calvo, thank you for instilling in me the earlier foundations of the scientific method and the passion to continually improve in my scientific endeavors. To my undergraduate mentor from Macalester College, Dr. Devavani Chatterjea, I owe gratitude for giving me my first research experience that culminated into an honors thesis and scientific publications. Devavani shared a passion for Immunology that is still alive in me to this day, and continues to be a source of inspiration, as a mentor, both professionally and personally.

I want to thank some of my closest friends for cheering me whenever things were not working out and for reminding me of my abilities and potential when my mood faltered me. Special thanks to my female friends Zaza Kabayadondo, Evelina Ayrapetyan, Jacqueline Handley, Michelle Miller, Simin Golestani, Diana Solano, and Chenan Zhang for your continued presence and advice.

Lastly, I want to thank my family. My parents instilled in me values such as perseverance, hard work, optimism, independence, and gratitude that proved essential for completing this challenge and I commend them for their encouragement, support and unconditional love all the way from Costa Rica. The arrival of my son, Maximilian, changed my life forever. Thus, I want to thank all of the lovely teachers from Sonnets Academy (Simone, Rebekah, Iesha, Jackie, Adriana, Christine) and nannies (Maribel) who care for Max so lovingly. To baby Max: Thank you for filling my days (and nights) with happiness.

This work could not exist without all of your contributions! THANK YOU.

ABSTRACT

The old dogma in the field of Biomaterials was to avoid as much as possible recognition by the immune system as “foreign”. Less than a decade ago, there has been a boon in technologies and strategies designed to appropriately engage with the immune system using defined components. Self-assembly allows the development of multi-subunit materials with facile synthesis and preparation methods, that are practical from an engineering perspective but also from a basic immunological standpoint, as it allows higher control over how individual parts affect a particular immune response outcome. In this thesis, we used peptide self-assembly to design the first anti-TNF immunotherapy in which the content of T cell and B cell epitopes was individually adjusted. In the past, peptide assemblies have been developed with the aim to target foreign antigens. Here, we show that peptide nanofibers in particular can be designed to target autologous or self-derived molecules, such as cytokines. Peptide assemblies consisting of TNF-derived B cell epitopes and foreign or non-TNF-derived T cell epitopes were designed to enable a TNF-specific autoantibody response without breaking T cell tolerance to the cytokine, which resulted in unique combinations of T cell and B cell responses, and protection in mouse models of TNF-mediated inflammation. Our results further indicate that peptide nanofibers represent a highly robust self-assembly platform capable of maintaining the fibrillization capacity despite co-presentation of high density, relatively hydrophobic, CD4 T helper cell epitopes. Collectively, the work presented in this thesis suggests a new peptide-based technology with immense potential for diverse immunotherapy applications.

CHAPTER 1: INTRODUCTION

Note: Sections 1.1-1.3 of this introduction chapter were reproduced with only minor modifications from reference 7 of this thesis: C. Mora-Solano and J. H. Collier. Engaging adaptive immunity with Biomaterials. J Mater Chem B Mater Biol Med. 2014. 2(17): 2409–2421, with permission from the Royal Society of Chemistry.

1.1 Summary

Adaptive immune responses, characterized by T cells and B cells engaging and responding to specific antigens, can be raised by biomaterials containing proteins, peptides, and other biomolecules. This section discusses major properties and processes that influence biomaterials-directed adaptive immunity, including: the physical dimensions of a material, epitope content, and multivalency. Selected strategies involving novel biomaterials designs will be discussed to illustrate these points of control and how they affect immunological recognition and activation. A particular group of biomaterials relevant to the present thesis are self-assembling peptides. Their physical and chemical properties, as well our current understanding of their mechanistic engagement of innate and adaptive immunity will be presented. The recent observation that these materials are self-adjuvanting (i.e. capable of stimulating an immune response to an antigen without the need of exogenous adjuvants) have expanded their application outside tissue engineering/wound healing into the fields of

immunomodulation and immunoengineering. Self-assembling peptide vaccines enable facile incorporation of functional epitopes and provide a versatile but simple platform to modulate T cell and B cell responses through adjustment of individual epitope content. This observation has led to the exciting perspective of using these biomaterials for therapeutic immunization against a variety of antigens. Original research stemming from our laboratory in recent years has discovered that self-assembling peptides are also relatively non-inflammatory, non-cytotoxic, and that induction of a vigorous antibody and T cell response does not adversely affect wound healing compared to more traditional adjuvants, suggesting that they have a relatively safer and non-inflammatory profile compared to other adjuvants. In this work, I will introduce the concept of active immunotherapy and our motivation to develop self-assembling peptide-based immunotherapies to attenuate Tumor Necrosis Factor (TNF), which is the focus of this thesis. TNF is a cytokine implicated in the inflammation process associated with a wide range of chronic and acute inflammatory conditions including rheumatoid arthritis (RA), psoriasis, and Inflammatory Bowel Disease (IBD), and it has been one of the first monoclonal antibody targets of commercial immunotherapy. The conclusion of this chapter will present a brief outline of the thesis.

1.2 Introduction

In the past few decades, researchers working in the field of Biomaterials have developed an expansive set of exciting new hybrid biological/synthetic materials and are applying them towards diverse clinical objectives, including tissue engineering, wound

healing, cell-based therapies, immunotherapies, and the delivery of genes, drugs, proteins, and other therapeutics for a broad spectrum of diseases. Arguably the dominant theme in contemporary biomaterials research is an ever-increasing reliance on incorporated biomolecules to confer specific biological activity [1]. Reasons for including biomolecules are extremely varied and include targeting (via antibodies or other affinity tags), cell adhesion, specific proteolysis, selective cell ablation, specific enzyme activity, homing factors for various cell populations, and modulators of inflammation, to name a few. However, along with the now commonplace integration of biological macromolecules into biomaterials come new considerations in biomaterials design, not the least of which are adaptive immune responses.

Previous materials generally lacking in potentially immunogenic components such as the metals, polymers, and ceramics in current widespread clinical use have been able to avoid adaptive immunity in most applications, but next-generation biomaterials will not necessarily have that luxury. Fortunately, the very explosion of available chemistries and strategies seen in biomaterials recently is enabling not just the avoidance of adaptive immunity, but a deeper understanding and engagement of immunological processes as well, as evidenced by the increasing introduction of new vaccine platforms and other immunomodulating biomaterials. We begin this chapter with an exploration of emerging concepts, strategies, and underlying basic knowledge that is enabling us to avoid, control, or exploit biomaterials-directed adaptive immune responses.

1.3 Basic Biomaterial Properties for Exploiting Adaptive Immunity

Adaptive immunity consists of T cell and B cell responses to specific antigens, and it is initiated by the interaction of these cells with antigen-presenting cells (APCs) in the lymph node. On the one hand, naïve T cells require appropriately presented antigen (signal 1), co-stimulation (signal 2), and the appropriate cytokine milieu (signal 3) to become properly activated [2,3].On the other hand, B cells need not only cross-linking of their B cell receptors (BCRs), but also activating signals from antigen-specific T follicular helper cells (T_{FH}) for maturation into long-lived memory B cells or antibody-producing plasma cells [4-6]. Both halves of this two-signal mechanism represent fundamental considerations for biomaterials design, for maximizing and for avoiding strong adaptive immune response (**Figure 1.1**) [2,3].

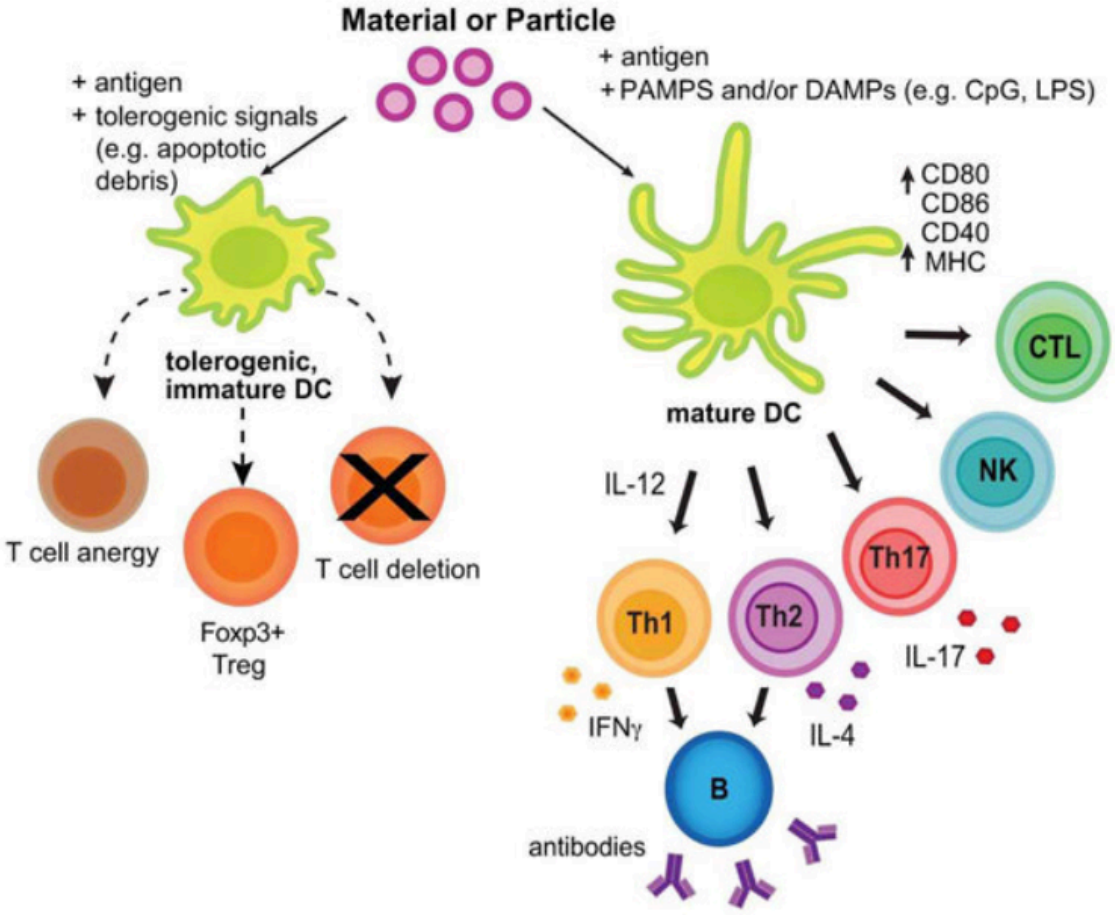


Figure 1.1 Canonical pathways for particles or materials to engage immune cells. Biomaterials can induce tolerance (left) or immunogenicity (right) to an antigen depending on the incorporation and/or modulation of tolerogenic signals (for example, apoptotic debris) or pathogen- or damage/danger-associated molecular patterns (PAMPs or DAMPs) recognized by pathogen recognition receptors (PRRs) on dendritic cells (DCs). Tolerance mechanisms can include T cell anergy, induction of T regulatory (Treg) cells, and antigen-specific deletion of effector T cells. Activation of DCs by antigen in the presence of PAMPs and/or DAMPS results in higher antigen presentation on MHC molecules, as well as increased expression of co-stimulatory molecules (CD80, CD86 and CD40). Mature DCs can then activate cytotoxic T lymphocytes (CTLs or CD8+ T cells), natural killer (NK) cells, or cytokine-producing CD4+ T helper cells (Th1, Th2 or Th17). B cells, on the other hand, can be directly activated by particles but also need input signals from DCs and T follicular helper cells (T_{FH}, not shown) to differentiate into antibody-secreting cells. Image reproduced with permission from Mora-Solano and Collier, Copyright 2014, from the Royal Society of Chemistry [7].

Antigens are taken up by APCs (i.e. dendritic cells, B cells, and macrophages) and processed, and the resulting epitopes are displayed on the cell surface within the major histocompatibility complex class II (MHCII). This epitope-MHC complex binds to the T cell receptor (TCR) to provide signal 1. Signal 2 is provided when the APC becomes activated and displays costimulatory receptors (e.g. CD80, CD86, CD40). Immunogenicity can be imparted to otherwise immunologically inert materials using specific design strategies to activate co-stimulation, for example by including danger-associated or pathogen-associated immunostimulatory ligands for pattern recognition receptors (PRRs) or chemistries capable of activating complement [8,9] [10-17]. These design strategies contrast with traditional vaccines prepared from live, attenuated, or inactivated whole pathogens, which contain a diverse mixture of antigens as well as molecules that can activate APCs and promote secretion of inflammatory cytokines, generally leading to strong immune responses. In the past decades, the fields of vaccinology and immunology have converged efforts toward a more rational design for adjuvants and provided new levels of control for specifying and shaping such responses. More detailed descriptions of the mechanisms by which innate immunity regulates adaptive immunity has been the focus of several reviews [18-21].

I will now highlight three of the most important compositional characteristics of biomaterials that influence adaptive immune responses: their epitope content, size, and multivalency. Together, these three factors strongly influence the pathways by which antigen-containing biomaterials are detected, processed, and responded to by the immune system.

Epitope content

Adaptive immune responses cannot proceed without competent epitopes, so efforts to specify the epitope content of a given biomaterial are an appropriate first-order point of control. Vaccines typically require the presence of a T-helper-epitope to activate CD4+ T cells, and either a B-cell specific or CD8+ T-cell-specific epitope, to induce neutralizing antibodies or cytotoxic responses, respectively [2,22,23]. In the fields of bioengineering and biomaterials, the word “epitope” has come to be used at times to indicate a biofunctional or biomolecular component, or a ligand in general, but here we are employing the classical definition: the sequence on a molecule that can be recognized by antibodies, by BCRs, or TCRs. Epitopes are usually peptide sequences, and they can be incorporated into biomaterials directly or can arise *in situ* as APCs process larger antigens, proteins, cells, or debris associated with the biomaterial.

Two pathways exist for antigen processing and epitope presentation [22,23]. In the classical MHC-II pathway, extracellular antigens are taken up via phagocytosis, endocytosis, or macropinocytosis, digested in endosomal/lysosomal compartments, loaded into MHC-II molecules, and presented on the APC surface for CD4+ helper T cells to recognize [22,23]. Intracellular antigens (after infection with intracellular pathogens), or extracellular ones that escape to the cytosol through cross-presentation pathways, are digested via the proteasome into short peptide fragments, transported into the endoplasmic reticulum, loaded into MHC-I, and presented on the APC surface for cytotoxic, CD8+ T cell recognition [22,23].Thus, a competent T cell epitope must successfully be processed through one of these entire pathways. A B cell epitope, on

the other hand, is simply a sequence (linear or conformational) on a peptide or protein that can bind antibodies or BCRs directly; processing is not necessarily required [24].

Currently, predictive algorithms are increasingly employed to determine the likelihood for a given amino acid sequence to act as a functional epitope [25]. In general, predictive power is greatest for MHC-I binding peptides, [25,26] but MHC-II [27,28] and B-cell epitope prediction [24] is rapidly improving. MHC-I epitope prediction can be based on multiple points along the antigen processing pathway, including proteasomal cleavage, MHC binding, engagement of TCRs, the 3D structure of the epitope, or a consensus combination of more than one of these considerations [26]. MHC-I molecules are known to bind peptides 8-10 amino acids (aa) long whereas MHC-II molecules can bind peptides 9-40 aa in length, even though the core binding motif is usually only 9aa long [28]. These length differences mean that an MHC-II-binding epitope can extend out of the open ends of the MHC surface and bind with different registers or aa contacts, making prediction more complicated than for MHC-I-binding epitopes. B cell epitope prediction is also challenging because discontinuous stretches of amino acids often form conformational epitopes, requiring knowledge or calculation of the 3D structure of the protein [24]. Although prediction tools continue to be refined and are not yet 100% reliable, an online resource such as the Immune Epitope Database and Analysis Resource (IEDB, www.iedb.org) is a helpful entry point for biomaterials researchers seeking to predict the epitope content of their constructs [29,30].

Consideration of epitope content is perhaps the most critical parameter for biomaterials-driven adaptive immune responses, since the presence or absence of T

and B cell epitopes on a particle, fiber, scaffold, or other biomaterial can mean the difference between no detectable immune response and a vigorous one. For example, peptides that self-assemble into nanofibers do not raise detectable antibody responses unless competent B and T cell epitopes are present in the peptide sequence, in which case the antibody responses are strong and durable [31-34].

Size

The physical dimensions of a biomaterial profoundly influence adaptive immune responses [4,35]. For particulate vaccines and delivery systems, size modulates biodistribution, active and passive targeting, cellular uptake mechanisms, and the intracellular fate of antigens [14,36-40], which cumulatively direct the magnitude and quality of the adaptive immune response elicited [9,10,14,34,41-49]. APCs such as dendritic cells and macrophages are capable of recognizing and responding to particles ranging from the size of viruses (10-200 nm), to bacteria (1-8 m), and cells (>1 m) [4,35,50],and immunomodulatory biomaterials have been designed in each of these ranges **(Figure 1.2).**

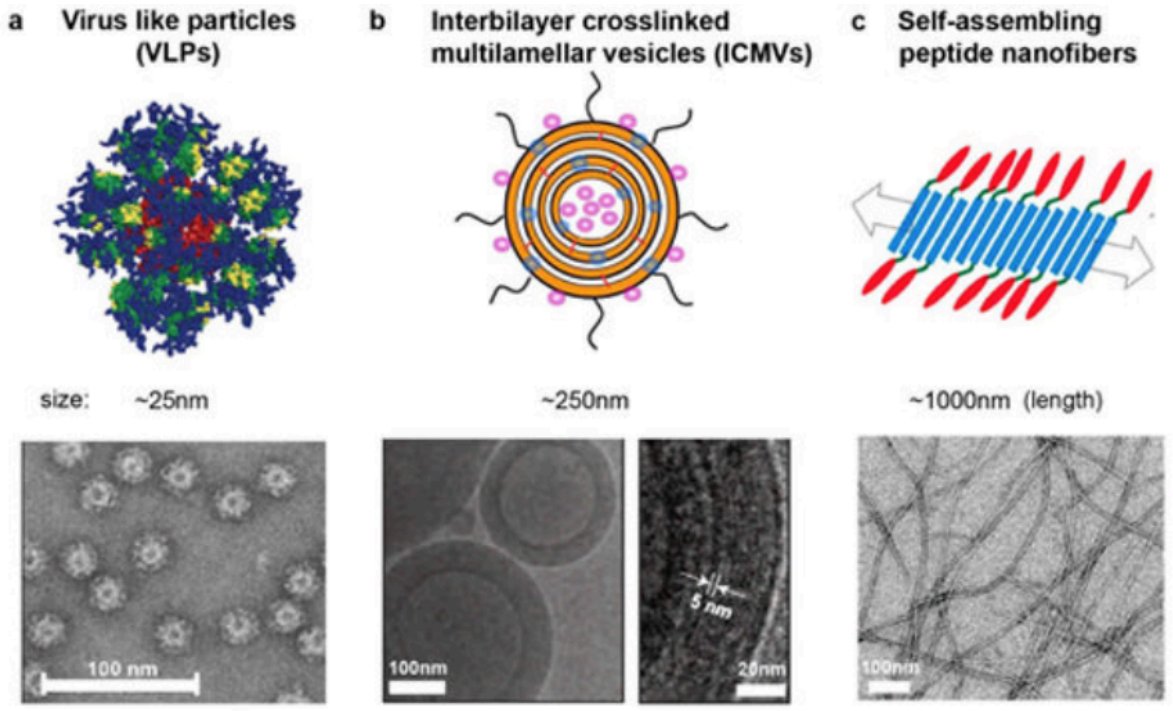


Figure 1.2. Biomaterials enabling antibody responses via the multivalent surface display of antigens can span a range of sizes. a. Virus-like particles (VLPs) and other self-assembled proteins are non-replicating nanoparticles that mimic the shape and size of viruses. They can be composed of viral- derived non-pathogenic proteins or synthetic sequences that self-assemble into icosahedral or rod-like structures. Shown is a representative VLP nanoparticle designed for multivalent display of eOD-GT6, a rationally designed HIV immunogen [51]. b. Interbilayer cross-linked multilamellar vesicles (ICMVs) are prepared from the fusion of maleimide-functionalized liposomes that co-encapsulate antigen (pink) in the aqueous core, and monophosphoryl lipid A (MPLA, blue), a TLR4 ligand, in the lipid bilayers. The maleimide groups in the precursor liposomes are used for cross-linking the bilayers (orange), surface immobilization of antigen, and conjugation of polyethylene glycol groups (PEG, black) that add chemical stability to the ICMVs [43]. c. Self-assembling peptide nanofibers composed of self-assembling peptide domains (blue) chemically synthesized in tandem with an antigenic peptide (red), form nanofibers in physiological buffers. The antigenic peptides are made accessible on the surface of the fibers by means of a flexible peptide linker [31]. Image reproduced with permission from Mora-Solano and Collier, Copyright 2014, Royal Society of Chemistry [7]. a. Jardine *et al.,* Copyright 2013, the American Association for the Advancement of Science [51]. b. Moon *et al.,* Copyright 2011, Nature Publishing Group [43]. c. Rudra *et al.,* Copyright 2010, Proceedings of the National Academy of Sciences of the United States of America [31].

As most immunotherapeutic platforms are delivered to peripheral tissues, size regulates whether or not biomaterials can access APC-enriched anatomical locations, such as the lymph nodes. It is critical that the biomaterial or its derivatives traffic correctly to and within the lymph node, so that it can interact with the necessary cell types to elicit a response. The lymphatic system mediates and regulates the transport of molecules and cells between tissue compartments and the blood [52,53].Entry into lymphatic vessels is possible owing to the presence of gaps and permeable cell-cell junctions between endothelial cells [38,52-54]. The anatomy of lymph nodes is composed roughly of a cortex, paracortex, and medulla circumscribed by a sinus. B cell follicles are located in the cortical region, while T cells localize to the paracortical region. Lymphocytes enter the lymph nodes at specialized endothelia called high endothelial venules (HEVs) and migrate within the nodes following specific chemokine gradients [52,53]. DCs, on the other hand, can be found throughout the node but are present in higher numbers near the T cell zone and the medulla [52,53]. Incoming fluid from lymph vessels is sampled first at the sinus, which is lined with mostly macrophages but also DCs [38,52,53,55]. In this region, molecules larger than 70kDa or 7nm in diameter drain along the sinus and can be internalized by APCs [14,38,53-55]. Lower molecular weight materials, in contrast, can reach other compartments of the lymph nodes directly, without being carried there by APCs, as they can be transported inside small channels in the lymph node known as fibroblastic reticular conduits (FRCs) [53,56,57]. B cells and immature resident DCs, but not mature immigrating DCs, are able to probe into these conduits to sample antigens [53,55,58,59]. Materials >100nm are less successful at passive

transport through the lymphatic system by interstitial flow, but can be carried to nodes following uptake and processing by migrating DCs [10,38,39]. Alternatively they can be specifically delivered to nodes via intranodal injections [60].

Owing to the strict size exclusion properties and permeability of the lymphatic system, small soluble antigens (<70kDa) arrive from a site of delivery or infection within minutes and drain through the FRCs [57-59]. Larger particles take longer to reach lymph nodes but are detectable, although at much lower intensity, anywhere between hours (<50nm) to days (>50nm) after peripheral injection, suggesting uptake by APCs at the lymph nodes or in tissues, respectively [10,14,34,38,39,41,43,46]. The cutoff size for effective drainage of particles to lymph nodes was found to be 45nm [38], which is larger than the size limit for rapid elimination via the kidneys at 5.5nm [37] but much lower than the size limit (>1μm) for rapid clearance by the reticuloendothelial system (liver, spleen, lymph nodes and bone marrow) [35]. While specifically investigating lymph node targeting, 30nm-size fluorescent virus-like particles (**Figure 1.2a**) and 20nm nanoparticles could be detected in lymph nodes within 2 hours.33,35 In contrast, larger (100nm, 500nm or 1μm) particles are barely detected in the lymph nodes by 24 hours and largely remain at the injection site [38,39,46]. Interestingly, particles <50nm delivered via the skin (subcutaneously or intradermally) can reliably target an impressive ~50% of DCs in the lymph nodes, of which CD8a+ DCs constitute a population important for cross-presentation of antigen to CD8+ T cells [38,39]. For example, 25nm particles modified with polyhydroxylated surfaces (to enhance complement binding) induced CD8 T cell responses at levels comparable to co-injection of soluble LPS and antigen [38].

Larger (>50nm) biomaterials also can elicit strong responses in the lymph nodes. Some of these materials have been carefully designed to degrade under certain environmental or cellular conditions, while others may function due to heterogeneity in the size of the particles or due to partial degradation, two alternatives that need to be investigated further. For example, ~200nm ICMVs **(Figure 1.2b)** were specifically designed for rapid degradation by phagosomal phospholipases following uptake by DCs to promote cross-presentation and CD8 T cell responses39. When these particles were synthesized with a malaria antigen that was incorporated to the surface in a multivalent display format, these particles elicited long-lasting (> 1 year) antibody responses following a prime/boost regimen, and the strong antibody responses correlated with sustained presence of ICMVs in the lymph nodes, formation of germinal centers, and development of TFH cells [10]. Similarly, ~1μm-long peptide nanofibers **(Figure 1.2c)** composed of the self-assembling peptide Q11 (QQKFQFQFEQQ) synthesized in tandem with the $OVA_{323-339}$ peptide (which contains both B cell and T cell epitopes) were found to elicit high IgG titer antibodies and a 100-fold higher frequency of germinal center B cells compared to alum-adjuvanted OVA peptide [31,32,34]. Finally, peptide amphiphiles conjugated to OVA-specific MHC class I peptide SIINFELK peptide (DiC16-OVA), that form cylindrical micelles 50-300nm in length and less than 10nm in diameter, were shown to significantly delay the growth of OVA-expressing tumor cells and extend the survival of tumor-bearing mice compared to immunization with soluble OVA administered in incomplete Freund's adjuvant [47].

Thus, in designing immunostimulatory biomaterials where specific targeting of lymph node-resident DC populations is warranted, small particles appear to the most suitable candidates. In particular, small particles with the proper immunostimulatory surface characteristics appear to be effective at targeting and activating a significant number of lymph node resident DCs, making them highly desirable for cross-presentation and CD8+ T cell activation responses. On the other hand, unless care is taken to achieve very small particles, slower trafficking by DCs and a bias toward CD4+ T cell and antibody responses seem to be the most likely route for most biomaterial particulates [10,31,32,34,41,48,49,58,61]. Yet, given that larger particles can still elicit CD4+ and CD8+ T cells [34,41,43,46-48,61,62], it is plausible that fragments from larger particles are capable of targeting lymph nodes directly, or that targeting APCs in peripheral tissues is sufficient to induce those responses. Although size is now a recognized parameter of major importance for designing immunostimulatory biomaterials, the ultimate fate of different nanoparticle and microparticle systems and how they and their byproducts contribute to adaptive immune responses continues to be under considerable investigation.

Multivalency

In addition to the identity of the epitopes, their multivalency is also critical to the adaptive immune response, particularly for B cell activation [4,63,64]. Multivalency in this context refers to the repetitive display of an antigen at high local density on the material. Synthetic multivalent materials cause crosslinking of BCRs that are specific for that

antigen, thus lowering the threshold for B cell activation [4,63,64]. Highly multivalent antigen presentation has been achieved for biomaterials by using synthetic scaffolds or recombinant proteins, and these can elicit strong antibody responses in both T-cell independent and T cell-dependent systems; here we focus primarily on the latter. The first multi-antigenic peptide (MAP) vaccine was designed over 25 years ago and consisted of a fully synthetic branching oligolysine macromolecule that incorporated multiple copies of peptide epitopes [65,66]. In most cases, the antibodies produced reacted to the native protein as well as the peptide.60 Further, incorporation of malaria antigen-specific B and T cell epitopes was found to protect mice after a malaria parasite challenge and protection required the presence of both the B cell and the T cell epitopes in the scaffold, suggesting a T cell dependence for antibody production [66].

The requirement for repetitiveness and organized multivalent display to elicit antibodies was later corroborated using viruses [67], recombinant proteins bearing multiple copies of the same epitope [68], and synthetic or derived particles mimicking viral structures known as virus-like particles (VLPs, **Figure 1.2a**) [11,42,44,45,51,69]. The organized MAP format promotes BCR activation and can reverse B cell tolerance to soluble antigens [70]. Some of these synthetic and bio-inspired multivalent vaccine constructs can promote T cell-dependent antibody responses in the presence of diminishing doses of adjuvant (also called dose sparing) or in the absence of exogenous danger signals [9,10,42,43,71]. For example, Moon, Irvine, and coworkers developed lipid nanoparticles composed of layers of stapled lipid vesicles entrapping recombinant protein antigens from a malaria parasite, and additionally coated the particles' surfaces with antigen for

multivalent display [10]. The multivalent presentation of the antigen increased by almost a full order of magnitude the antibody titers compared to nanoparticles that only encapsulated the antigen for controlled release. When delivered to mice in the presence of monophosphoryl lipid A (MPLA), these particles required a much lower dose of both antigen and adjuvant to elicit broad and durable humoral responses **(Figure 1.2**). Further, the responses included germinal center formation and differentiation of CD4 T cells to become T Follicular Helper (TFH) cells. Also, multivalent antigen effects on B cells are also likely to be an important component of the responses seen with self-assembled peptides (**Figure 1.2**) [31-33].

1.4 Self-assembling peptide materials

In part to provide chemically defined scaffolds with which to mechanistically study biomaterial/immune interactions, and in part to efficiently engineer multicomponent materials for tissue engineering and vaccines, in our group we have designed biomaterials using molecular self-assembly. Molecular self-assembly is defined as an organization of individual molecules into multi-subunit structures that occurs without outside management or input. The size scale for this event can be self-limiting and results in structures of predictable size (i.e. nanoparticles), or “infinite” in size in one or more dimensions (i.e. nanofibers and nanotubes) [72]. There are biological advantages to self-assemblies, such as increased complexity and added functionality, but also practical advantages from a materials engineering perspective, owing to their simpler synthesis, chemical definition, and modularity.

Peptide self-assembly is driven by non-covalent forces, including hydrophobic, ionic, hydrogen bonding, Van der Waals, and π-stacking interactions[72]. These forces can prevail or be encouraged by the properties of the solvent such as hydrophobicity/hydrophilicity, pH, and salt content, but can also be designed and applied on demand through enzymatic modification or by light, etc [73,74 75]. The specific amino acid content can dictate the forces that will drive self-assembly, for example, hydrophobic amino acids include aliphatic (A, I, L, M, V) and aromatic (F, Y, W) residues, hydrophilic but uncharged amino acids (S, T, N, Q) partake in hydrogen bonding, and charged residues (H, K, R, E, F) enable complementary ionic interactions driving the ability for self-assembly into secondary conformations (beta-sheets, alpha helices) and into the diverse array of three-dimensional structures found not just in (biologically-sourced) proteins but also in non-biological supramolecular materials [72].

Peptide nanofibers undergo hierarchical self-assembly over time into stable beta-sheet rich structures that at low concentrations can be injected, while at high concentrations solidify into hydrogels for tissue engineering and cell delivery applications [76]. The discovery that the self-assembling peptide Q11 can be functionalized with biological epitopes recognized by immune cells without the need of an externally supplied adjuvant [31] opened up a new era of research into design principles favoring specific immune applications. The focus of this thesis is the design of immunologically active nanofibers for active immunotherapies.

Immune mechanism of beta-sheet peptide nanofiber assemblies. Using gels and nanofibers composed of self-assembling peptides, proteins, and peptide/polymer conjugates, we have recently observed that peptide assemblies evoke a vigorous antibody response but almost no signs of inflammation. This response shares similarities with decellularized matrices previously used in tissue repair applications (**Figure 1.3**) [34]. For example, the fibrillizing peptide Q11 assembles into supramolecular nanofibers and hydrogels, and it raises strong and durable antibody responses of a mixed Th1/Th2 balanced phenotype when it is attached to peptides or proteins containing a competent B cell or T cell epitope [31]. Other self-assembling peptides elicit similar responses [32]. When OVAQ11 peptide nanofibers were delivered intraperitoneally, again there was no detectable infiltration of inflammatory cell types or production of inflammatory cytokines [34]. Analyzing the behavior of T cells responding to these materials, we found that the materials induced differentiation into T follicular helper cells, but T cells were only moderately responsive in terms of Th1/Th2 differentiation, producing modest amounts of both IFNγ and IL-4 compared with alum-adjuvanted positive controls [34]. Q11 nanofibers conjugated to protein antigens raised antibodies primarily of the IgG1 isotype, suggesting a Th2 polarization for these materials [77,78].

Tests of self-assembled peptide materials presenting the OVA peptide epitope in T cell-knockout mice showed that T cells were required for the strong antibody responses these materials elicit [32]. This does not rule out, however, that T-independent and T-dependent processes may act in parallel to influence different aspects of the total

response, a possibility that may provide interesting future study. Although we have endeavored to determine the signaling mechanism by which self-assembled peptide nanofibers lead to vigorous antibody responses, to date only myeloid differentiation factor 88 (MyD88), a shared adapter protein downstream of several TLRs, has been identified as a necessary signaling component,28 Further, we have ruled out the necessity of TLR-2 (and by association, of TLR-1 and TLR-6 with which TLR-2 dimerizes to form active complexes[79]), TLR-4, TLR-5, and the NOD-like receptor, NALP3, which is involved in inflammasome signaling and secretion of mature inflammatory cytokines such as IL-1β [32,33,77,80] .

Recent studies yet to be published have aimed to clarify the role of MyD88 in the immunogenicity of peptide nanofibers. In particular, global deletion of MyD88 suppressed CD4 T cell cytokine responses elicited by peptide nanofibers. Thus, MyD88 is required for both T cell and antibody responses induced by nanofiber peptide vaccines. Intriguingly, deletion of the gene coding for MyD88 in either DCs or CD4 T cells did not suppress T cell responses, indicating that there are redundant MyD88-dependent and MyD88-independent pathways that contribute to the immunogenicity of peptide nanofibers. In vivo uptake of these materials, measured after intraperitoneal immunization, revealed that dendritic cells were the main APC responsible for processing and presentation of peptide epitopes to T cells, despite significant internalization by macrophages. These results complemented previous studies showing that immunization with peptide nanofibers elicits limited inflammatory cell engagement [34]. These data suggest that peptide nanofibers do not seem to contain the inflammatory

cues necessary to activate macrophages or engage processes that significantly alter their inflammatory potential. Understanding how macrophages' involvement or lack thereof contribute to the non-inflammatory profile of peptide nanofibers should be analyzed more deeply in the future.

On the other hand, self-assembling peptides (nanofibers or peptide amphiphilic micelles) can also stimulate CD8 T cell responses when designed with competent CD8 T cell epitopes [47,62], for example the CD8 T cell epitope from OVA protein ($OVA_{257-264}$, SIINFEKL). Immunization of OT I mice, which express transgenic T cells that specifically recognize this peptide bound to MHC class I (presented by H-2Kb molecule in the C57BL/6 mouse strain) [81], with self-assembling nanofibers enabled IFNγ secretion from CD8 T cells [62]. It also protected mice after challenge with OVA-expressing influenza virus strain PR8-OVA (in peptide nanofibers) or OVA-expressing tumors (in the case of peptide amphiphilic micelles), indicating that self-assembling peptides can elicit protective cytolytic T cell responses. When responses were compared against Peptide/IFA immunization, peptide/IFA was found to elicit persistent antigen presentation at the site of injection, which was detected for nearly one month post-immunization, while Q11-OVA nanofibers elicited a more transient presentation but better recall response [62]. In agreement with prior peptide/IFA studies [82], boosting elicited a diminished expansion of OVA peptide-specific CD8 T cells, suggesting hyporesponsiveness, which is thought to occur during chronic antigen exposure [83,84]. These results affirm that peptide nanofibers elicit a modest but yet effective T cell activation that is significantly less inflammatory than the responses elicited by other

adjuvants such as IFA [82] or Alum [34,85]. Self-assembling peptides are increasingly being employed to elicit responses against therapeutically relevant targets, such as cocaine to curb cocaine addictive behavior [86], cancer [87,88], malaria [33], bacteria [89], and viruses [90-92].

Peptide nanofibers have also been employed as materials for wound healing. In the absence of an exogenous adjuvant, prior immunization of mice with peptide nanofibers elicited antibody titers and recruited more T cells to the dermal wound bed, but did not alter wound healing rates compared to unimmunized animals in three different dermal wound models [93]. In contrast, immunization of peptide nanofibers mixed with CFA adjuvant delayed wound healing despite eliciting similar IgG titers, and it prolonged the biomaterials-specific CD4 T cell response, which was significantly more slanted toward Th1 than Th2 [93]. These results indicated that peptide nanofibers elicit immune responses that are compatible with tissue engineering applications, despite their immunogenicity. The responses they elicit mirror xenografted decellularized tissues, such as small intestinal submucosa (SIS) in humans, which is bio-compatible despite eliciting a strong Th2 anti-biomaterial antibody response [94,95]. (**Figure 1.3**). Collectively, these studies illustrate that strong antibody and (CD4 and CD8) T cell responses can occur without inflammation or rejection of the material, opening up possibilities for active immunomodulation using biomaterials, both in the context of tissue repair and as a platform for rational design of novel immunotherapies.

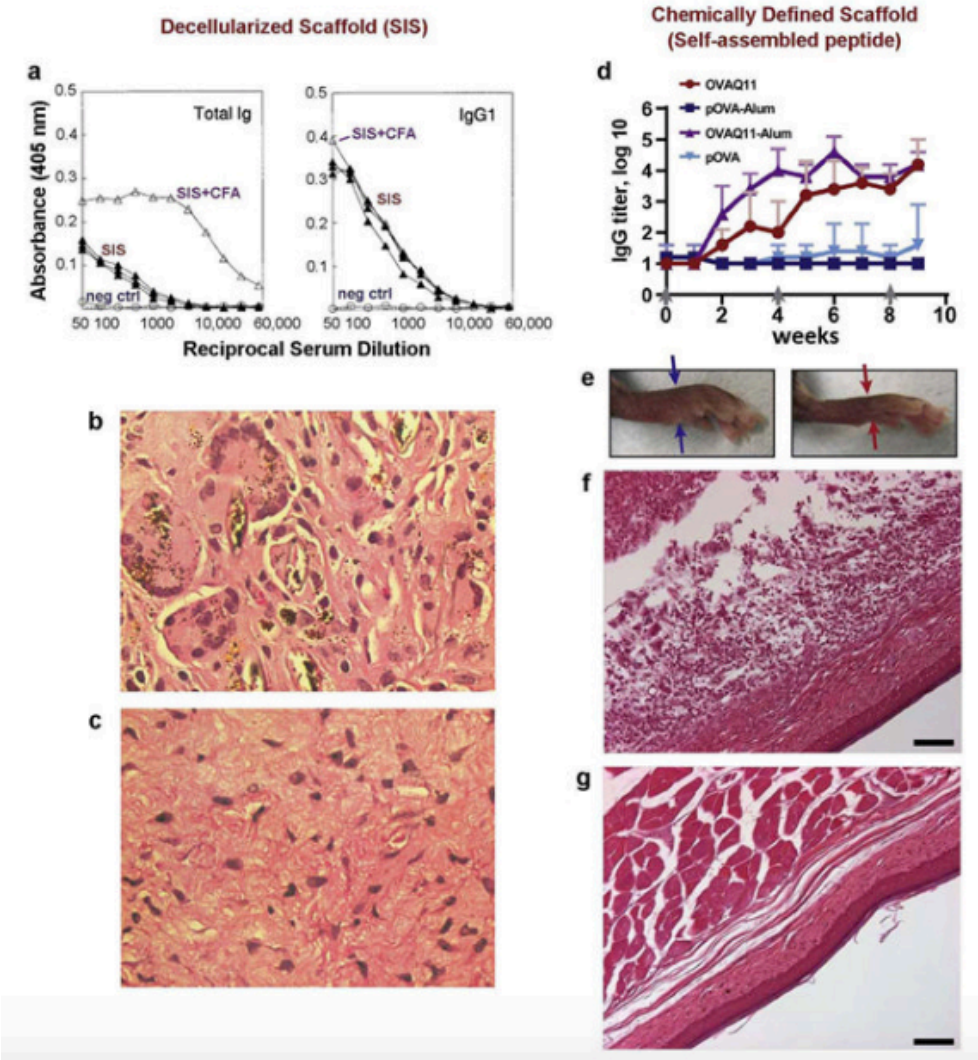


Figure 1.3 Antibody and tissue responses elicited by decellularized xenogeneic matrices and self-assembled peptide materials. a. SIS decellularized matrices[95] elicit significant IgG responses, with IgG1 being the major isotype. b. In mice, non-decellularized xenogeneic tissue elicits a rejection response, with necrosis and inflammation evident c. whereas decellularized SIS is well integrated into the tissue, exhibiting resolved inflammation and remodeling. (Both xenogenic muscle tissue and SIS were implanted subcutaneously, imaged at 28 days, H&E stained and imaged at 40× magnification). d. Similarly, self-assembled peptide materials [34] raise strong antibody responses (showing total IgG titers against self-assembled OVAQ11, OVA peptide delivered in alum (pOVA-Alum), self-assembled OVAQ11 delivered in alum (OVAQ11-Alum), and soluble OVA peptide (pOVA)). e. Like SIS, self-assembled peptide matrices do not elicit significant inflammation when injected into mouse footpads (gross swelling in footpads injected with OVAQ11 in alum (left) and OVAQ11 (right). g. At day 8, H&E staining showed significant necrosis, swelling, and inflammation for alum-adjuvanted OVAQ11 (f), but no inflammation for OVAQ11 (g).

Figure 1.3 continued. Scale bar 50μm for f and g. Image reproduced with permission from Mora-Solano and Collier Copyright 2014, the Royal Society of Chemistry [7]. a-c reproduced from Allman *et al.*, Copyright 2001, with permission from Wolters Kluwer [95] d-g reproduced with permission from Chen and Pompano *et al.,* Copyright 2013, with permission from Elsevier [34].

1.5 Tumor Necrosis Factor Signaling in health and Disease

Dysregulated Tumor Necrosis Factor (TNF, formerly TNFα) has been implicated in the pathogenesis of several chronic inflammatory and autoimmune conditions. Active TNF is a homotrimer, a type II transmembrane protein (tmTNF), which undergoes enzymatic cleavage by metalloprotease TNF alpha converting enzyme (TACE or ADAM17), to form a soluble cytokine (sTNF) [96-98]. Both TNF and Lymphotoxin alpha (LTα, or formerly known as TNFβ) bind to TNFR1 and TNFR2 receptors to exert their biological activity. Both receptors share similar extracellular domains, but intracellularly they are thought to engage unique signaling pathways [99]. TNFR1 is thought to be important for the induction of acute inflammation and apoptotic signaling via NFκB, whereas TNFR2 mediates immune regulation. TNFR1 is constitutively expressed on most cell types, while TNFR2 is induced upon immune (hematopoietic) and endothelial cell activation [100,101]. TNF initiates a complex transcriptional program that results in secretion of several inflammatory cytokines (IL-1, IL-6, IFNγ, IL-2) and anti-inflammatory cytokine IL-10 [102], among others, which can affect further TNF regulation. Physiologic levels of TNF are necessary for the control of infections [103], maturation of humoral (antibody) responses, and the genesis of secondary lymphoid tissues [104,105]. Elevated and uncontrolled levels of systemic TNF are associated with septic shock and detected

in patients suffering from immunopathologies, such as Rheumatoid Arthritis (RA), psoriasis, and inflammatory bowel disease [106,107]. It is also dysregulated in Alzheimer's Disease (AD), and in autoimmune disorders such as lupus and Multiple Sclerosis (MS) [108].

Currently there are five FDA-approved TNF inhibitors used in the clinic: Infliximab, Adalimumab, Etanercept, Golimumab, and Certolizumab Pegol [101]. These agents comparably bind, with picomolar affinities, to both tmTNF and sTNF [109-112], and are thought to work by competitively inhibiting binding to its receptors [113]. Infliximab is a 75% human (complement-fixing IgG1) and 25% mouse (antigen-binding region) chimeric anti-TNF monoclonal antibody, Adalimumab is a human IgG1 anti-TNF discovered by phage display, Etanercept is a fusion protein comprising the Fc portion of human IgG1 and the extracellular domain of TNFR2, Golimumab [110] is a human monoclonal anti-TNF antibody obtained from immunization of mice transgenic for human Ig genes, and Certolizumab Pegol is a monovalent humanized antigen-binding fragment (Fab) chemically modified with polyethylene glycol (PEG) (for increased stability) and devoid of an Fc region [114]. Independent reports about the biophysical interactions between these agents with tmTNF and sTNF indicate that these agents show comparable binding affinities by Surface Plasmon Resonance to sTNF and to mTNF expressed on cells [109]. Hence, differences in efficacy observed in patients may be affected by infusion route, relative stability, and pharmacokinetics rather than on drug efficacy.

Despite the effectiveness of these biologics, a major shortcoming is that all of them can be associated with significant immunogenicity, requiring higher dosing or combination therapy with immunosuppressive drugs (i.e. methotrexate) to counteract the development of anti-drug antibodies (ADAs) [115]. A meta-analysis on the immunogenicity of anti-TNF inhibitors has indicated that all agents induce some level of immunogenicity to varying levels (with the immunogenicity of infliximab > adalimumab > certolizumab > golimumab > etanercept), and that ADAs can reduce clinical response by nearly 70%[116]. Other reported adverse reactions include infections and, although rare, the induction of autoimmunity, for example antinuclear antibodies (ANAs) and anti-double-stranded DNA (anti-dsDNA) antibodies, among others [117].

Newer agents to potentially control or cure these diseases include Jakinibs (small molecule inhibitors of Janus kinases, most of which are in preclinical stage of development, and tofacitinib, which is the only FDA-approved Jakinib for RA) [118]. The principal drawback of these drugs is the concomitant inhibition of signaling for multiple cytokines. For example, tofacitinib inhibits JAK1/JAK3 and to a lower extend JAK2 signaling required for common gamma chain cytokines (IL-2, IL-4, IL-7, IL-9, IL-15, IL-21), IL-12, IL-23, IFNγ, and IL-6, among others, which may play a more critical role than others in the pathogenesis of these conditions. In addition, given that patients may have different pathophysiological profiles, pan-inhibition can result in drug-induced immunosuppression and higher risk/susceptibility to serious infections requiring hospitalization [118].

These adverse effects from current therapies has prompted the idea of using active immunization against TNF as an approach to overcome the drawbacks of passive immunotherapy with monoclonal antibodies. Further discussion of these strategies is discussed in chapter 3 of this thesis.

1.6 Overview of this thesis

The goal of this research project was to develop active immunotherapies targeting inflammation through blockade of active TNF signaling. An active immunotherapy is desirable in anti-TNF therapy to improve upon the current clinical use of passive immunotherapy using purified biologicals. This research was able to assess the potential of immunization against TNF to develop polyclonal B cell responses using peptide nanofiber assemblies. In chapter 1, I overviewed essential biomaterial properties considered for the design of immunoactive materials, needed to instruct the adaptive immune system to engage with the material to elicit productive and appropriate responses. In addition, we summarized the background on peptide supramolecular assemblies, with specific emphasis on self-assembling beta-sheet peptide nanofibers, in terms of the chemical, physical, and immunological qualities. Next, we overviewed the current understanding of TNF biology and signaling mediated by current TNF-blocking strategies utilized in the clinic. Chapter 2 contains the detailed description of the materials and methods employed in this research project. Chapter 3 consists of the main manuscript produced from this thesis, exploring the development of peptide assemblies as a platform for active immunotherapy targeting TNF. Chapter 4 is also

written in a manuscript format with introduction, results, and discussion section, though it presents additional supporting data not included in Chapter 3. Finally, chapter 5 is a general discussion of the positive outcomes of the thesis and how the findings fit in the broader context of designing supramolecular assemblies in clinical applications, ending with conclusions and a proposed model obtained from these investigations.

CHAPTER 2: MATERIALS AND METHODS

Note: Detailed step-wise protocols for synthesizing and evaluating immunologically active self-assembled peptide materials are presented in Appendix I and have been adapted from:

Mora-Solano, C., Wen, Y., Han, H. & Collier, J. H. Practical considerations in the design and use of immunologically active fibrillary peptide assemblies, *Methods in Molecular Biology*, in press (2017).

2.1 Peptide Synthesis Materials. Unless otherwise indicated, peptide synthesis materials were purchased from NovaBiochem, and other reagents were purchased from Sigma-Aldrich. Peptide synthesis was performed on Rink amide AM resin (Loading ≈ 0.7 mmol/g, 200-400 mesh) using 9-fluorenylmethoxycarbonyl (Fmoc)-protected amino acids, appropriately side-chain-protected. All activation steps were performed with 2 - (1H - Benzotriazole - 1 - yl) - 1,1,3,3 - tetramethyluronium hexafluorophosphate (HBTU) and 6-Chloro-1-hydroxybenzotriazole dehydrate (Cl-HOBt). Coupling reactions were performed in N,N-dimethylformamide (DMF), and resin washes were performed with DMF and Dichloromethane (DCM). Diisopropylethylamine (DIPEA) was utilized in activation steps, and 20% piperidine in DMF was utilized for deprotection steps. N-terminal functionalization was performed with acetic acid (acetylation), Biotin-ONp (biotinylation), 5-(and-6)-Carboxytetramethylrhodamine (5(6) - TAMRA), or N-hydroxy succinimidyl ester of fluorescein (NHS-fluorescein). Resin cleavage/deprotection was performed using trifluoroacetic acid (TFA), triisopropylsilane

(TIS), and water. Peptides were precipitated and washed using diethyl ether. For immunization materials, sterile wáter and sterile 10X phosphate buffered saline (PBS, Fisher Scientific, Cat#BP399-500) were used. Pyrogenicity was measured using the limulus amebocyte lysate (LAL) chromogenic endpoint assay kit (Lonza).

2.2 Peptide Synthesis. All peptides (Table 1) were synthesized using standard Fmoc solid-phase peptide synthesis (SPPS), purified by reverse-phase high performance liquid chromatography (HPLC), and verified using matrix-assisted laser desorption/ionization mass spectrometry (MALDI-MS) on a Bruker Ultraflextreme MALDI-TOF mass spectrometer using α-cyano-4-hydroxycinnamic acid as the matrix, as described previously [31,119,120]. Syntheses were performed on a CS Bio 136 or 336 peptide synthesizer using Fmoc-protected amino acids with standard side-chain protecting groups, Rink amide resin, and DMF as the solvent. Epitope peptides were synthesized both with an appended C-terminal Q11 domain and as free peptides. Three epitope peptides were investigated: TNF_{4-23}, the mouse TNF-derived B cell epitope (SSQNSSDKPVAHVVANHQVE), PADRE (aKXVAAWTLKAa, where X = cyclohexylalanine; a = D-Ala), and Vaccinia $I1L_{7-21}$ (QLVFNSISARALKAY, VAC). To form self-assembling versions of these epitopes, they were synthesized in tandem with a $(Ser\text{-}Gly)_2$ linker repeat and the fibrillizing domain of Q11 (SGSGQQKFQFQFEQQ). A negative control scrambled version of TNF_{4-23} (SKHVNVDNESHSVPSQAAVQ) was also synthesized to investigate any effects that could be non-antigen-specific. Free epitope peptides (incapable of self-assembly) were also biotinylated for use with

Streptavidin-coated plates for peptide-specific antibody ELISA. All peptide sequences are shown in **Table 1**.

Table 1. Summary of Peptide Sequences.

Peptides synthesized and investigated	
Q11	Ac-QQKFQFQFEQQ-Am *Self-assembling sequence, forms β-sheet fibers*
TNF_{4-23} (B)	NH2-SSQNSSDKPVAHVVANHQVE-COOH *B-cell epitope from mouse TNF, exposed in soluble form of TNF*
PADRE (T)	NH2-aKXVAAWTLKAa-COOH, X = cyclohexylalanine, a = D-alanine *Pan DR T-helper epitope*
Vaccinia $I1L_7$ (T)	NH2-QLVFNSISARALKAY-COOH *T-helper epitope from Vaccinia*
TNFQ11 (B)	NH2-SSQNSSDKPVAHVVANHQVE-SGSG-QQKFQFQFEQQ-Am *Self-assembling peptide presenting the TNF B-cell epitope*
$scTNF_{4-23}$ (B) sequence	NH2-SKHVNVDNESHSVPSQAAVQ-COOH, sc = scrambled *Scrambled version of self-assembling TNF B-cell epitope peptide*
PADREQ11 (T)	NH2-aKXVAAWTLKAa-SGSG-QQKFQFQFEQQ-Am *Self-assembling peptide presenting the PADRE T-cell epitope*
VACQ11 (T)	NH2-QLVFNSISARALKAY-SGSG-QQKFQFQFEQQ-Am *Self-assembling peptide presenting the PADRE T-cell epitope*

2.3 Preparation of Vaccine Formulations. Unless otherwise indicated, a typical vaccine formulation contained TNFQ11 (B cell epitope), PADREQ11 (or VACQ11, T cell

epitope), and unmodified Q11 at a total final concentration of 2 mM in PBS. The concentration of TNFQ11 was fixed at 1 mM (50 mol %) for all experiments. The concentration of PADREQ11 was titrated from 0.002mM (0.1 mol %) to 0.75mM (37.5 mol %). The concentration of VACQ11 in the nanofibers was adjusted from 0.002mM (0.1 mol %) to 1.25mM (50 mol %, with 1 mM TNFQ11 and 0.25 mM Q11). To prepare a vaccine formulation for immunization, lyophilized peptides were weighed in separate tubes, intermixed by vortexing for 30min, and then dissolved in sterile water at a total concentration of 8 mM. The peptides were allowed to dissolve and equilibrate overnight at 4 °C. Peptide solutions were then diluted with sterile water and 10x concentrated PBS to a final concentration of 2 mM in 1x PBS, and incubated for at least 3 h at room temperature for complete assembly [89]. To prepare nanofiber vaccines with scrambled TNF, TNFQ11 was replaced with the same molar amount of scrambled TNFQ11. For vaccine formulations adjuvated with 0.1 mg/mL CpG, water was replaced with equal volume of 1 mg/mL CpG in water during the assembly step. Endotoxin measurements were conducted on all immunizing formulations using the Limulus Amebocyte Lysate (LAL) kit (Lonza) as described previously [120]. All solutions were confirmed to be lower than 0.5 endotoxin units (EU) per mL and within acceptable limits for mouse study [121].

2.4 Transmission Electron Microscopy (TEM). Vaccine formulations were diluted to 0.2 mM in PBS and vigorously vortexed. Five microliters of 0.2 mM peptide nanofibers were deposited onto Formvar/carbon coated 400 mesh copper grids (Electron Microscopy Sciences), washed, stained with 1% w/v uranyl acetate in water, and dried.

Samples were imaged on an FEI Tecnai Spirit TEM.

2.5 Thioflavin T (ThT) Binding Fluorescence assay. Peptide mixtures were prepared as described above and diluted to 4 mM for testing. 100 μL of each solution was mixed 1:1 v/v with a freshly prepared solution of 100 μM Thioflavin T in 1 X PBS, and allowed to incubate for 20 minutes at room temperature, protected from light. To measure ThT fluorescence, excitation was set at 440nm and fluorescence was recorded at 490nm on Spectramax M5 plate reader. Responses were compared against a blank sample containing ThT alone (no fibrils) and against Q11, which readily forms fibers and elicits a positive fluorescence reading from ThT binding.

2.6 Intrinsic peptide fluorescence assay for in vitro T epitope peptide titration. Peptide mixtures formulated at different T epitope (PADRE or VAC) concentrations were prepared in the same manner as for immunizations. To determine the incorporation of T cell epitope into the nanofibers, T cell peptide concentration was assessed indirectly by intrinsic aromatic amino acid fluorescence (Tryptophan/W for PADRE and Tyrosine/Y for VAC). Prepared peptide solutions were sedimented by centrifugation (12,000 *g* for 5 min), the supernatant was removed, and the nanofibers were re-suspended in 1X PBS buffer. Fluorescence was measured on SpectraMax M5 microplate reader. For PADRE-containing co-assemblies (aKXVAAWTLKAa, where X = cyclohexylalanine; a = D-Ala), W fluorescence was recorded with excitation at 284nm and emission at 330nm. For Vaccinia $I1L_{7\text{-}21}$ (QLVFNSISARALKAY) -containing co-

assemblies, Y fluorescence was recorded, with excitation at 274nm and emission at 300nm. Fluorescence of resuspended nanofibers and supernatant fractions was compared against intact (non-sedimented) peptide mixtures and 1X PBS buffer (no fibrils).

2.7 Mice and Immunizations. Female, wild-type C57BL/6 mice (MHC class II haplotype: I-A^b) were purchased from Harlan-Envigo laboratories or Charles River laboratories. Experiments conducted at the University of Chicago were approved by the University of Chicago Institutional Animal Care and Use Committee, and studies performed at Duke University were approved by the Duke University Institutional Animal Care and Use Committee. All procedures were in compliance with the NIH Guide for the Care and Use of Laboratory Animals. Mice 8-12 weeks old were used for experiments. Mice were anesthetized and immunized with 100 μL (200 nmol total peptide) vaccine formulation subcutaneously (50 μL each at the left and right flank). Two Booster immunizations were performed on week 4 and 8, with a half dose (100 nmol total peptide).

2.8 Anti-TNF antibody ELISA. Sera collected from the submandibular vein at designated time points were analyzed for antibody titers by ELISA. Briefly, plates were coated with 1 μg/mL streptavidin in PBS overnight at 4 °C, washed, and then coated with 20 μg/mL biotinylated peptide epitopes (PADRE or TNF) in PBS. Alternatively, recombinant mouse TNF cytokine (Peprotech) was coated at 1 μg/mL in PBS (50 μL

each well) to detect TNF cytokine specific antibodies. Plates were washed with PBS containing 0.05% Tween 20 (PBST) and then blocked with PBST containing 1% bovine serum albumin (PBST-BSA) for 1h at room temperature. Serum was serially diluted in PBST containing 1% BSA (PBST-BSA) in 10-fold steps from $1:10^1$ to $1:10^6$, applied to coated wells, and incubated for 2 h at room temperature. To detect total IgG, HRP conjugated Fcγ fragment specific goat anti-mouse IgG (Jackson Immunoresearch) was used as the detection antibody. For antibody isotyping, HRP-conjugated IgG subtype-specific, i.e. IgG1, IgG2b, IgG2c and IgG, antibodies were utilized (Southern Biotech). A titer was defined as the highest dilution that produced an absorbance signal higher than the mean + 3•SD of naive mouse serum. "ND" refers to serum samples with absorbance indistinguishable from pre-immune serum at 1:100 dilution and were categorically given a value of zero, to indicate the lack of a measurable titer.

2.9 T Cell ELISPOT. One week after final boost, brachial, axial, and inguinal draining lymph nodes were collected. Single cell suspensions were prepared and plated at 0.5 x 10^6 cell per well (200 μL) in a 96 well plate (Millipore) pre-coated with anti-mouse IL-4 and IFN-γ capture antibodies (BD Bioscience). Cells were stimulated with TNF peptide (5 μM) or PADRE (1μM). Phytohemagglutinin (PHA, 10 μg/mL) or purified hamster anti-mouse CD3 antibodies (clone: 145-2C11, University of Chicago) were utilized as positive controls. Cells were stimulated in a CO_2 incubator at 37°C for 48h. To detect IL-4 and IFN-γ secreting cells spots, biotinylated anti-mouse IL-4 and IFN-γ detection antibody pairs, HRP-streptavidin, and AEC substrate set were used sequentially

following the manufacturer's general guidelines and concentrations (BD Biosciences). Plates were imaged and counted on an ImmunoSpot Analyzer (Cellular Technology, Ltd.). Graphs depict calculated number of spots per 250,000 cells.

2.10 Intraperitoneal LPS Challenge. To induce TNF cytokine mediated acute inflammation, mice were challenged with 1 mg/mL lipopolysaccharide (LPS, serotype 055: B5) from *E. coli* (Sigma) in sterile PBS intraperitoneally at a dose of 10 mg/kg one week after the final booster immunization. The mice were carefully monitored for 72 h. Body temperature and body weight were recorded. Humane endpoints were set at: 1) >20% weight loss, 2) significant hypothermia (rectal temperatures below 32°C [52] or 3) inability to ambulate, drink, and eat. Immediately before euthanasia, blood samples were collected for analysis of concentrations of TNF cytokine and antibody titers.

2.11 Listeria infection. Immunized mice were challenged one week after the last boost with 10^5 colony-forming units (CFU) of *Listeria monocytogenes (Lm*-GFP strain) (200 μL) by intraperitoneal injection. Negative controls included mice immunized with sterile PBS and mice immunized with the vaccine without T cell epitope (uncompromised ability to clear infection). Mice receiving a therapeutic TNF-neutralizing monoclonal antibody of 500μg in 200μL sterile PBS were employed as the positive control (clone MP6-XT22, Biolegend). The spleen and liver were harvested 48h later. The organs were placed in 5 mL sterile 0.05% Tween-20 in water, diced with scissors, and homogenized with a Tissue Tearor hand held homogenizer (Biospec Products). The

homogenized sample (5 mL for the spleen or 6 mL for the liver) was serially diluted 3 times at 1:10 dilution in sterile 0.05% Tween-20 in water. 100 μL (spleen) or 120 μL (liver) of undiluted, 10-, 100-, and 1000-fold diluted solutions were plated on Brain-Heart Infusion Agar (BD Biosciences) in quadrant-divided Petri dishes. The plates were allowed to air dry inside a sterile hood, then incubated upside down for up to 48 h in a 37°C incubator. The off-white *Listeria* colonies were counted and the total CFU per organ were calculated using the formula: Total CFU= CFU count x dilution factor x 50 (corrected for total organ homogenate volume).

2.12 Surface Plasmon Resonance (SPR). To assess the quality of serum antibodies raised by peptide assemblies, dissociation rates were measured using a BioRad ProteOn XPR36 Protein Interaction System at the University of Chicago Biophysics Core Facility. To bind TNF, a ProteOn HTG sensor chip (BioRad) with capability to capture Histidine-tagged proteins was conditioned and pre-activated following the manufacturer's instructions before each run. Next, His-tagged recombinant mouse TNF (Genscript) was diluted to 100 nM in PBST and flowed through the vertical lanes of the chip at a rate of 25 μL/ min for 5 min. PBST-BSA was then run through the horizontal lanes of the chip at a rate of 25 μL/ min for 2 min to reduce non-specific adsorption. Serum samples from multiple experiments (n= 8 for TNFQ11/Q11/VACQ11 immunization, n=5 naive serum, n=5 CFA serum) were collected 1 week after the second booster immunization and stored at -80°C before experiments. Prior to each run, samples were pooled and diluted by five-fold in PBST-BSA buffer. Additional

controls included 100 μM anti-TNF (clone MP6-XT22) antibody, blank PBST buffer, and pre-immune sera. The non-specific background signal of pre-immune sera was subtracted from the signals of sera samples and anti-TNF antibody. To measure antibody binding affinity to the recombinant TNF on the chip, samples and controls were flowed horizontally at a flow rate of 25 μL/min for 5 min. After that, running buffer was flowed over the horizontal lanes of the chip at a rate of 25 μL/min for 30 minutes. Absorption and desorption raw data were plotted and fit using KaleidaGraph Software (Synergy).

2.13 Statistical Analysis. Mean ± standard deviation was plotted. Statistical analysis was performed using ANOVA with Tukey's HSD post hoc comparisons (>2 groups) or unpaired t test (2 groups) on GraphPad Prism software. Significance between specific groups was defined at $p<0.05$, as indicated in the figure legends.

CHAPTER 3: Active Immunotherapy for soluble TNF-mediated inflammation using self-assembled peptide nanofibers

3.1 Summary

Therapeutic antibodies represent a dominant class of biopharmaceuticals, but they commonly require repeated injections and elicit neutralizing immune responses that can diminish their efficacy. As an alternative, active immunotherapies that raise the therapeutic antibodies directly within patients have begun to receive interest. The challenge in such an approach is to raise protective and adjustable levels of antibodies while at the same time avoiding strong T cell responses that could lead to T cell-mediated autoimmunity. Here we demonstrate the design of a therapeutic vaccination platform against soluble TNF-mediated inflammation using non-adjuvanted supramolecular peptide nanofibers. In comparison with other bioconjugate vaccines requiring adjuvants, peptide nanofibers are minimally inflammatory, can raise protective responses without any adjuvant, and enable the facile assembly of predetermined mixtures of selected B cell epitopes and T cell epitopes. These properties facilitated tuning the strength of the anti-TNF antibody response and focusing the T cell response on exogenous and non-autoreactive T cell epitopes. Immunized mice raised anti-TNF antibody titers that could be smoothly adjusted by varying the ratio of B cell epitopes to T cell epitopes in the nanofibers. In a lethal model of acute inflammation induced by intraperitoneal delivery of lipopolysaccharide (LPS), mice were rescued by prior immunization with non-adjuvanted peptide nanofibers. In contrast, immunizations with peptide nanofibers co-mixed with CpG adjuvant lessened the protective effect against

LPS and correlated with a more Th1 inflammatory T cell and B cell response. Further, anti-TNF vaccination using non-adjuvanted peptide nanofibers did not diminish the ability of mice to clear infections of *Listeria monocytogenes*, which requires functional membrane TNF signaling. Collectively this work suggests a new peptide-based technology for active immunotherapies capable of selectively targeting soluble TNF and tuning of the quality of the adaptive (B cell and T cell) immune response.

Note about contributions: Dr. Yi Wen assisted with TEM imaging of the peptide co-assemblies, and repeated the PADRE and VAC LPS protection experiments at Duke University to increase the experimental replicates. Huifang Han synthesized all of the peptides used in this chapter. Dr. Michelle Miller assisted with *Listeria* infection and ELISPOTs. Finally, Dr. Joel Collier and Dr. Rebecca Pompano helped with conception of the idea for the project and discussion of experiments. This chapter was written by Carolina Mora Solano and Joel Collier and will be submitted for publication, which will be similar in content but different numbering for the figures.

3.2 Introduction

Monoclonal antibodies and other biologics have seen tremendous growth in the last few decades and are now dominant strategies for the treatment of a variety of conditions, including chronic inflammation, transplant rejection, autoimmunity, infectious diseases, and cancer. They have been a tremendous boon to healthcare, and their design, engineering, and manufacturing continue to be advanced, but there remain

drawbacks to their use [122]. They are costly to develop, produce, store, and distribute. Many require repeated injections, thereby diminishing patient compliance, and they commonly fail owing to primary unresponsiveness or the induction of antibodies that neutralize the therapeutic molecule and diminish its efficacy over time [101].

A promising but not yet clinically successful way to overcome the disadvantages of monoclonal antibodies is active immunotherapy: stimulating the patient's own immune system to produce therapeutic antibodies against a specific problematic self-molecule. This approach has significant potential advantages compared with exogenous antibodies and other biologics, including lower cost, fewer doses required, improved patient compliance, and better tolerance to the treatment. Further, active immunotherapies can raise polyclonal responses, which may have a better capacity to interfere with the target of interest. In the area of active immunotherapy, TNF (tumor necrosis factor) has received particular interest owing to its central role in a variety of chronic inflammatory conditions such as rheumatoid arthritis, psoriasis, and Crohn's disease [123,124]. Recently, several TNF-directed active immunotherapy strategies have been studied. These include recombinant TNF molecules engineered to contain exogenous CD4 T helper epitopes [125,126], TNF proteins containing unnatural amino acids [127], native TNF conjugated to carrier proteins such as keyhole limpet hemocyanin (KLH) or virus-like particles (VLPs) [128]LeBuanec:2006kz}[129-133] , as well as peptide [134] and DNA autovaccines against TNF [135]. Currently no active immunotherapy targeting

TNF has been clinically approved, though a kinoid consisting of TNF conjugated to keyhole limpet hemocyanin (KLH) is in clinical trials [136].

The key objective of active immunotherapy is to raise a predictable and adjustable B cell/antibody response without an autoreactive T-cell response [124]. This achieves the controllable production of therapeutic antibodies without mounting an autoimmune response against the cells producing the cytokine through complement- or antibody-mediated cytotoxicity [111,112]. To accomplish this, it has been generally believed that three components are necessary: 1) B-cell epitopes from native human TNF [137]; 2) non-autologous T-helper epitopes from a foreign source, incorporated via a carrier protein or by engineering such peptides into a chimeric TNF molecule [125,126,128,132,133]; and 3) in most cases an adjuvant [138]. For example, the TNF-kinoids currently being investigated clinically consist of TNF protein (B-cell epitope source) conjugated to KLH (T-cell epitope source) and formulated with Montanide ISA 51 adjuvant in an oil-in-water emulsion [133].

Peptide vaccines that do not contain any potential TNF T-cell epitopes and only contain TNF B-cell epitopes reduce the likelihood of a T-cell response to native TNF, and so these have potential safety advantages, but they tend to be poorly immunogenic. TNF B-cell epitope peptides conjugated to carrier proteins have been studied only in mice, using strong adjuvants such as complete Freund's adjuvant (CFA) [134], which is not acceptable for human use. Further, the adjuvants required in most subunit vaccines

cause inflammation, present challenges for regulatory approval, and may not necessarily induce the T-helper phenotype and antibody isotypes that are most therapeutic.

Here we report an anti-TNF active immunotherapy that does not require supplemental adjuvants, based on a supramolecular peptide system in which exogenous T-cell epitopes and TNF B-cell epitopes can be co-assembled into long nanofibers with a wide range of possible stoichiometries. This is a departure from peptide-carrier conjugates, which contain only a fixed number of T cell epitopes and only have room for a limited number of B cell epitope peptides to be conjugated. More importantly, the peptide nanofibers that the strategy is based on have been previously shown to be remarkably non-inflammatory [34] and they raise strong B-cell and T-cell responses without supplemental adjuvants [31,34,89]. Other recent work also found in a similar fibrillizing peptide vaccine against S. aureus that the relative ratio of B cell epitopes and T cell epitopes in the materials had a strong influence on the strength and phenotype of the subsequent immune response [89]. Both this previous work and the current work investigating a range of peptide combinations has been enabled by the non-covalent modular construction the materials, which makes it straightforward to economically generate a set of nanofibers containing a range of specified epitope combinations for further testing in vitro and in vivo [89,119,139,140]. In the work reported here, this control over epitope ratio was exploited to adjust the titer of anti-TNF antibodies and select promising formulations for evaluation in animal models of inflammation. In mice,

these unadjuvanted peptide nanofibers protected against an otherwise lethal intraperitoneal injection of lipopolysaccharide (LPS), which induces massive TNF-mediated inflammation, but immunizations did not diminish the mice's ability to clear infections of *Listeria monocytogenes*. Fascinatingly, when peptide nanofibers were adjuvanted with CpG, this protective effect against LPS was abolished, correlating with a more Th1-polarized response compared to the unadjuvanted and protective nanofibers. Collectively, these results indicate that unadjuvanted supramolecular systems such as the one reported here represent attractive new platforms for development as active immunotherapies.

3.3 Results

Self-assembling nanofibers induce anti-TNF antibodies

Self-assembled nanofibers employed the Q11 fibrillizing sequence [31,34,77,78,89,141]. Epitope-bearing peptides were synthesized with Q11 at the C-terminus and the epitope at the N-terminus (sequences in Materials and Methods). The peptide TNFQ11 contained an N-terminal B-cell epitope from mouse TNF, residues 4-23 (SSQNSSDKPVAHVVANHQVE), identified in pioneering work by Bachmann and co-workers as being able to raise antibody responses against soluble TNF but not transmembrane TNF when conjugated to VLPs [132]. Owing to this targeted response, this peptide did not compromise the ability to clear bacterial infections, whereas formulations containing whole TNF did [132]. This B-cell epitope-containing peptide was

co-assembled with peptides PADREQ11 or VACQ11, which contain an N-terminal $CD4^+$ T-cell epitope, either the synthetic pan-DR epitope PADRE [142], or $I1L_{7-21}$ (VAC), an $I\text{-}A^b$ (the MHC II haplotype in C57/BL6 mouse strain)-restricted epitope from Vaccinia I1L protein [143]. In physiological buffers, all three peptides self-assembled to form nanofibers in binary mixtures with unmodified Q11, and in ternary mixtures of TNFQ11, Q11, and PADREQ11 or VACQ11 (**Figure 3.1A**). The reproducible co-assembly of all three peptides (see more TEM images in Chapter 4) corresponds with extensive previous work investigating other epitope-tagged Q11 peptides, which have been shown repeatedly to be able to stoichiometrically assemble into integrated nanofibers of controlled composition [77,78,89,119,139,140]. Again, this B cell epitope peptide was selected owing to its previously reported ability to raise IgG antibodies that react specifically against the soluble form of TNF but that only weakly bind to the membrane-bound form of TNF [128,132], contrasting with biologicals that bind both membrane-bound and soluble TNF [101]. This choice was made to maximize the production of neutralizing antibodies against the circulating cytokine and minimize chances for autoimmunity. It is thought that antibodies raised against this B cell epitope are capable of binding soluble TNF monomers and disrupting trimer formation, a process required for TNF activity [132]. PADRE was selected as the T cell epitope not only for its high affinity for MHC class II molecules in humans and in C57BL/6 mice [142], but also because we have previously had success blending it with B cell epitopes in fibrillar peptide assemblies [89]. VAC was chosen as an alternative to PADRE with expected differences in affinity for MHC-II and T cell phenotypes [143]. In co-assembled peptide nanofibers (**Figure 3.1B**), simple

adjustment of the relative ratios of the T-cell epitope and B-cell epitope can be used to vary the resultant antibody titer and the phenotype of the T cell response [89]. Here we hypothesized that nanofibers incorporating strong foreign T-cell epitopes would provide the necessary T cell help required, while the repetitive presentation of TNF B cell epitopes would serve to break B cell tolerance but not T cell tolerance to native TNF [67]. In our first proof-of-concept we wanted to know whether a T cell epitope would be required to elicit an anti-TNF IgG response. Hence, we immunized mice with assemblies that did or did not contain a foreign CD4 T cell epitope and evaluated responses against TNFQ11 over time (**Figure 3.2A**) Immunizations containing 1mM TNFQ11 / 0.05mM PADREQ11/ 1.95mM Q11 were effective at eliciting moderate antibodies titers that reacted against the TNF_{4-23} peptide by ELISA (**Figure 3.2B**). Mice immunized with nanofibers containing VACQ11 (1mM TNFQ11/ 0.25mM VACQ11 / 0.75mM Q11) also raised detectable antibody titers (**Figure 3.2C**). In contrast, nanofibers lacking any T cell epitopes failed to raise any detectable antibodies two independent experiments (**Figures. 3.2B, C**).

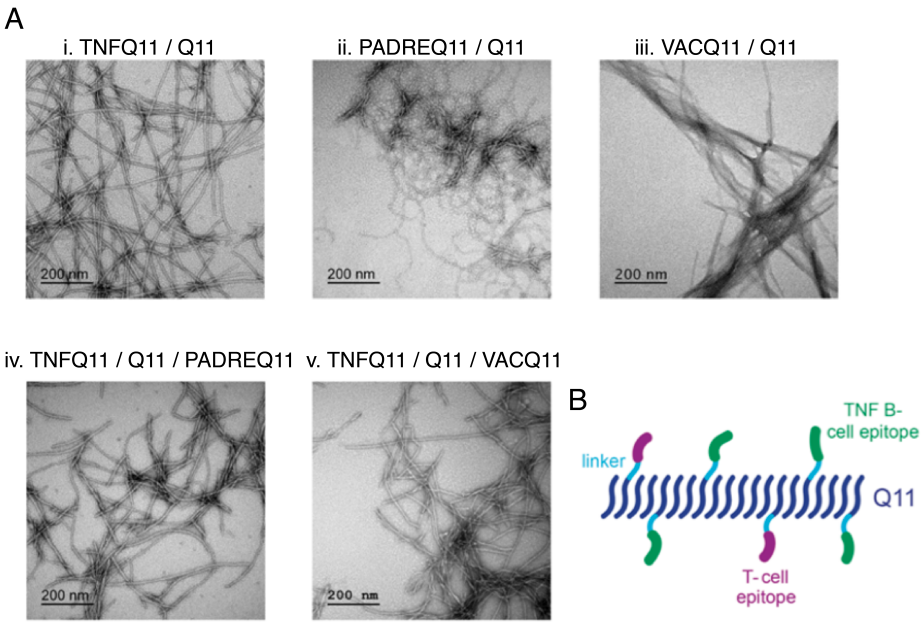


Figure 3.1 Co-assemblies of B cell and T epitopes form nanofibers by TEM. A) Peptides were individually weighed, combined and vortexed to mix, then formulated at 8mM in sterile filtered water and allowed to self-assembled into nanofibers overnight at 4 ˚C. The next day, peptides were diluted to 2 mM in a final concentration of 1 x PBS buffer and incubated RT for at least 3 hours. Peptides were diluted to 0.2 mM in water, loaded onto 400 mesh carbon grids and stained with 1% uranyl acetate to visualize nanofiber morphology by TEM. Scale bar for all images = 200nm. Formulations included: i) 1 mM TNFQ11 / 1 mM Q11; ii) 1 mM PADREQ11 / 1 mM Q11; iii) 1 mM VACQ11 / 1 mM Q11; iv) 1 mM TNFQ11 / 0.95 mM Q11 / 0.05 mM PADREQ11 mixture; v) 1 mM TNFQ11 / 0.75 mM Q11 / 0.25 mM VACQ11. B. Schematic of co-assembled peptide nanofibers (fibrillizing core in navy blue) containing defined amounts of B-cell epitopes (green) and T-cell epitopes (magenta), separated by a flexible linker (light blue).

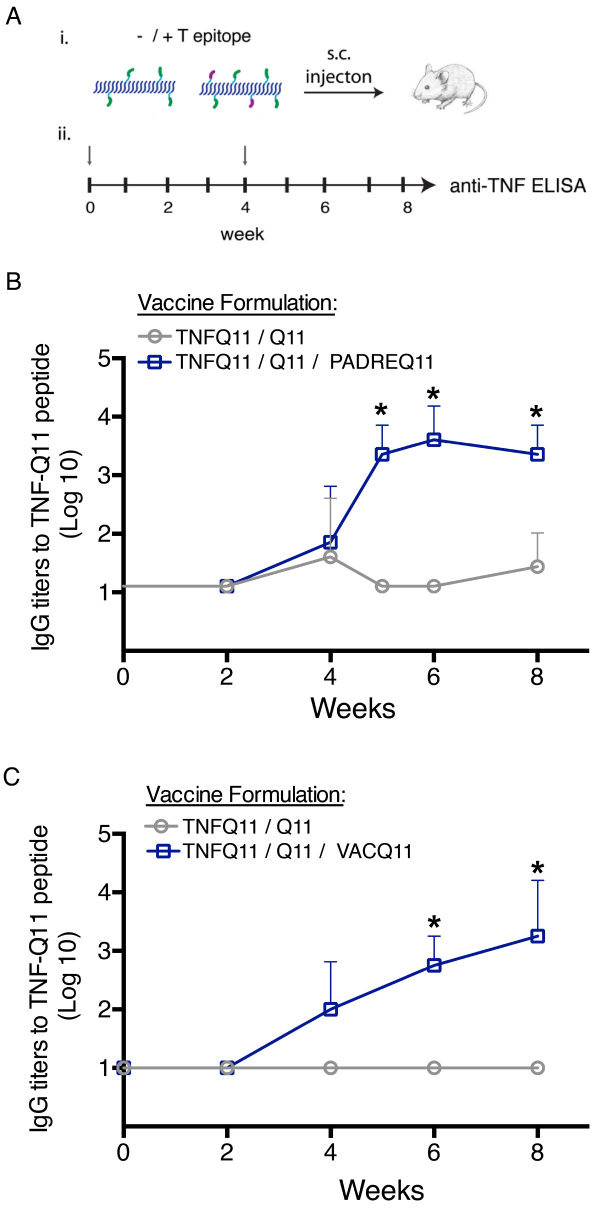


Figure 3.2 Foreign T cell help is required to break B cell tolerance to mouse TNF. A) Schematic of experiment. Mice were immunized subcutaneously (s.c.) with 200 nmol total peptide assemblies that did or did not contain a T cell epitope, and boosted on week 4 with a half dose (100 nmol) of the same peptide formulation. The induction of anti-TNF IgG antibodies was evaluated over time against TNFQ11 by ELISA from blood drawn at the indicated time points. B) TNF-specific IgG antibody responses were detected in the sera of mice immunized with peptide co-assemblies containing PADREQ11 T cell epitope (B) or VACQ11 T cell epitope (C). In either case, formulations lacking T cell epitopes (1 mM TNFQ11 / 1mM Q11) did not elicit measurable anti-TNF IgG antibodies. Lines represent means ± SD. * $p<0.05$, by one-way ANOVA followed by Tukey's multiple comparison test; n=5 per group.

To evaluate the specificity of the response we measured reactivity of the induced antibodies against TNF cytokine and PADRE or VAC peptides by ELISA. We found that the majority of antibodies bound to TNF cytokine or TNF peptide more than the foreign T cell epitopes (**Figures. 3.3**). In particular, no detectable antibodies were raised against PADRE (**Figure 3.3A**), and weak titers were raised against VAC (**Figure 3.3B**). Further, these responses were lost when a scrambled version of TNF_{4-23} was used as the B cell epitope (Shown and discussed during the protection experiments in figures 3.12-3.14)**.** The above results prompted us to evaluate also whether immunization with the peptide elicited antibodies that could cross-react with human TNF given the high sequence homology between mouse and human TNF (**Figure 3.4**). Cross-reactivity against human TNF was observed in serum samples from immunization for up six months and the anti-IgG titers were of similar magnitude compared to TNF peptide (**Figure 3.4A**). In a separate experiment, we tested whether cross-reactivity was observed in serum of mice immunized with formulations that contained different doses of PADREQ11 peptide, and found that responses were similar across doses against both TNF peptide and human TNF, except at the highest dose of PADRE tested of 0.75mM, with only one mouse out of four showing detectable anti-human TNF IgG titers (**Figure 3.4B**). Surface plasmon resonance (SPR) was performed to evaluate the binding quality of the polyclonal antibodies in the serum. Antibodies raised against TNF in the VAC-Q11 system had average K_{off} rates of 7.89×10^{-5}, similar to those of an anti-TNF monoclonal antibody (4.97×10^{-5}), and slower than the K_{off} rates for CFA-adjuvanted formulations (1.32×10^{-4}) (**Figure 3.5**). Overall, these results indicate that

self-assembling nanofibers co-presenting both self-derived B cell epitopes and foreign T cell peptides can overcome B cell tolerance and raise specific antibody titers without the use of supplemental adjuvants.

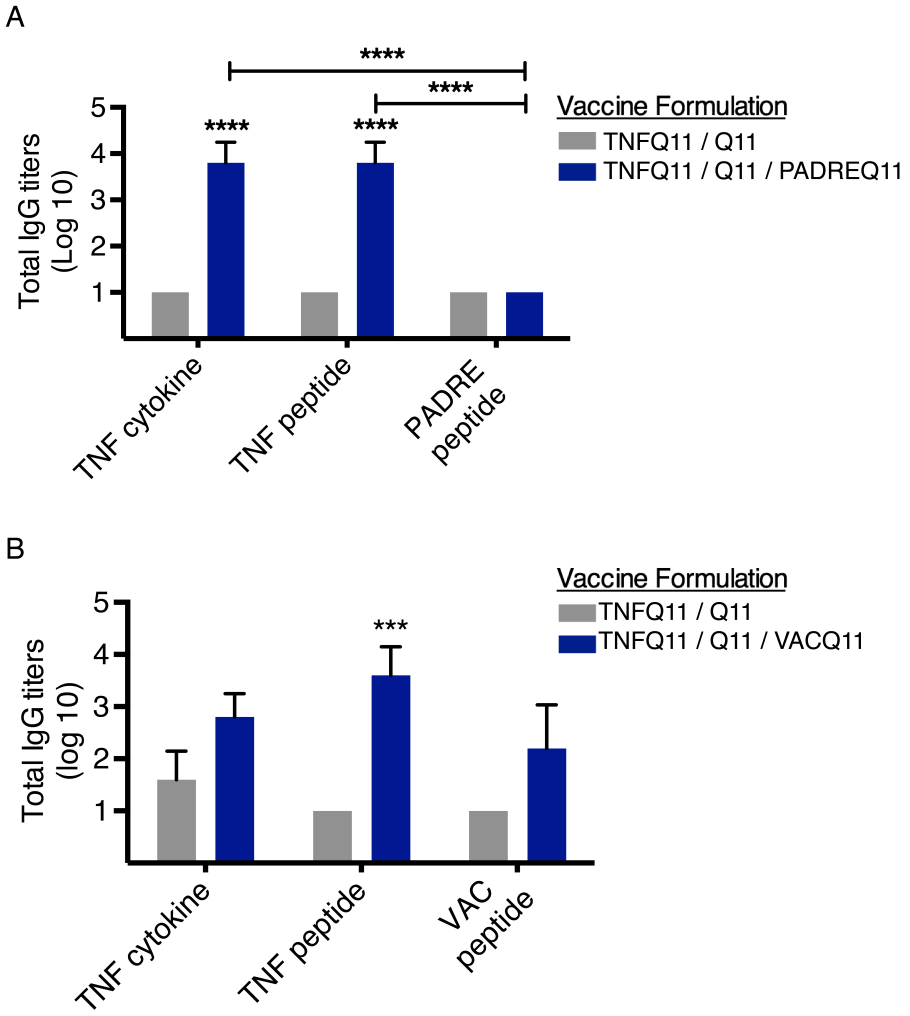


Figure 3.3 T-cell epitope-containing assemblies raised significant IgG responses against TNF peptide and TNF cytokine, with minimal antibody responses against the T-cell epitopes. IgG titers in sera from mice immunized with the indicated formulations was measured against TNF cytokine (mouse), TNF-derived B cell peptide, and T cell epitope peptides PADRE (A) or VAC (B) by ELISA. A) PADREQ11-containing co-assemblies elicited IgG that was similarly reactive and specific to TNF protein and TNF peptide. (B) VACQ11-containing co-assemblies elicited IgG that was more reactive against TNF peptide compared to TNF cytokine, but minimally cross-reactive against VAC peptide. Bars indicate means ± SD. * $p<0.05$, ** $p<0.01$, *** $p<0.001$, **** $p<0.0001$ by one-way ANOVA followed by Tukey's multiple comparison test; n=3-5 per group.

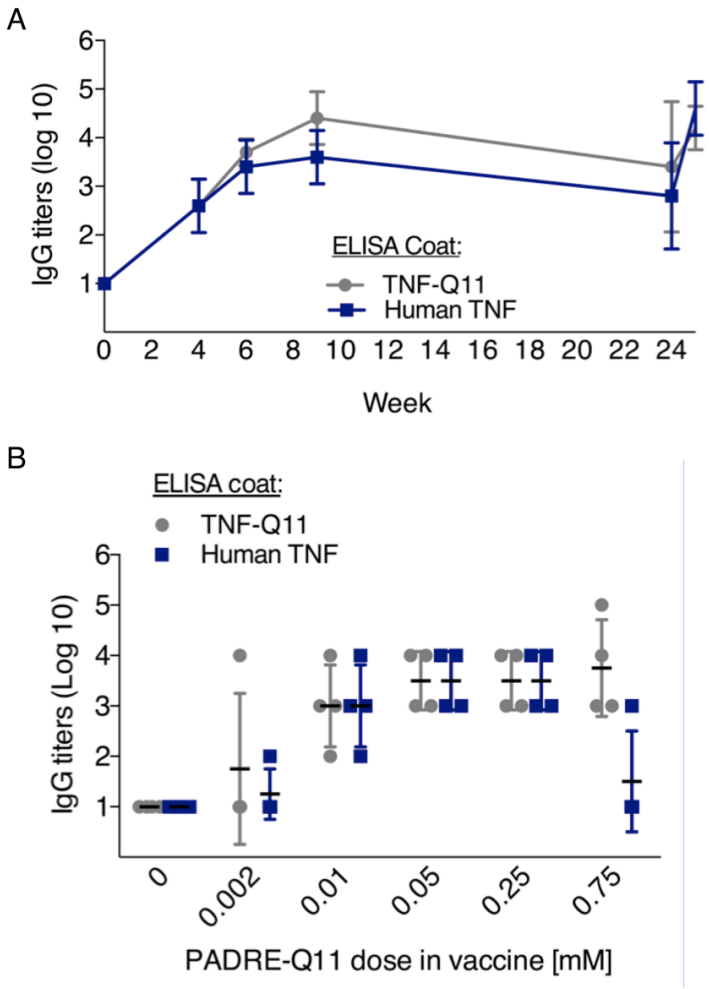


Figure 3.4 Vaccination using mouse TNF-derived antigen raises antibodies that also react with human TNF cytokine. A) Mice were immunized on week 0 with 200 nmol of peptide formulation 1 mM TNFQ11 / 0.95 mM Q11 / 0.05 mM PADREQ11, and boosted three times with 100nmol on weeks 4, 8, and 24. Blood was collected post-immunization at the time points indicated and the serum tested for human TNF-reactive IgG antibodies by ELISA. A) Similar IgG titers against human TNF compared to TNFQ11 peptide coated on ELISA plates were obtained at each time point suggesting that peptide immunization elicits cross-reactive antibodies. B) Mice were immunized with formulations consisting of a fixed dose of mouse TNF peptide and a variable dose of PADREQ11 adjusted to 2mM total peptide with Q11, as indicated, and the serum from week 8 was evaluated for human TNF IgG antibodies by ELISA. Increasing doses of T helper epitope PADRE resulted in an increase in IgG titers against TNFQ11 peptide with comparable cross-reactivity against human TNF cytokine, except at the highest PADREQ11 dose of 0.75mM, at which titers against human TNF cytokine were significantly reduced. For A and B, n= 4-6 mice per group.

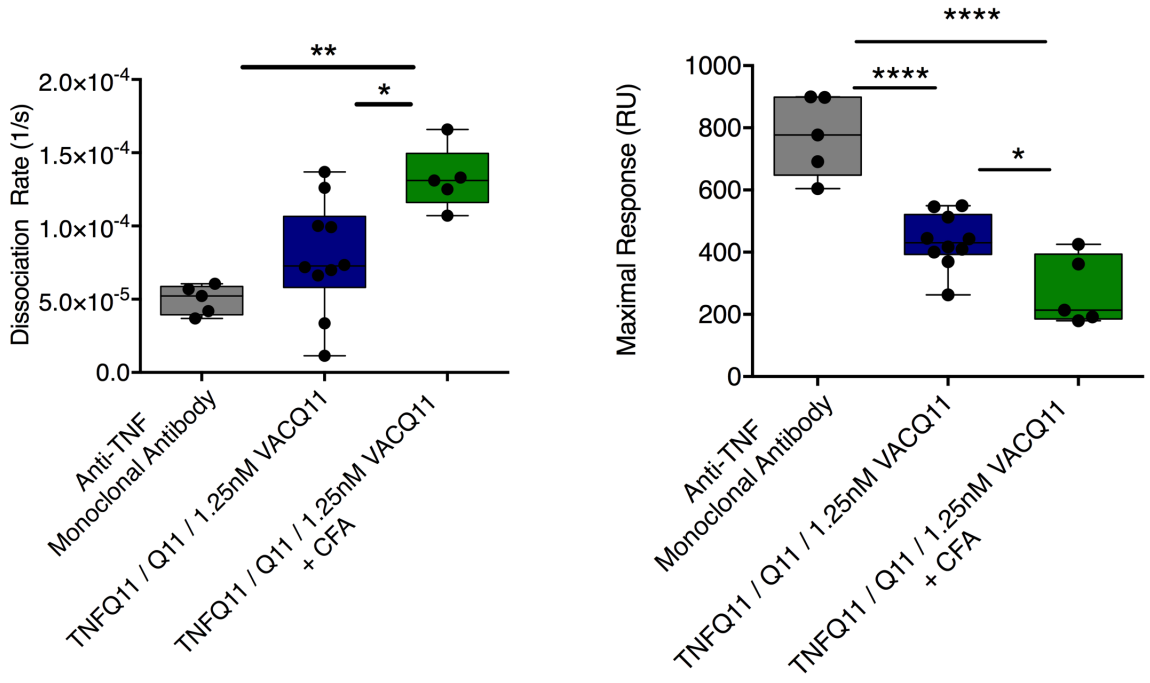


Figure 3.5 Serum polyclonal antibody binding measurements by SPR. Pooled serum from mice immunized with peptide assemblies with or without CFA adjuvant were tested for binding mouse TNF coated on SPR chip, and compared against a purified commercial anti-TNF monoclonal antibody (MP6-XT22 clone). For antibody binding, samples and monoclonal antibody were flowed for 5 min. After that, running buffer was flowed for 30 minutes to measure unbinding. Calculated dissociation rates (left) and maximal binding response units (right) before buffer was flowed over are shown. n=8 mice, 2 pooled samples of 4 mice each for TNFQ11 / Q11/ 1.25mM VACQ11 samples and n= 5 for TNFQ11 /Q11/ 1.25mM VACQ11 + CFA samples. Pre-immune pooled serum samples (n= 5) were used for background subtractions. Dissociation rates were more similar between those induced from peptide immunization without CFA and commercial anti-TNF monoclonal antibodies, and slower than dissociation rates for CFA-immunized serum.

Anti-TNF antibody responses were adjustable by titrating the T cell epitope content.

We expected that titrating the amount of PADREQ11 or VACQ11 in the nanofibers relative to the amount of TNF B-cell epitopes would influence the strength of the antibody response, based on previous observations of similar nanofibers formulated for a MRSA vaccine [89] To test PADREQ11, we made nanofibers where 50% of Q11 peptides were appended with the B cell epitope (TNFQ11), and the balance contained a mixture of PADREQ11 and unmodified Q11. The three peptides were mixed as dry powders prior to self-assembly in a process shown previously to produce mixed peptide fibrils [89,139]. The formulated nanofibers contained as little as 0.002mM (0.1%) PADREQ11 and as much as 0.75mM (37.5%) PADREQ11, a range spanning several hundred-fold differences in concentration. As PADREQ11 was titrated into the nanofibers, it progressively improved TNF-specific IgG titers up to formulations containing 0.05mM (2.5%) PADREQ11. Interestingly, increasing the PADREQ11 content beyond this diminished the antibody responses (**Figure 3.6A**). These results are consistent with the previous vaccination study using PADREQ11 in combination with another B cell epitope from *S. aureus* [89], which also showed a similar maximum titer at intermediate levels of PADRE incorporation. We next measured the titers of specific IgG phenotypes to determine whether PADRE affected the polarization of this response. PADRE-Q11

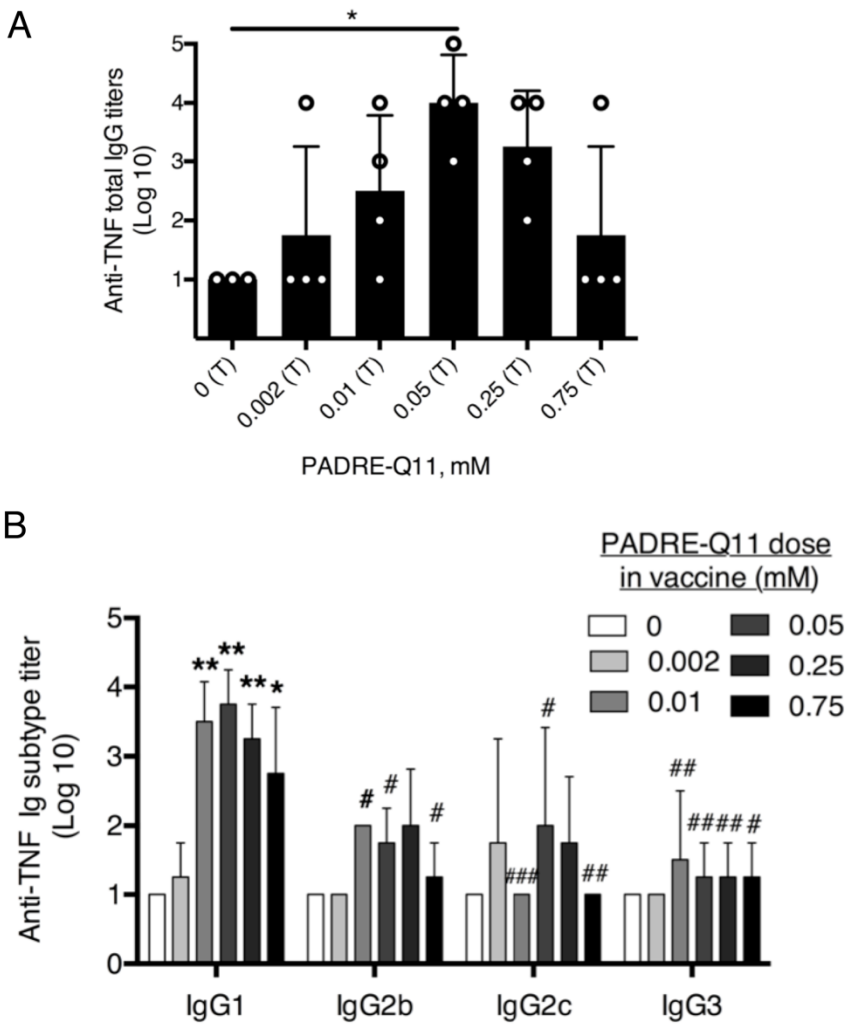


Figure 3.6 The strength and quality of anti-TNF antibody responses can be modulated by the amount of PADRE T cell epitope within nanofibers. C57BL/6 mice were immunized with vaccine formulations consisting of a fixed molar ratio of 1 mM TNFQ11 peptide (B-cell epitope) and progressively increasing amounts of PADREQ11 (T cell epitope), and adjusted for total peptide concentration with unmodified Q11. The amount of T cell epitope is shown in mM in the figure legends and axes. A) Nanofibers containing PADREQ11 showed a clear maximum in anti-TNF IgG titers at 0.05 mM PADREQ11 by ELISA. B) Immunization with PADRE-containing nanofibers elicited predominantly IgG1 isotype responses. Means ± SD shown. ND = not detected. * $p<0.05$, ** $p<0.01$ compared to 0mM PADREQ11; and # $p<0.05$ compared to the IgG1 response at the equivalent formulation by ANOVA followed by Tukey's multiple comparison test. n=4-6 mice per group, from 2 independent experiments.

appeared to favor IgG1 to a greater extent, although we were able to detect Ig2b and IgG2c in some mice (**Figure 3.6 B**).

To determine whether this bell-shaped curve is specific to PADRE or may be more generalizable to other T cell epitopes, we investigated a second CD4 T cell helper epitope from Vaccinia virus (QLVFNSISARALKAY, VAC). This epitope has not been tested before in peptide nanofiber vaccine formulations. We tested VACQ11 concentrations from 0.002mM (0.1%) up to 1.25mM (62.5%). Similar to PADREQ11 IgG responses, we found that antibody responses strengthened as the VACQ11 content increased, but unlike PADREQ11 the titers did not decrease at the highest VACQ11 doses (**Figure 3.7A**). To test if there were any differences in the quality of the antibodies, we also investigated the IgG subclasses raised by nanofibers containing VAC T cell epitope. Formulations with VACQ11 elicited IgG1, IgG2b, IgG2c, and IgG3 at more similar levels, compared to PADREQ11 (**Figure 3.7B**). These results demonstrated a simple method, adjusting the T cell epitope content in the nanofibers is able to tune the quantity and quality of anti-TNF antibodies.

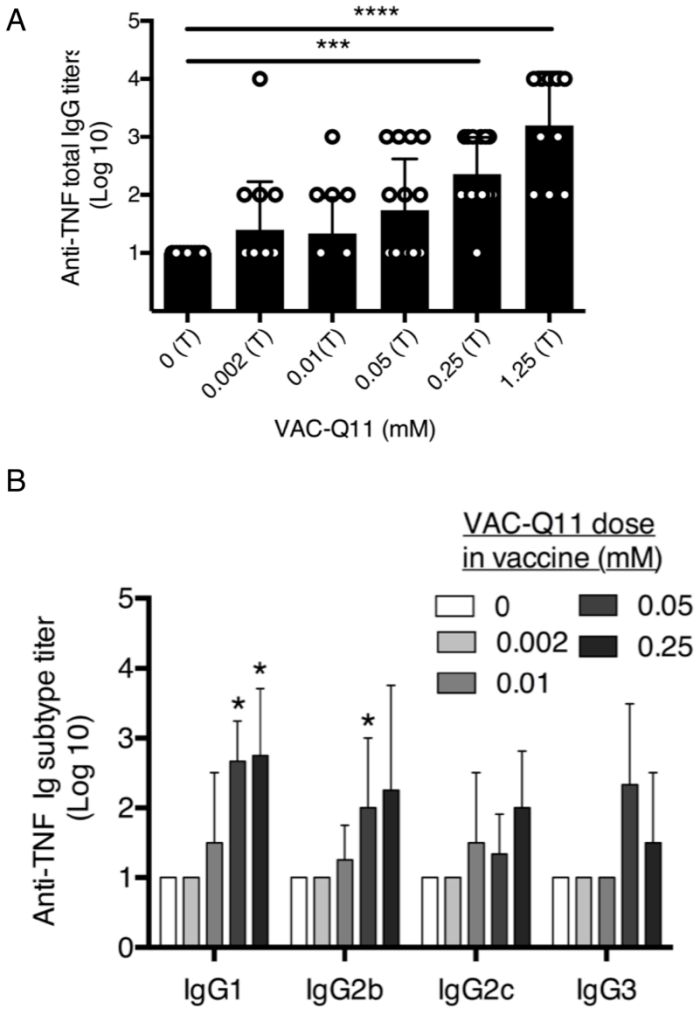


Figure 3.7 The strength and quality of anti-TNF antibody responses was modulated by the amount of VAC T cell epitope within nanofibers. C57BL/6 mice were immunized with vaccine formulations consisting of a fixed molar ratio of 1 mM TNFQ11 peptide (B-cell epitope) and progressively increasing amounts of VACQ11 (T cell epitope), and adjusted for total peptide concentration with unmodified Q11. The amount of T cell epitope is shown in mM in the figure legends and axes. A) Nanofibers containing VACQ11 showed a positive correlation between the magnitude of anti-TNF cytokine IgG titers and dose of VAC T cell epitope. B) Immunization with VAC-containing nanofibers elicited IgG responses that were more balanced between IgG1, IgG2b, IgG2c, and IgG3 (d). Means ± SD shown. ND = not detected. * $p<0.05$, ** $p<0.01$, *** $p<0.001$ ****$p<0.0001$ compared to 0mM PADREQ11; and # $p<0.05$ compared to the IgG1 response at the equivalent formulation by ANOVA followed by Tukey's multiple comparison test. For A, n= 9-15 mice per group and for B, n= 5 per groups from 3 and 2 independent experiments, respectively.

Cell-mediated immunity depended on T cell epitope concentration and was focused on the exogenous T cell epitopes, not the TNF component.

A significant potential limitation of active immunization strategies for blocking TNF-mediated inflammation is the possibility of inducing cell-mediated immunity against TNF-expressing cells [111,112]. TNF has important functions in host defense and secondary lymphoid organization, so cell-mediated immunity could lead to increased levels of inflammation, tissue damage, immunosuppression, or potential autoimmunity [104,105]. We hypothesized that using a foreign T cell epitope (PADRE or VAC) would minimize T cell responses to endogenous targets yet still facilitate therapeutic antibody titers against the desired B cell epitope of TNF. To test this, we collected draining lymph node cells from immunized mice and investigated how T cell epitope dose influenced the strength and polarization of the T cell response using ELISPOT for IL4 and IFNγ production. T cell responses to PADRE depended on the dose of the T cell epitope, in a similar manner to the dose-responsiveness of the antibody titers. The responses were highly focused on the foreign T cell epitope and not the TNF B cell-derived antigen, which elicited minimal IL-4 or IFNγ spots across all formulations that were statistically equivalent to unstimulated controls (**Figure 3.8**). The overall PADRE-specific phenotype was Th2-dominant, with considerably more IL4-secreting cells **(Figure 3.8A)** than IFNγ-secreting cells **(Figure 3.8B)** at each peptide dose increment studied. In fact, only we were only able to detect IFNγ production at the lowest doses of 0.002 mM PADRE and 0.01 mM PADRE (**Figure 3.8B**). Overall, T cell cytokine

production was maximized at 0.002mM dose of PADRE and decreased thereafter, with 0.25mM PADRE eliciting minimal IL-4 production, and 0.75mM PADRE completely ablating the production of both IL-4 and IFNγ cytokines. Further, we found that the doses that most stimulated B cell/antibody responses did not necessarily correspond with those eliciting the strongest T cell responses. Interestingly, the optimal dose for antibody responses of 0.05mM PADRE was associated with the presence of moderate levels of IL-4 and the absence of any IFNγ-production, which correlate with our prior findings that T_{FH} cells peak at this dose and are mostly associated with providing B cell help for antibody production.

Compared to PADRE, T cell responses to VAC-containing nanofibers were more balanced between IL4 and IFNγ (**Figure 3.9**)**,** and in correspondence with VAC formulations' broader IgG antibody isotype responses (**Figure 3.7B**). Similarly, the responses elicited were dose-dependent with the mid-dose of 0.05mM eliciting maximal IL-4 and IFNγ spots, a dose that was higher than the optimal dose for PADRE (**Figure 3.9A**). In stark contrast to PADRE, we were able to detect weak IL-4 responses that were at or below 50 spots per 250,000 cells after stimulation with TNF B cell epitope. These responses were statistically significant at 0.05mM dose of VAC but decreased and were statistically comparable to unstimulated controls at 0.25mM and 1.25mM doses of VAC for IL-4 production (**Figure 3.9A**). No significant IFNγ production was observed after TNF B cell peptide stimulation across all VAC-containing formulations (**Figure 3.9B**). Additionally, the amount of VAC T cell epitope necessary for eliciting

maximal T cell responses was different than the amount eliciting maximal antibody responses, with 0.05 mM eliciting maximal T cell responses (both IL4 and IFNγ and 1.25 mM eliciting maximal antibody titers). In contrast to PADRE, we found formulations which elicited moderate VAC-specific Th1 responses at 0.05mM and 0.25mM VAC (**Figure 3.9B**). In agreement with PADRE ELISPOT data, increasing the doses of VAC in the vaccines resulted in a diminished T cell response, suggesting that higher content would similarly ablate cytokine production. Thus, by creating a range of nanofibers with varying epitope contents, different combinations of T cell responses and antibody responses can be generated, and from these options specific attractive formulations can be selected for advancement into further development depending on the specific therapeutic application or target. Moving forward, we selected combinations of antibody and T cell responses most likely to produce neutralizing anti-TNF antibodies without significant T cell responses against the TNF-derived B cell epitope.

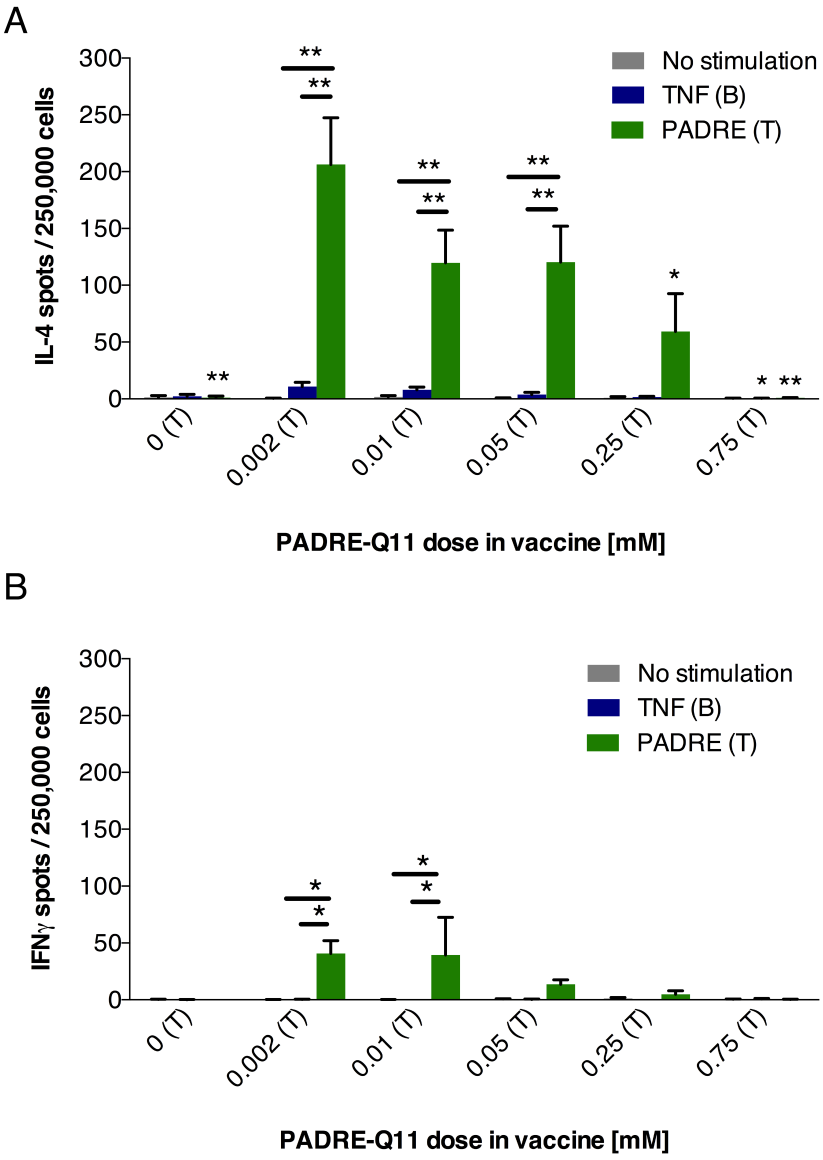


Figure 3.8 PADRE-containing co-assembled nanofibers elicited dose-dependent IL-4/Th2 dominated T-cell responses against the foreign T cell epitope PADRE, but not the endogenous TNF B-cell epitope. Cytokine-secreting cells from mice immunized with TNFQ11 combined with the indicated doses of PADREQ11 were quantified ex vivo by ELISPOT after re-stimulation of lymph node cell suspensions with single peptides. A) IL-4/Th2 or B) IFN-γ/Th1 spots were counted after stimulation with media (no stimulation), TNF (B epitope) or PADRE (T epitope.) Bars correspond to mean spots per 250,000 cells ± SD. n= 4-6 mice per group from 2 independent experiments. *p<0.1, **p<0.05, ***p<0.01 by ANOVA with Tukey's comparison test. Asterisks not paired between groups indicate differences from highest response group (0.002mM PADREQ11 formulation).

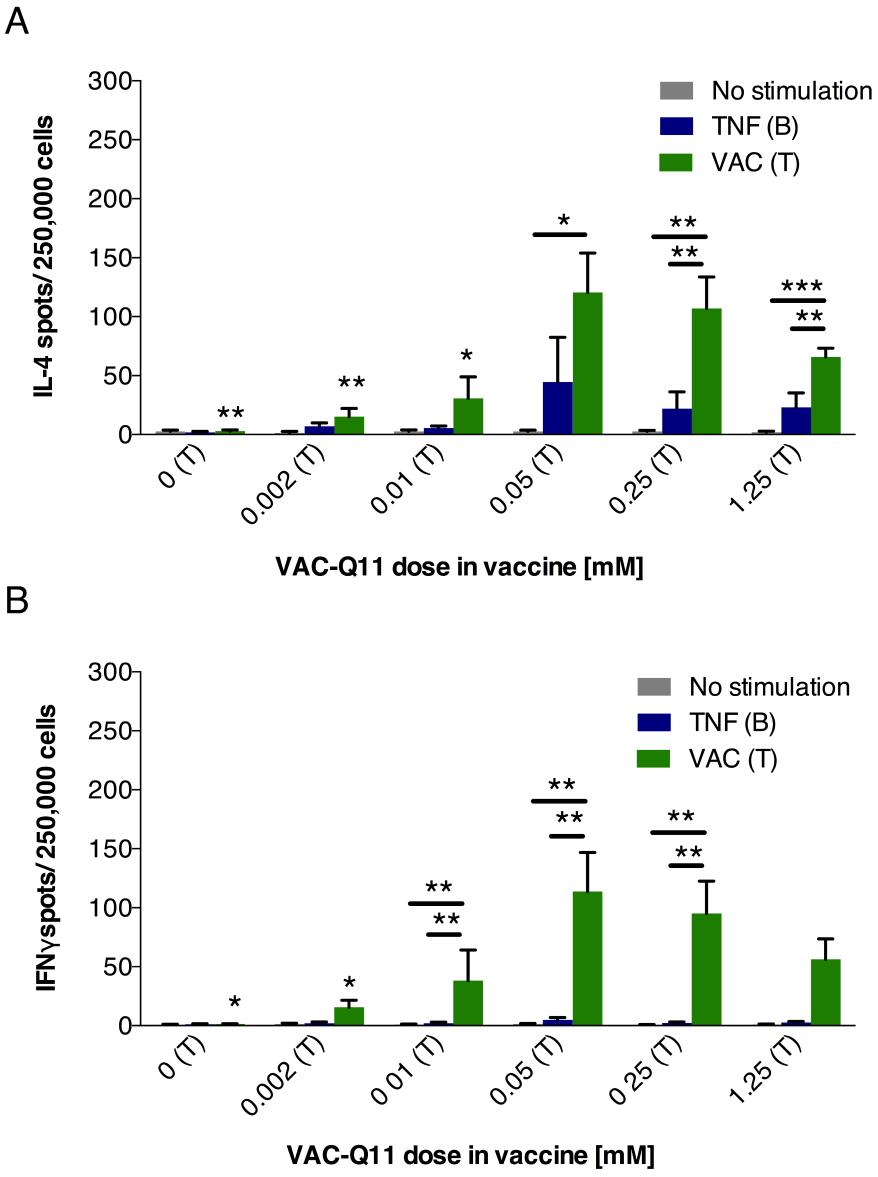


Figure 3.9 VAC-containing co-assembled nanofibers elicited dose-dependent, balanced Th1/Th2 responses focused against the foreign T cell epitope VAC, not the endogenous TNF B-cell epitope. Cytokine-secreting cells from mice immunized with TNFQ11 combined with the indicated doses of VACQ11 were quantified ex vivo by ELISPOT after re-stimulation of lymph node cell suspensions with single peptides. A) IL-4/Th2 or B) IFN-γ/Th1 spots were counted after stimulation with media (no stimulation), TNF (B epitope) or PADRE (T epitope.) Bars correspond to mean spots per 250,000 cells ± SD. n= 4-6 mice per group from 2 independent experiments. *p<0.1, **p<0.05, ***p<0.01 by ANOVA with Tukey's comparison test. Asterisks not paired between groups indicate differences from highest response group (0.05mM VACQ11 formulation).

Vaccination protected from TNF-mediated inflammation in mice.

Our next goal was to evaluate if anti-TNF active immunotherapy with peptide assemblies provided protection in a mouse model of TNF-mediated inflammation. We used a model in which intraperitoneally delivered lipopolysaccharide (LPS) induces shock-like symptoms, including weight loss, hypothermia, and death, with mice removed from the study upon reaching predetermined cutoffs for weight and temperature [144-146]. In the first set of experiments, we challenged mice previously immunized with PADRE-containing assemblies. We tested two formulations of PADRE that differed only in the quantity of TNF-derived B cell epitopes (1mM and 0.2mM) but otherwise had the optimized formulation of T cell epitope of 0.05mM. Hence, these formulations differed in their B:T epitope molar ratios. Both formulations raised statistically equivalent levels of anti-TNF IgG antibody titers in immunized mice (**Figure 3.10A**) We then injected immunized and unimmunized control with i.p. LPS. Without vaccination, all control mice injected with LPS succumbed within 12 hours by exceeding the predetermined cutoff for hypothermia, 32°C, whereas immunized mice recovered to baseline temperatures approximately 48h post-challenge (**Figure 3.10B**). We also measured the percentage of mice that recovered from LPS-induced symptoms over 72h. While naïve control mice succumbed by 12h, immunization protected mice by 90% (with 1mM TNFQ11: 0.05 mM PADREQ11: 0.95mM Q11) and 100% (0.2mM TNFQ11: 0.05mM PADREQ11: 1.75mM Q11) (**Figure 3.10C**). Body temperatures (**Figure 3.11**) and weights (**Figure 3.12**) of individual mice are also included and show that immunized mice experienced neither

extreme hypothermia nor extreme weight loss during the 72-hour monitoring period of the study.

We then tested protection by VACQ11-containing assemblies in this mouse model (**Figure 3.13**) and included additional controls: formulations lacking T cell epitopes or those with a scrambled B cell epitope. Neither of these formulations raised any detectable anti-TNF IgG titers. In contrast, immunization with peptide assemblies elicited IgG titers of 10^3 and incorporation of CpG into the peptide assemblies elicited the highest titers of anti-TNF antibodies in this study (**Figure 3.13A**). After LPS injection, formulations lacking T cell epitopes or those with scrambled B cell epitope conferred no protection, and experienced indistinguishable hypothermia compared to unimmunized mice injected with LPS and all the mice in these three groups succumbed within the first 12 hours of the experiment (**Figure 3.13B**). Paradoxically, incorporation of CpG into the peptide assemblies elicited the highest titers but only partial protection, with only 40% surviving the LPS challenge (**Figure 3.13C**) a marked diminishment compared to the fully immunized mice, which exhibited 90% protection. Individual body temperature (**Figure 3.14**) and weights (**Figure 3.15**) show the similar kinetics in the symptoms experienced by the controlled group immunized with formulations lacking T cell epitope or a scramble B cell epitope. Moreover, the traces for body temperature of CpG-immunized group showed faster kinetics in 4 out of 6 mice, perhaps by exacerbating the production of TNF or other inflammatory mediators. These surprising results indicated that high antibody titers are not the only requirement for protection, that other factors influencing the phenotype of the immune response can impact the

therapeutic efficacy of active immunotherapies, and that the unadjuvanted nature of peptide nanofibers has advantages over formulations containing CpG in this model. Notably, these experiments were repeated in two different locations (Univ. Chicago and Duke University), in different animal facilities, and by different researchers (CMS and YW), indicating the robustness of the finding.

We further compared vaccine formulations adjuvanted with CpG and without CpG. To explore these phenotypic considerations further, we compared the Th1/Th2 bias between unadjuvanted formulations and those containing CpG (**Figure 3.16**). Our results indicate the both formulations elicit modest levels of IL-4 producing cells, yet the CpG group had an augmented number of IFNγ spots, suggesting that the addition of CpG strongly biased the response toward Th1 (**Figure 3.16A**). Specifically, the ratio of IFNγ-producing cells to IL4-producing cells in ELISPOTs was around 0.2 for unadjuvanted nanofibers and around 5.0 for adjuvanted nanofibers, a difference of a factor of 25 (**Figure 3.16B**). Upon sacrifice, circulating TNF values were also measured, showing that mice with poor enough clinical measurements to warrant removal from the study had significantly elevated circulating TNF, whereas mice that recovered returned their TNF levels to baseline (**Figure 3.16C**). Further study will be required to ascertain whether a causal relationship exists between this observed Th2 phenotype and the protective ability of peptide nanofiber vaccines, but at this point the correlation is striking.

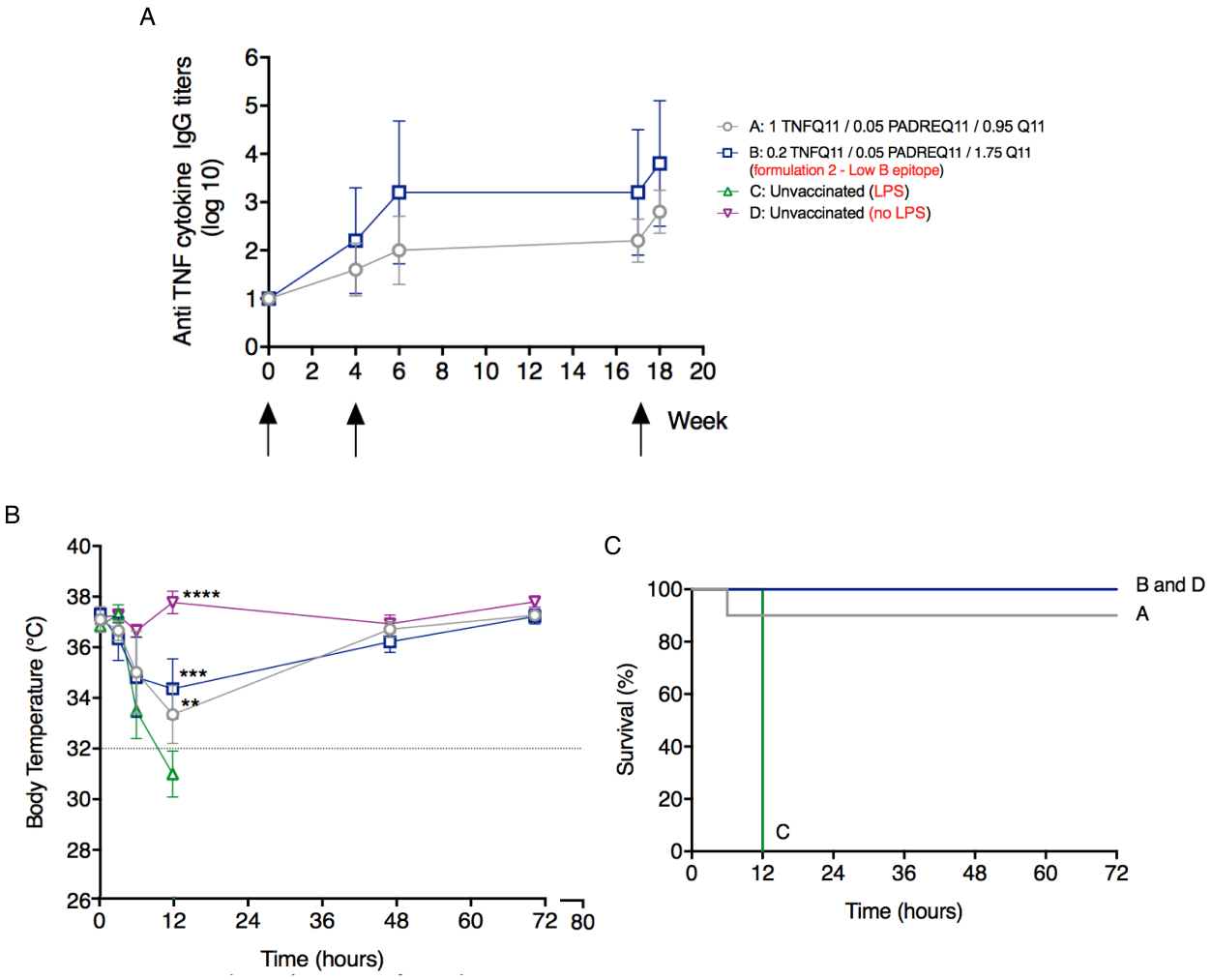


Figure 3.10 Immunization with PADREQ11/TNFQ11/Q11 peptide nanofibers protects mice from LPS-induced inflammation. Mice were challenged with 10mg/kg of O55:B5 LPS from *E. coli.* to evaluate protection from TNF-mediated inflammation induced by LPS. A) Immunized mice received a primary immunization of 200nmol and 2 boosts with 100 nmol of peptide nanofibers (arrows). Tested formulations: A= 1 mM TNFQ11 / 0.95 mM Q11/ / 0.05mM PADREQ11, B = 0.2 mM TNFQ11 / 1.75 mM Q11/ 0.05 mM PADREQ11. A) Anti-TNF IgG titers were not statistically different between the two tested doses of TNF-derived B cell epitope in the vaccine formulation prior to challenge. B) Body temperature and C) survival after LPS challenge was monitored for 72 hours. Significant protection was attained with formulations A and B, respectively, both of which rescued from LPS-induced death (Group C) and exhibited similar survival by 72h to unimmunized mice mock-injected with PBS buffer (group D). n: group A=10; B/C =5; n group D=4. **p<0.01, ***p<0.001, ****p<0.0001 by one-way ANOVA with Tukey's post hoc test.

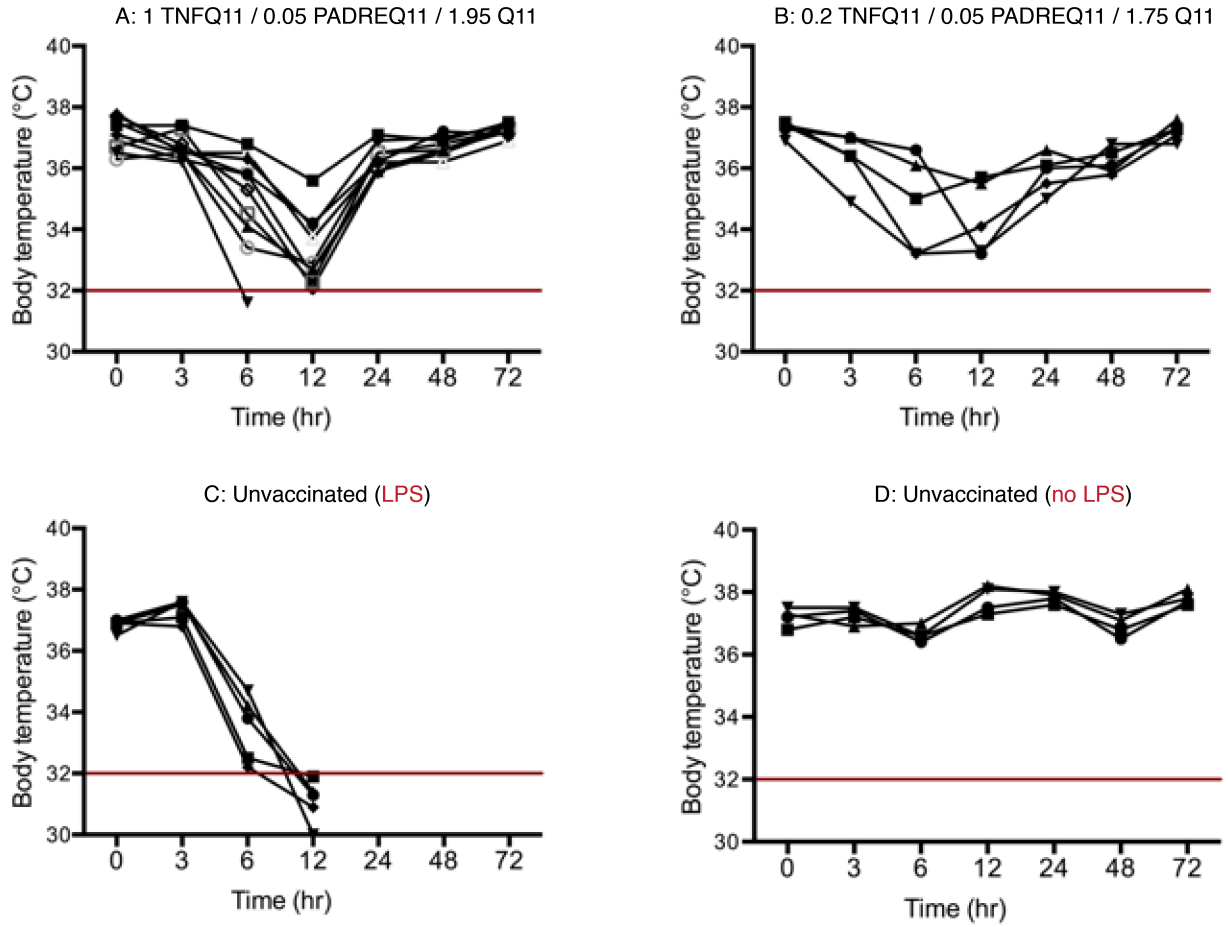


Figure 3.11 Individual body temperature traces after LPS challenge of PADRE-immunized mice. Vaccinated and unvaccinated controls were challenged intraperitoneally one week after their last boost with 10mg/kg LPS (Groups A-C) or mock-injected with sterile PBS (Group D). Body temperature was monitored periodically for 3 days for lethal hypothermia at 32 degrees (dotted line), at which point mice were euthanized. Tested formulations included: A) 1 mM TNFQ11 / 0.95 mM Q11 / 0.05 mM PADREQ11; B) 0.2 mM TNFQ11 / 1.75 mM Q11 / 0.05 mM PADREQ11. Control groups including: C) Unvaccinated mice injected with LPS. D) Unvaccinated mice mock-injected with PBS. In the absence of LPS, body temperature is unaffected over the course of the study (group D). In contrast, unimmunized mice injected with LPS exhibited significant hypothermia by 12 hours (Group C), while mice vaccinated with peptide nanofibers exhibit moderate hypothermia that resolves within 24 hours. n for A/B =10 mice, n for C = 5, n for D= 4.

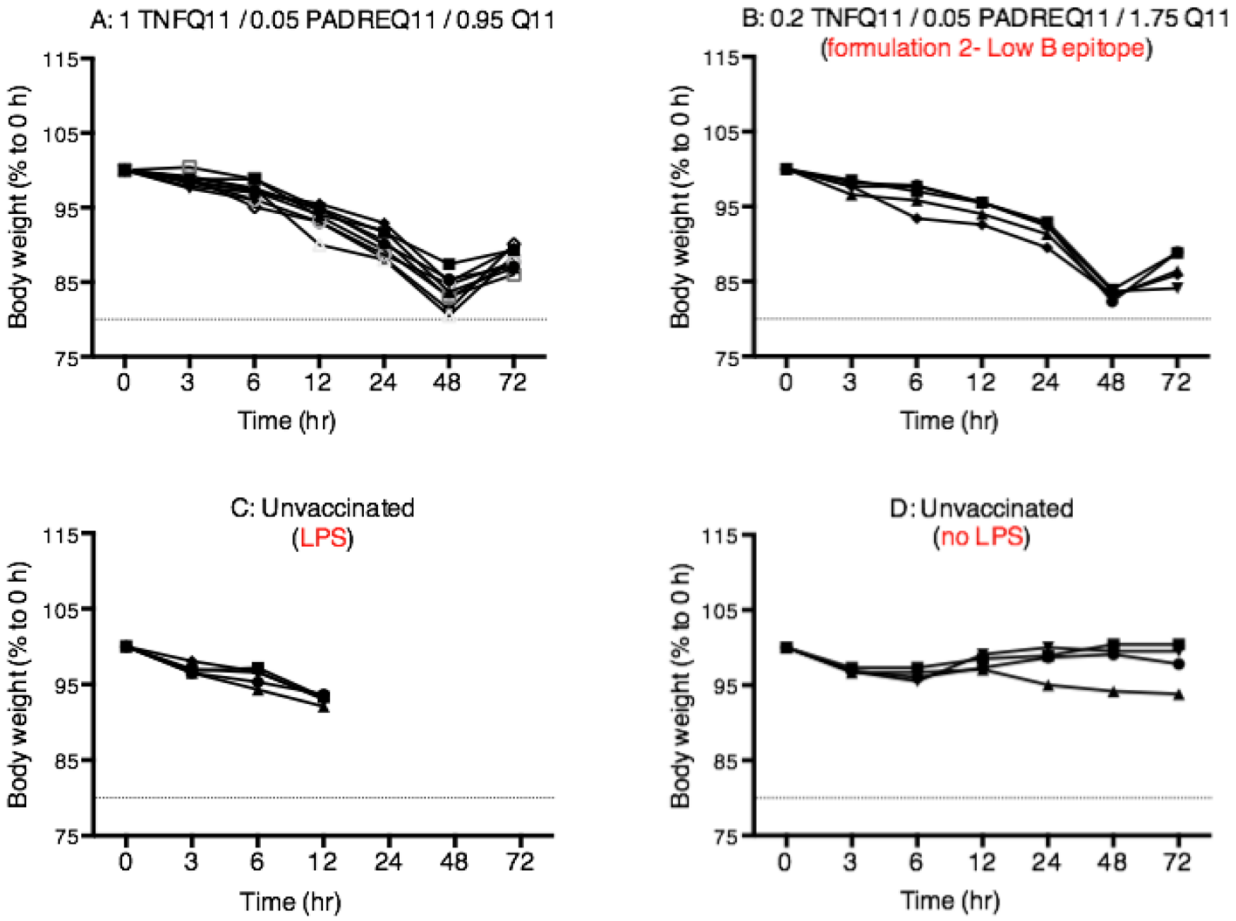


Figure 3.12 Individual weight traces after LPS challenge of PADRE-immunized mice. Vaccinated and unvaccinated controls were challenged i.p one week after their last boost with 10mg/kg LPS (Groups A-E) or mock-injected with sterile PBS (Group F). Tested formulations included: A) 1 mM TNFQ11 / 0.95 mM Q11 / 0.05 mM PADREQ11; B) 0.2 mM TNFQ11 / 1.75 mM Q11 / 0.05 mM PADREQ11. Control groups including: C) Unvaccinated mice injected with LPS. D) Unvaccinated mice mock-injected with PBS. Groups C succumbed to LPS before reaching the end of the study. Groups immunized with TNF / Q11 / PADREQ11 nanofibers were similarly protected from extreme weight loss (>20% baseline) by 72h to untreated group (group D). n for A/B =10 mice, n for C= 5 mice, n for D= 4 mice.

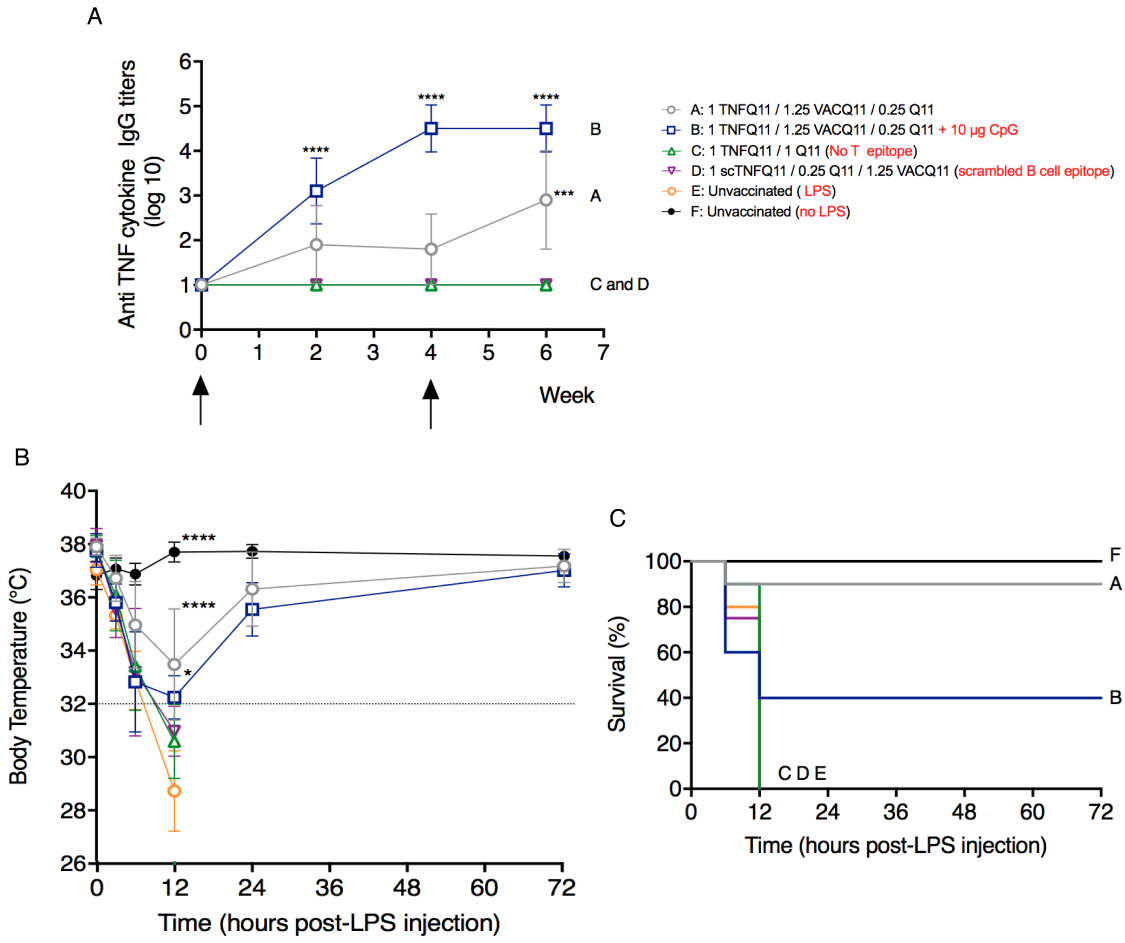


Figure 3.13 Protection from LPS in VAC-containing nanofibers with and without CpG adjuvant, or with a scrambled TNF sequence. The formulations tested included: A) 1 mM TNFQ11 / 0.25 mM Q11 / 1.25 mM VACQ11; B) 1 mM TNFQ11 / 0.25 mM Q11 / 1.25 mM VACQ11, adjuvanted with 10μg CpG; and control groups C) Formulation without T cell epitope consisting of 1 mM TNFQ11 / 1 mM Q11; D) Scrambled TNF B cell epitope formulation consisting of 1 mM scrambled TNFQ11 / 0.25 mM Q11 / 1.25 mM VACQ11. E) Unvaccinated mice injected with LPS. F) Unvaccinated mice mock-injected with PBS. A) Anti-TNF cytokine titers were evaluated by ELISA prior to LPS challenge. Mice immunized immunized with VACQ11-containing nanofibers VACQ11 exhibited anti-TNF IgG titers 6 weeks. In the presence of CpG, antibodies are induced within 2 weeks and are of increasing magnitude. B) Body temperature and C) survival after LPS challenge was monitored for 72 hours. CpG-adjuvanted formulations were protective albeit to a lower degree compared to unadjuvanted nanofiber formulations. Control formulations that did not contain a T cell epitope or contained a scrambled TNF sequence did not protect against LPS challenge. N for A, B, C = 10; D, E= 5; F= 4. $p<0.05$, $***p<0.001$, $****p<0.0001$ by one-way ANOVA with Tukey's post hoc test.

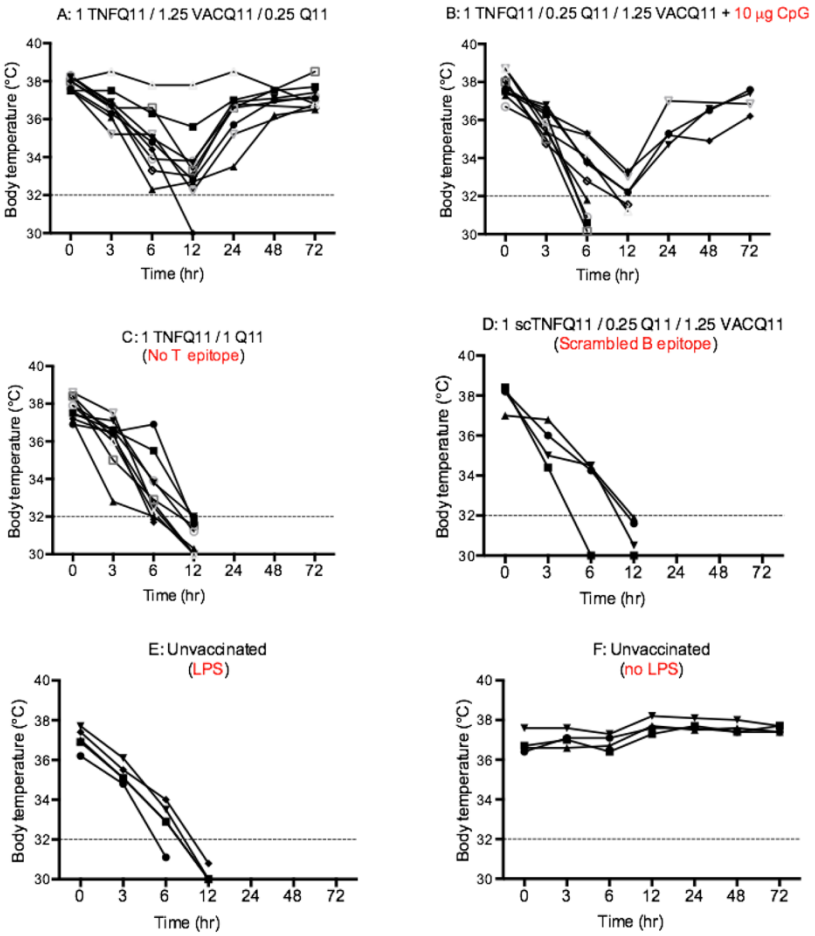


Figure 3.14 Individual body temperature traces after LPS challenge of VAC-immunized mice. Vaccinated and unvaccinated controls were challenged i.p one week after their last boost with 10mg/kg LPS (Groups A-E) or mock-injected with sterile PBS (Group F). Body temperature was monitored periodically for 3 days for lethal hypothermia at 32 degrees (dotted line), at which point mice were euthanized. Tested formulations included: A) 1 mM TNFQ11 / 0.25 mM Q11 / 1.25 mM VACQ11; B) 1 mM TNFQ11 / 0.25 mM Q11 / 1.25 mM VACQ11 adjuvanted with 10μg CpG; Control groups included C) Formulation without T cell epitope consisting of 1 mM TNFQ11 / 1 mM Q11; D) Scrambled TNF B cell epitope formulation consisting of 1 mM scrambled TNFQ11 / 0.25 mM Q11 / 1.25 mM VACQ11; E) Unvaccinated mice injected with LPS; F) Unvaccinated mice mock-injected with PBS. In the absence of LPS, body temperature was unaffected over the course of the study (group F). In contrast, mice that were unimmunized or immunized with sub-optimal formulations and then injected with LPS exhibited significant hypothermia by 12 hours (Groups C-E). Mice vaccinated with optimized unadjuvanted peptide nanofibers exhibited better protection compared to mice immunized with peptide nanofibers adjuvanted with CpG as well as unimmunized mice. n for A-C =10 mice, n for D: n for D/E= 5 mice, n for F= 4 mice.

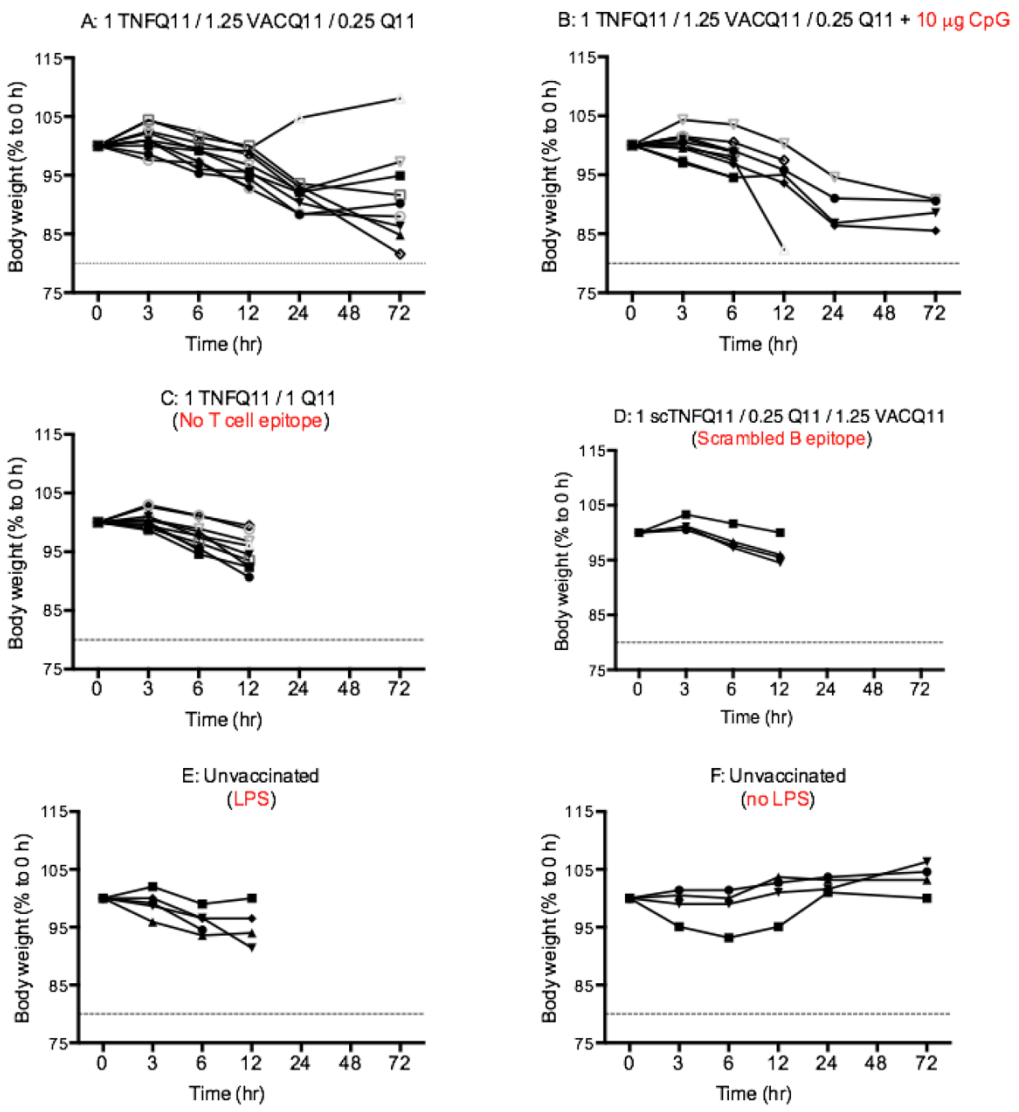


Figure 3.15 Individual weight traces after LPS challenge of VAC-immunized mice. Vaccinated and unvaccinated controls were challenged i.p one week after their last boost with 10mg/kg LPS (Groups A-E) or mock-injected with sterile PBS (Group F). Tested formulations included: A) 1 mM TNFQ11 / 0.25 mM Q11 / 1.25 mM VACQ11; B) 1 mM TNFQ11 / 0.25 mM Q11 / 1.25 mM VACQ11, adjuvanted with 10μg CpG; Control groups including: C) Formulation without T cell epitope consisting of 1 mM TNFQ11 / 1 mM Q11. D) Scrambled TNF B cell epitope formulation consisting of 1 mM scrambled TNFQ11 / 0.25 mM Q11 / 1.25 mM VACQ11. E) Unvaccinated mice injected with LPS. F) Unvaccinated mice mock-injected with PBS. Groups C-E succumbed to LPS before reaching the end of the study. Better protection was observed for mice immunized with VAC-containing formulations that did not contain CpG, which did not reach the endpoint for extreme weight loss of >20% baseline. n for A-C =10 mice, n for D/E= 5 mice, n for F= 4 mice.

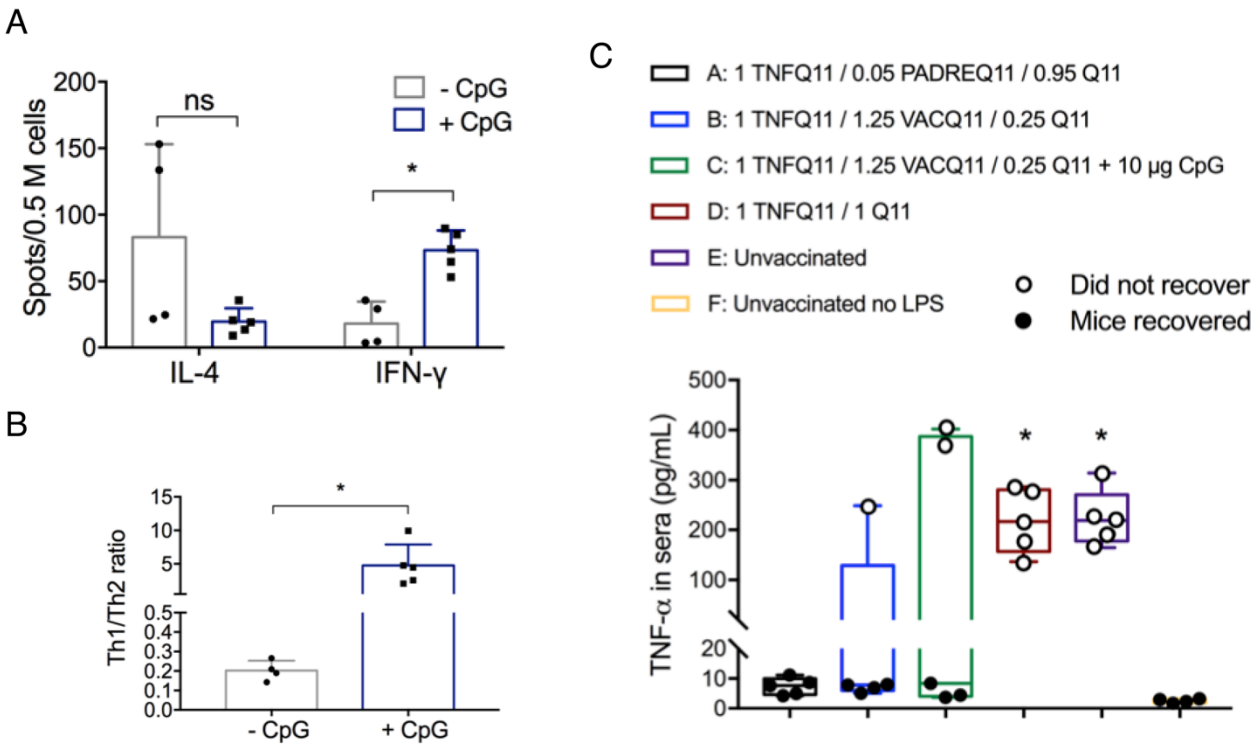


Figure 3.16 CpG adjuvantation of optimized peptide nanofibers resulted in a robust Th1 polarization of the T epitope-specific T cell cytokine response.
A) Mice were injected with 1mM TNFQ11 / 0.25 Q11 / 1.25 mM VACQ11 peptide nanofibers formulated without or with CpG, and VAC T cell peptide responses were assessed one week after the last boosting immunization by ELISPOT. In the absence of CpG (-CpG), an IL-4 skewed cytokine response was elicited by peptide assemblies. In contrast, the presence of CpG (+CpG) adjuvant shifted the T cell response toward significant IFNγ production. B) Th1/Th2 ratio calculation from the T cell ELISPOT results depict a robust shift in T cell polarization from Th2 in self-adjuvanted peptide nanofibers to Th1 in peptide nanofibers adjuvanted with CpG. C) TNF cytokine levels were examined in the mice at either the time of death (for mice that succumbed to LPS) or at endpoint of the study at 72 hours (for mice that survived). TNF ELISA results indicated a significantly higher TNF concentration in the blood of mice that did not recover (clear circles) compared to mice that recovered after LPS challenge. CpG adjuvantation increased the proportion of mice that did not recover, which also exhibited the highest levels of systemic TNF. Significance was assessed by an unpaired T-test (A, B) and one-way ANOVA. N=5 mice per group.

The ability to clear infections was not impaired by peptide nanofiber vaccination

We hypothesized that vaccination with TNF/VAC nanofibers would not diminish the ability to clear infections because the B cell epitope chosen was previously found to raise antibodies against soluble TNF, not transmembrane TNF [128,132]. An inadvertent targeting of transmembrane TNF, which is expressed on activated macrophages and lymphocytes could lead to destruction of these cells and an impaired ability to respond to infection [103,132]. Indeed, mice receiving 0.5mg of highly purified anti-mouse TNF monoclonal antibody (clone MP6-XT22) that were challenged intraperitoneally with 1×10^5 CFU of *Listeria* showed elevated CFUs in their livers and spleens 48 hours later (**Figure 3.17A**). In contrast, mice immunized with TNFQ11/VACQ11 showed CFUs indistinguishable from unimmunized mice or those that had received non-functional nanofibers lacking the VAC T-cell epitope (**Figure 3.17B**). These findings indicated that TNF/VAC nanofibers did not compromise the ability of the animals to suppress *Listeria* infectivity, even when they raised high titers of anti-TNF antibodies (Titers of 4 were raised by the mice immunized with TNFQ11/VACQ11 nanofibers in this experiment, **Figure 3.16C**).

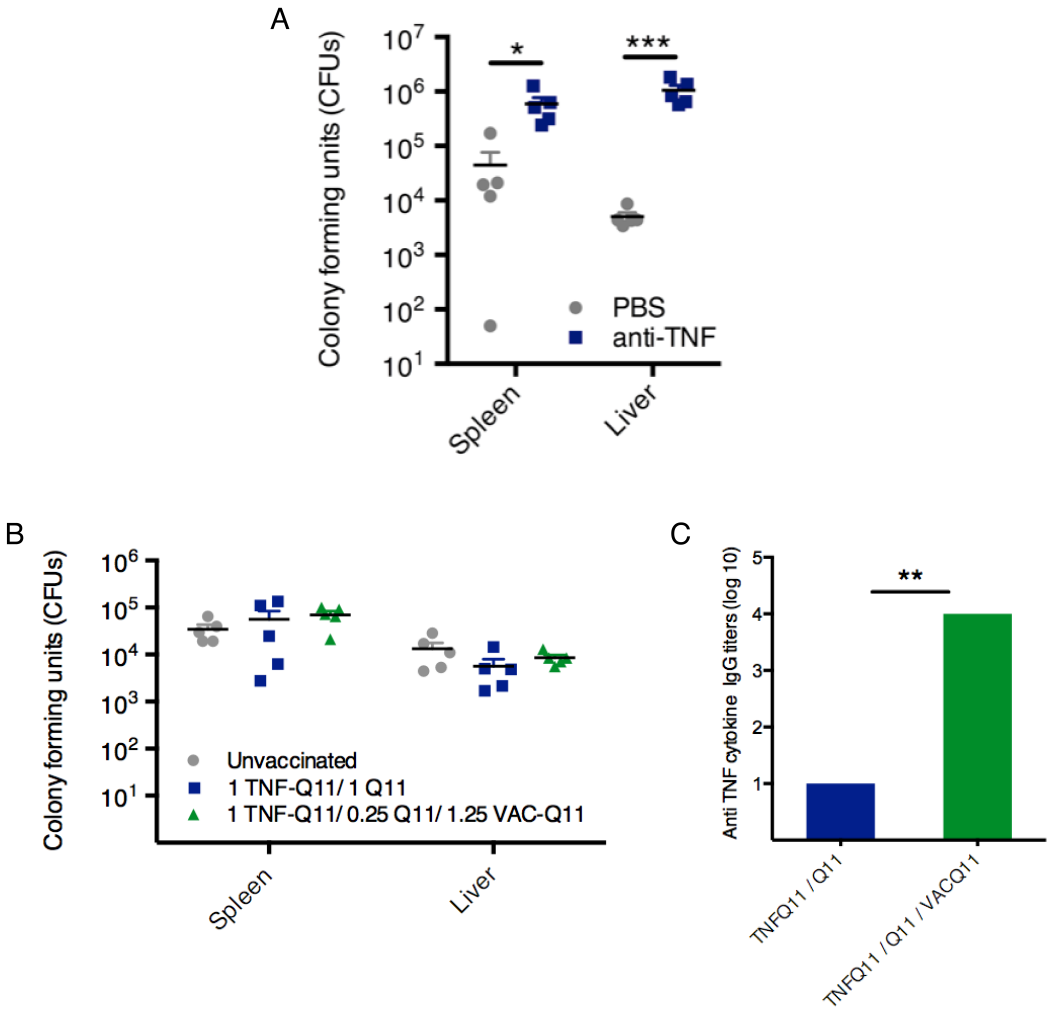


Figure 3.17. Vaccination with peptide assemblies did not increase susceptibility to infection by *Listeria monocytogenes*. A) Unimmunized mice were injected i.p. with 0.5 mg of anti-TNF antibody or PBS buffer 3 hours prior to i.p challenge with 1 x 10^5 dose of *Listeria* colony-forming units (CFU). Antibody treatment resulted in significantly elevated CFU counts in infected organs 48 hours later compared to the untreated mock-injected group. B) Unimmunized mice and mice immunized with the indicated nanofiber formulations, that either contained an optimized dose of T cell epitope or no T cell epitope, were challenged i.p. with the same dose of *Listeria* as in A. None of the groups exhibited statistically significant differences in total CFU counts per organ. C) Immunized mice were boosted one week before Lm challenge and anti-TNF IgG titers were evaluated on the day of challenge before infection with *Listeria*. Anti-TNF IgG titers were significantly different between mice immunized with optimized formulations that contained VAC T cell epitope compared to mice that were immunized with nanofiber formulations lacking the presence of T cell epitope VAC. n=5 mice per group. Lines indicate means ± SEM. Each mouse is indicated by a symbol. *p<0.05, **p<0.01, ***p<0.001 2-way ANOVA. In C, significance was assessed using an unpaired T test.

3.4 Discussion

The current results indicate that supramolecular peptide materials may be suitable for development as systems that can raise therapeutic antibody responses against autologous targets, a departure from previously described uses of these materials that have focused primarily on their use as scaffolds for cell culture and delivery or as vaccines against cancer or infectious diseases [72,147]. Platforms that share structural similarities with Q11 and which may be interesting to study in this regard include other peptides that form into long, high-aspect ratio nanofibers. For example the peptide KFE8 has been explored previously in vaccinations against West Nile virus [90] and cocaine addiction [86]; the peptide RADA4 has been explored as a depot-forming material in vaccines against hepatitis B [92]; the peptide EAK16 has been investigated in vaccines against HIV [91]; the peptide Ac-AAVVLLLW-COOH has been explored in anticancer vaccines [88]; and Q11 has been explored in applications including malaria [33], influenza [34], S. aureus vaccines [89], and cancer [87]. Other high-aspect self-assemblies include those composed of peptide amphiphiles, which have been explored in anticancer vaccines [47] and vaccines against group A streptococcus [148]. Despite the range of infectious diseases that peptide assemblies have already been developed toward, this still represents a small portion of the current breadth of application for peptide self-assemblies overall, which further includes 3D cell culture, matrices for regenerative medicine, and the controlled release or delivery of cells and therapeutics [72,147]. Because these materials share structural similarities, it may be useful to

determine whether they represent, as a class, advantageous platforms for active immunotherapy against autologous targets.

Advantages that supramolecular assemblies appear to have is that they are non-inflammatory [34], they do not require supplemental adjuvants, and they do not strongly engage Th1-type T cell responses[34,93] (**Figures 3.16A, B**), which correlates with their good performance in the mouse model studied here. Another advantage is the modularity of the system, which allows the adjustment of the epitope content within the material simply by mixing different amounts of component peptides prior to fibrillization. In the results reported here, this adjustment had a large influence on the titer of antibodies raised, as well as the strength of Th1 and Th2 T-cell responses to the PADRE epitope. It was straightforward to compare the ratio between T cell epitopes and B cell epitopes from as low as 1:500 to beyond 1:1. It would be comparatively more difficult to adjust the epitope ratio and content widely within other systems such as carrier proteins, engineered conjugates, or kinoids, because such steps commonly require cloning or an individually optimized conjugation reaction for each particular formulation. Nanofibers containing variable amounts of VAC or PADRE produced unique dose-response curves for antibody and T cell responses (**Figures 3.6-3.9**). For both epitopes, the formulations generating the greatest antibody responses did not match those generating the strongest effector T cell responses (**Figures 3.6-3.9**). For the PADRE T-helper epitope, antibody responses were greatest at 0.05 mM peptide, whereas T cell responses were greatest at 0.002 mM PADRE. For the VAC T-helper epitope, antibody responses were greatest at 1.25 mM peptide (the highest dose tested)

whereas T cell responses were greatest at 0.05 mM. Another previously investigated series of T/B epitope combinations in a Q11-based vaccine against methiciliin-resistant Staphylococcus areus (MRSA) likewise exhibited a strong dose-response curve, with different formulations favoring antibody or T-effector responses [89]. Together these studies indicate that peptide assembly can be utilized to efficiently generate a series of different epitope ratios, and these can be selected for preferred combinations of T- and B-cell responses. Previous studies have supported the concept that antigen dose influences the differentiation of CD4 Th1/Th2/T_{FH} phenotypes [149]. High antigen dose also increases the amount of peptide:MHC class II molecules displayed on antigen-presenting cells, thereby increasing TCR signaling strength and duration on specific T cells [150]. While low antigen doses are thought to favor Th1 differentiation, intermediate-to-high antigen doses induce Th2-dominated responses [REF]. High antigen dose or recognition of pMHC by high affinity TCRs is also thought to favor T_{FH} cell differentiation or anergy [150].

Continuing development of these materials will likely focus on studying the duration of antibody responses, as active immunotherapies require predictable half-lives and self-limiting responses for safe clinical use. They will also be explored in specific disease models of chronic, acute, or congenital inflammatory conditions.

CHAPTER 4: Nanofiber self-assembly of T and B cell epitope-bearing Peptide Mixtures for Anti-TNF Active Immunotherapy.

4.1 Summary

In this chapter, we incorporate further additional TEM imaging of the peptide co-assemblies evaluated in chapter 3 that will not be included in the scientific manuscript. Here, we corroborated that beta-sheet rich sequences like Q11 are surprisingly robust and maintain the fibrillary morphology despite incorporation of epitopes at high density. The ability for self-assembly is a pre-requisite for immunogenicity of this type of biomaterials. Thus, confirmation that all of the tested immunizing formulations produced fibrillary structures affirms that the response we observe is the result of interactions between the epitope-bearing biomaterial and the immune system.

4.2 Introduction

Self-assembling peptides are a category of supramolecular materials with important therapeutic potential and are actively being developed to elicit highly specific immune responses for the treatment of a variety of infectious and non-infectious diseases and conditions [120]. In the case of Q11 (QQKFQFQFEQQ)[141], normally the fibrillizing peptide sequence is expanded at its N-terminus with a ligand, though C-terminal expansion has also been shown to be capable for self-assembly [62], and the peptides can be fluorescently labeled or biotinylated post-synthesis (see Appendix I for

protocols). In the past, we have shown that multiple N-terminal sequences can be incorporated while maintaining the nanofibrillar morphology. Some of the biofunctional ligands include cell growth-related peptides [119,139,140], proteins [77,78] and immunogenic epitope antigens[31,33,86,87,89,151]. The modular nature provided via self-assembly greatly facilitates the combination and optimization of ligands and, as presented in this chapter, of T cell and B cell epitope mixtures, which in turn allows for the independent adjustment of B cell and T cell responses [89]. Although in general these materials are straightforward to prepare, working with them requires an important practical consideration: the self-adjuvanting capacity of these materials is strongly dependent on the self-organization into nanofibers [32], and multi-epitope formulations must be composed of nanofibers that contain predictable quantities of each of the desired epitopes such that delivery or injection of material is consistent across experiments and within experiments. In other words, systems where different peptides self-sort into mutually exclusive nanofibers can result in fibers with suboptimal or absent functionality [139,140]. This consideration is the focus of this chapter within the specific application as an active immunotherapy platform to target disease-causing self-molecule TNF.

4.3 Results

Fibrillization of individual TNF (B) cell epitopes and foreign T cell epitopes is facilitated with Q11 sequence modification.

Prior investigations of high-aspect ratio supramolecular materials have underscored how nanofribrillar morphology largely correlates with capacity for adjuvanticity, namely B cell/antibody and CD4 as well as CD8 T cell responses [32,47,62,78,93,120]. Therefore, we investigated the morphology of the individual peptides and their mixtures by Transmission Electron Microscopy (TEM). In physiological buffers, Q11, TNFQ11, PADREQ11, and VACQ11 self-assembled to form nanofibers individually, whereas the soluble TNF B cell epitope did not form any particulate or fibrillar structures **(Figure 4.1).** In addition, we verified that the nanofibrillar structures observed contained β sheet surfaces by Thioflavin T (ThT) staining, which fluoresces in the presence of β sheet-rich structures [152]. Indeed, we observed an enhancement in ThT binding fluorescence in all peptides with the exception of the soluble TNF B-cell epitope peptide, consistent with the TEM results (**Figure 4.1F**). Interestingly, the magnitude of the ThT signal for PADREQ11 nanofibrils was lower while the ThT signal for VACQ11 nanofibrils was higher with respect to Q11. These results correspond with the nanofiber morphology observed by TEM, where the PADRE epitope appeared to modulate nanofiber thickness and decrease the persistence length of the nanofibers, which appeared more flexible compared to unmodified Q11 nanofibers (**Figure 4.1D**). In contrast, the VAC epitope seemed to preserve the relatively more rigid nanofiber

structure similarly to unmodified Q11, with increased lateral fusion of nanofibers into branch-like aggregates (**Figure 4.1E**).

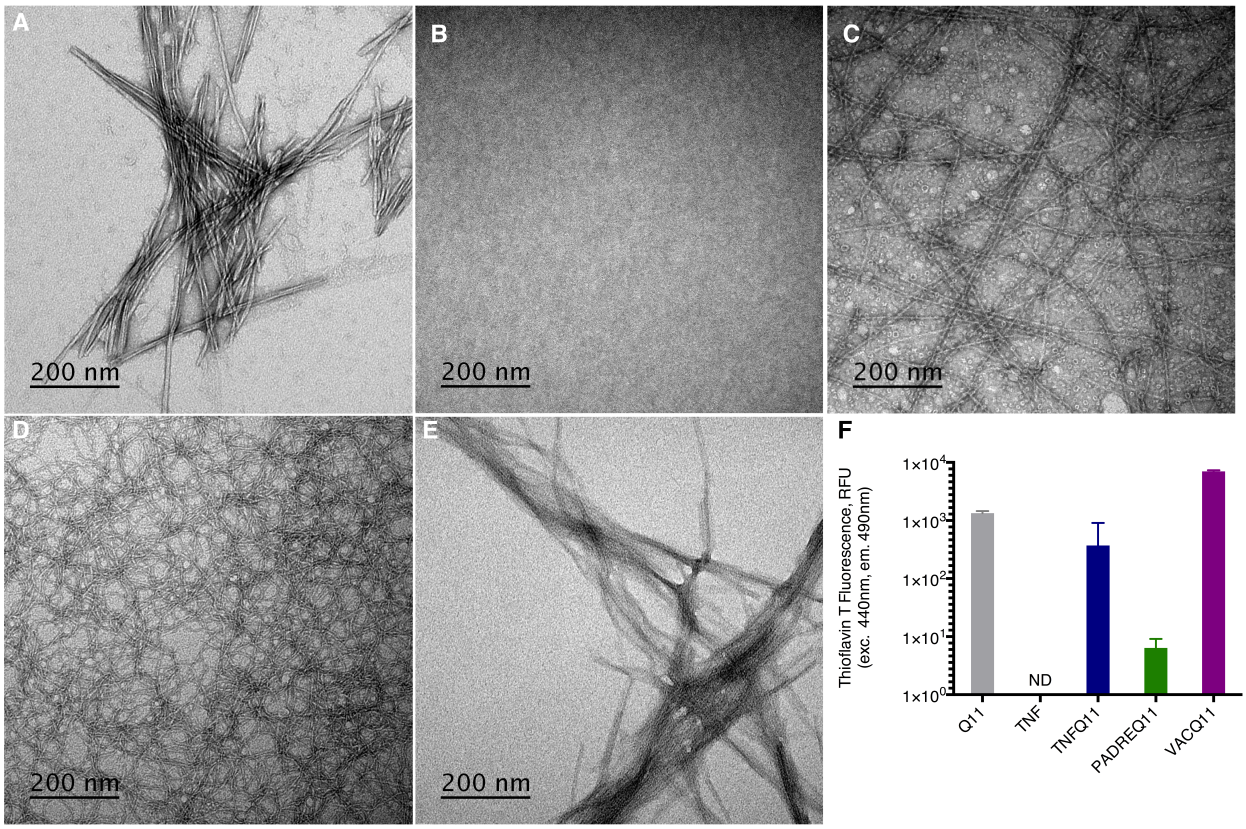


Figure 4.1 Transmission Electron Microscopy (TEM) and Thioflavin T (ThT)-binding fluorescence of individual peptides. Q11 (A), TNF (B), TNFQ11 (C), PADREQ11 (D), and VACQ11 (E) peptides. Thioflavin T fluorescence (F) confirmed the presence of β-sheet nanofibers in all samples, with the exception of unassembled TNF peptide. For TEM, 200 μM peptide solutions were negatively-stained with 1% uranyl acetate and imaged on an FEI Tecnai Spirit TEM. For ThT assay, 4 mM total peptide solutions were mixed 1:1 v/v with 100 μM ThT in 1 X PBS buffer and incubated for 20min at RT. ThT fluorescence was measured on SpectraMax M5 (excitation 440nm/emission 490nm).

To explore possible contributing factors to the highly entangled morphology of VACQ11 nanofibers, we explored pH effects. Between pH 5.1 – 7.4, morphology was not affected (not shown). In addition, we tested the morphology of VACQ11 in water and found that it was capable of forming long, regular, unbranched nanofibers in water; however, it formed more flattened, laterally aggregated fibrillar structures in PBS (**Figure 4.2A and 4.2B**). ThT staining of VACQ11 peptide in water confirmed that the fibers were predominantly β-sheet (**Figure 4.2C**). Hence, these observations indicated that Both the VAC and PADRE epitope could be tolerated within the Q11- based nanofibers, but subtle morphological differences existed for PADREQ11 and VACQ11 when they formed pure nanofibers.

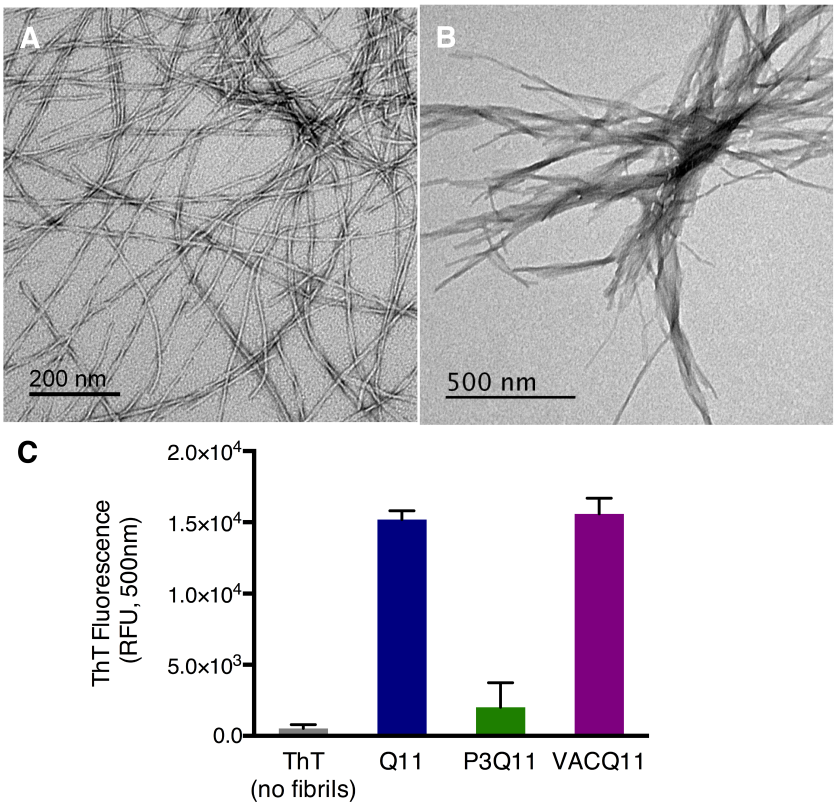


Figure 4.2 TEM and ThT of VACQ11 in water revealed long and homogenous fibers. (A, C). VACQ11 in PBS produced irregular, flattened, laterally aggregated clusters (B). Samples lacking peptide (no fibrils), Q11 (known β-sheet structure), and P3Q11 (a non-fibrillizing variant of Q11[32] were used as controls for the ThT assay (C).

Binary mixtures of epitope-bearing Q11 peptides with unmodified Q11 adopt morphologies more typical of Q11.

Next, we investigated nanofibers containing equimolar mixtures of Q11 with one other epitope-bearing peptide, either TNFQ11, scrambled TNFQ11, PADREQ11, or VACQ11 (**Figure 4.3**). As suspected, nanofibers of mixed peptides produced morphologies with nanostructures in between those of each pure peptide**.** For example,

TNFQ11 and scrambled TNFQ11 mixed with Q11 formed longer fibers with longer persistence lengths than pure nanofibers of TNFQ11 **(Figure 4.3A-B and Figure 4.1c).** PADREQ11/Q11 mixtures produced entangled fibers of mixed diameters and lengths **(Figure 4.3C),** and VACQ11/Q11 mixtures formed straight nanofibers with slight lateral aggregation, indistinguishable from Q11 (**Figure 4.3D**).

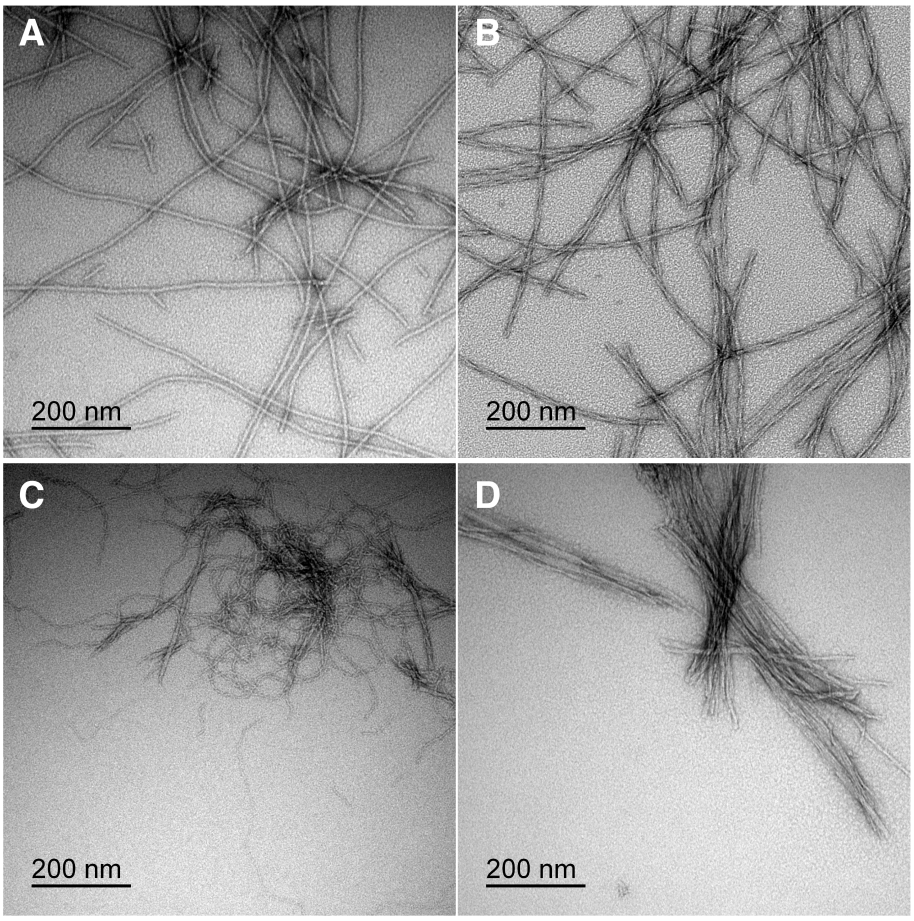


Figure 4.3 TEM of binary peptide mixtures with Q11 (1:1 molar ratio, 1mM each). TNFQ11/Q11 (A); scrambled TNFQ11/Q11 (B); PADREQ11/Q11 (C); VACQ11/Q11 (D).

Titration of T cell epitopes in Nanofiber Assemblies

We next explored how the dose of the T cell epitope affected the nanofibril morphology by TEM. We evaluated the morphologies of ternary mixtures by systematically varying the dose of PADREQ11 or VACQ11 in the co-assemblies, while maintaining a fixed quantity of 50 mol% TNFQ11 (1 mM), and adjusted with Q11 to achieve formulations with equimolar total peptide concentration. The doses tested covered the range of T cell epitope concentrations evaluated in mice. For PADREQ11 co-assemblies, we titrated PADREQ11 from 0.1 mol% to 37.5 mol%. While low-dose (0.1 mol%) and mid-dose (2.5 mol%) PADREQ11 maintained the nanofiber morphology observed for Q11 **(Figure 4.4A-B),** the high dose (37.5 mol%) reflected a structure similar to that observed for 1:1 PADREQ11:Q11 (**Figure 4.4C**). For VACQ11 co-assemblies, we titrated VACQ11 from 0.1 mol% to 50 mol%. All formulations formed similar nanofibers (**Figure 4.5**), with the highest VACQ11 content exhibiting longer, somewhat twisting nanofibers (**Figure 4.5C**). Lastly, we observed that scrambled TNFQ11 co-assemblies also form nanofibers. No meaningful differences in morphology were observed in the scrambled TNFQ11 co-assemblies compared to TNFQ11 co-assemblies (**Figure 4.6**).

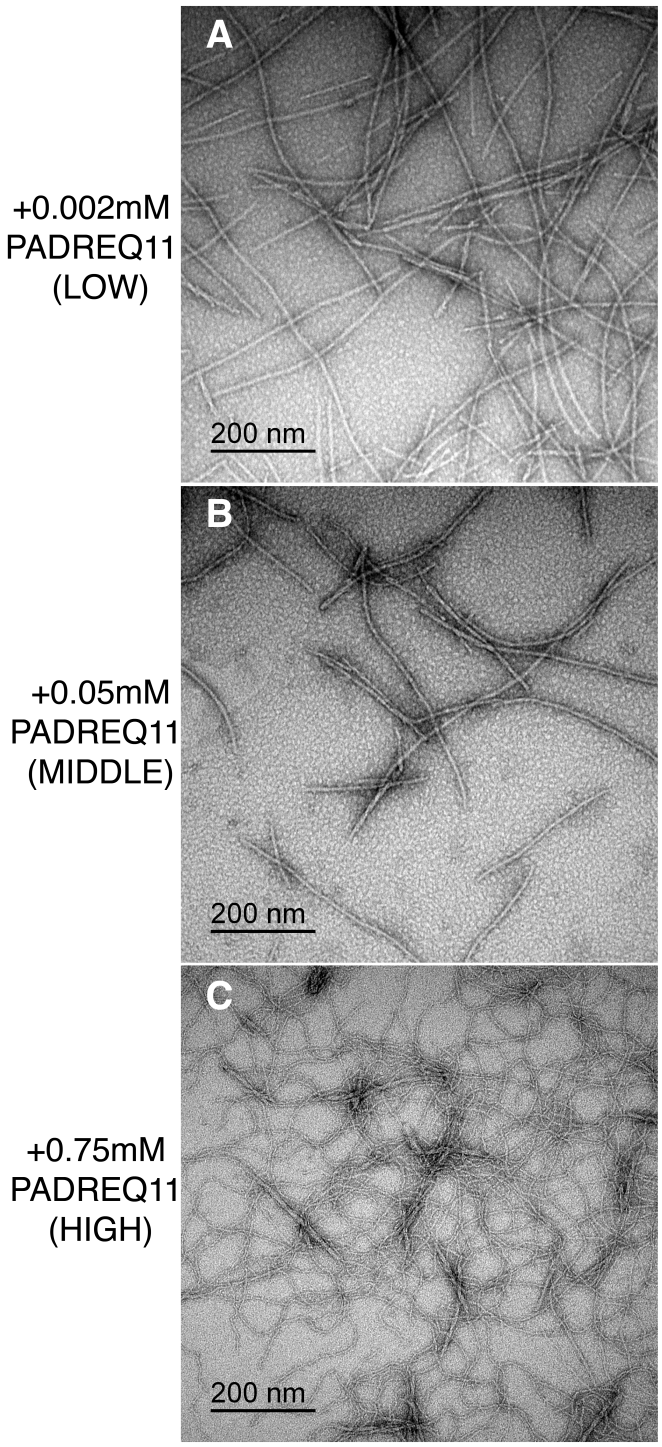


Figure 4.4 TEM micrographs of ternary complexes incorporating PADREQ11 T cell epitope peptide. A) low-dose formulation of 0.1% PADREQ11 (1 mM TNFQ11 / 0.998 mM Q11 / 0.002 mM PADREQ11). B) mid-dose formulation of 2.5% PADREQ11 (1 mM TNFQ11 / 0.95 mM Q11 / 0.05 mM PADREQ11.), and C) high-dose formulation of 37.5% PADREQ11 (1 mM TNFQ11 / 0.25mM Q11 / 0.75 mM PADREQ11).

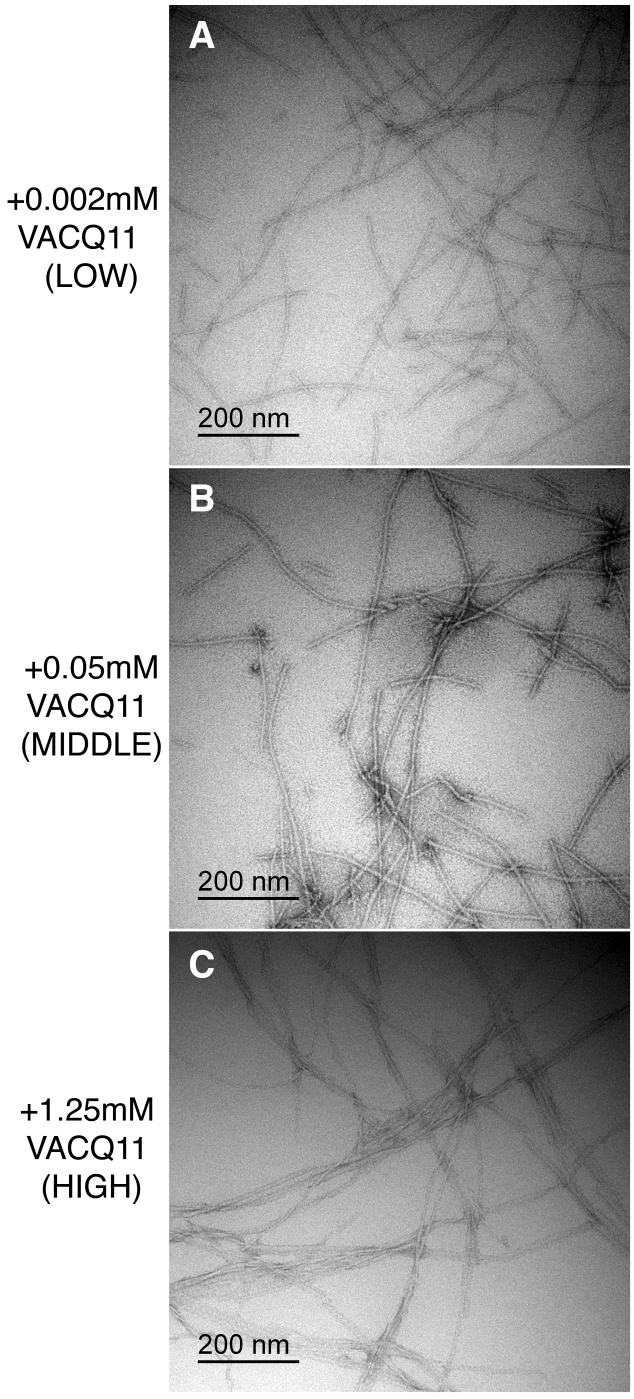


Figure 4.5 TEM micrographs of ternary complexes incorporating varying concentrations of VACQ11 T cell epitope. A) low dose of 0.1% VACQ11 (1 TNFQ11 / 0.998 Q11 / 0.002 mM VACQ11.), B) mid-dose of 2.5% VACQ11 (1 TNFQ11 / 0.95 Q11 / 0.05 mM VACQ11.), and C) a high dose of 50% VACQ11 (1 TNFQ11 / 0.25 Q11 / 1.25 mM VACQ11).

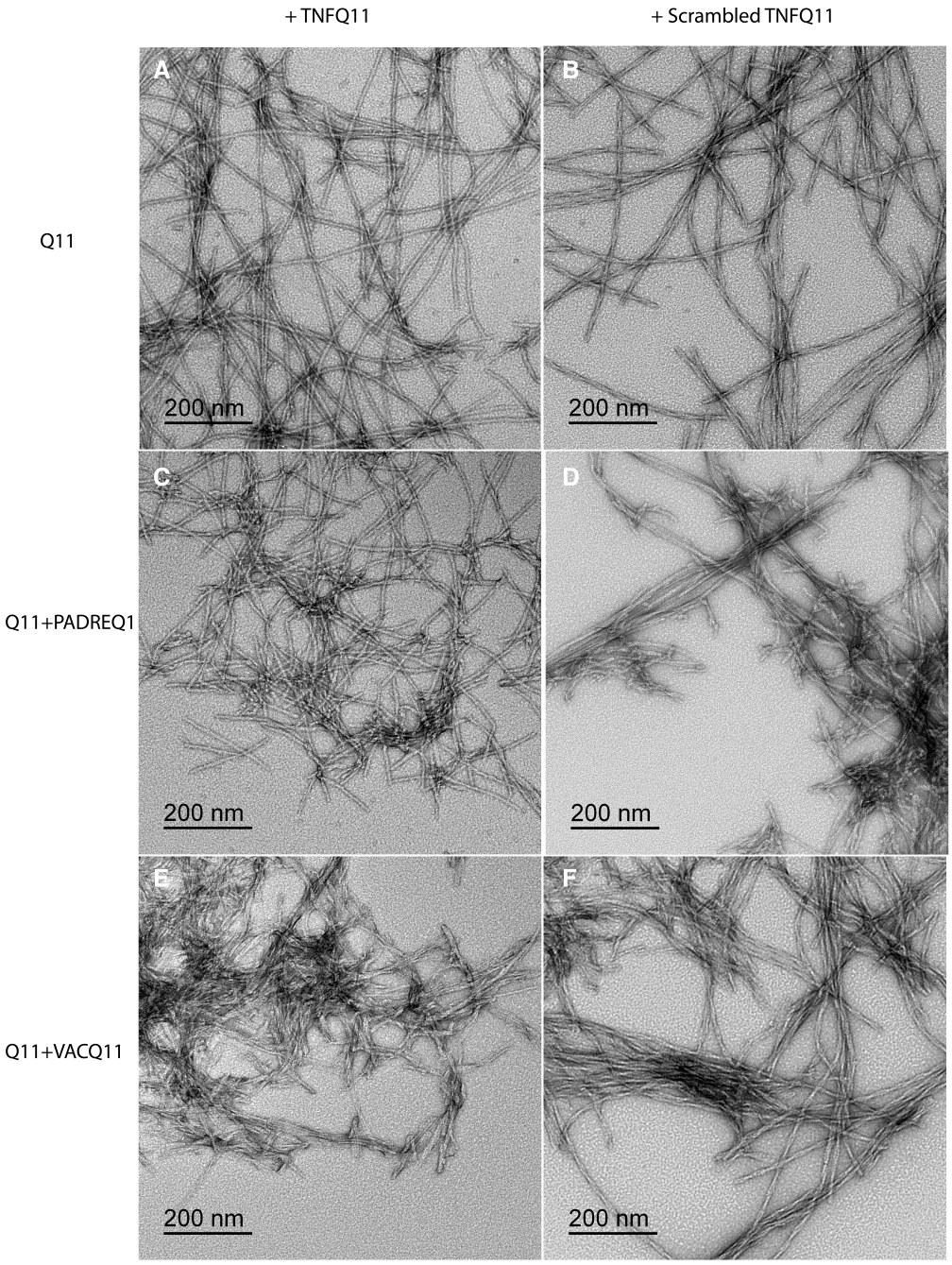


Figure 4.6 Co-assemblies with scrambled TNFQ11 peptide of optimized formulation for anti-TNF antibodies. TEM micrographs of ternary complexes incorporating TNFQ11 (left) are indistinguishable to ternary complexes with scrambled TNFQ11 peptide (right) A) 1 mM TNFQ11 / 1 mM Q11. B) 1 mM scrambled TNFQ11 / 1 mM Q11. C) 1 mM TNFQ11 / 0.95 Q11 / 0.05 mM PADREQ11. D) 1 mM scrambled TNFQ11 / 0.95 mM Q11 / 0.05 mM PADREQ11. E) 1 mM TNFQ11 / 0.25 mM Q11 / 1.25 mM VACQ11). F) 1 mM scrambled TNFQ11 / 0.25 mM Q11 / 1.25 mM VACQ11).

4.4 Discussion

Overall, the co-assembly of TNFQ11, PADREQ11, and VACQ11 corresponds with extensive previous work investigating other epitope-tagged Q11 peptides, which have been shown to be able to co-assemble into integrated nanofibers of controlled composition [77,78,89,119,140]. With specific regard to PADREQ11, however, high content in the nanofiber led to less rigid-appearing nanofibers, perhaps because PADRE is a rather hydrophobic epitope. The hydrophobicity of the VAC epitope may also contribute to the additional lateral aggregation observed for nanofibers containing high amounts of VACQ11.

CHAPTER 5: GENERAL DISCUSSION

The work presented in this thesis contributes to the fields of Biomaterials and Immunology on more than one level. Broadly, in the recent history of the field of Biomaterials, the interaction between synthetic materials and the human body has been intentionally minimized to avoid any sort of immune reaction. Almost all current clinically utilized devices and therapies based on biomaterials are engineered to be as immunologically inert as possible. For example, the metals used in orthopedic implants, the polymers used in soft tissue reconstruction, and the ceramics used in dental and orthopedic applications are minimally immunogenic. While all implanted materials engage inflammatory processes to some extent, the engagement of adaptive immunity has largely been avoided in the field of Biomaterials until very recently.

Over the past 5-7 years, the former principle of avoiding all adaptive immune responses with biomaterials is being replaced with a perspective that the immune system should be actively engaged, engineered, and optimized to achieve specific beneficial therapeutic effects [153]. A sub-field variously termed “Immune Engineering, Immunoengineering, or Biomaterials Immunology” has coalesced and is now visibly represented in the research community of Biomaterials, Biomedical Engineering, and their related disciplines. Laboratories active in this area seek to combine engineering approaches with basic immunological principles to develop new technologies to treat a broad range of diseases and conditions, including cancer, infectious disease, degenerative disorders, autoimmunity, tissue repair, and others. Our laboratory has contributed to this field by designing supramolecular systems capable of engaging the immune system with specificity, and we are working to engineer systems where the

phenotype of the overall immune response can be systematically adjusted [77,78,89]. This thesis is part of this overall shift in paradigm currently moving through the field by exploring whether and how T cell and B cell epitope content and dose affect adaptive immune response phenotypes and protection against a therapeutically relevant self-antigen displayed by self-assembling peptide nanofibers.

From a technological standpoint, this thesis represents several novel advances specifically. First, the strategy of immunizing an individual against a specific problematic cytokine is a concept that has been explored previously [125,126], [128-134] but there is no current clinically efficacious technology that has been successful. In this regard, the design of a self-adjuvanting system with promising efficacy in mice establishes a critical proof-of-concept. Subsequent group members in the Collier lab will be continuing this work to further develop it within specific diseases including arthritis. Other group members are applying the concepts learned to other cytokines, including IL17 and IL1.

Previous studies using the Q11 system have evaluated efficacy at provoking an antibody or a T cell response in response to *foreign* antigens, including those from *Staphylococcus aureus* [89]. These previous studies established the principle that varying the dose of T- and B-cell epitopes within peptide nanofibers is a viable strategy for adjusting the strength and phenotype of epitope-specific immune responses. However, until the work presented in this thesis, it was an open question whether supramolecular peptides could be used to elicit responses against *self*-antigens. The work described in this thesis targeted TNF, an endogenous molecule, and it demonstrated that peptide assemblies can be also designed to elicit appropriate responses aimed at limiting or

controlling elevated levels of self-molecules through active immunotherapy. Within this, several specific findings were particularly notable. The most significant of these findings are:

1. Peptide assemblies can be designed with precisely chosen combinations of peptide epitopes to elicit highly specific antibody or T cell responses. With an increasing reliance on peptides to direct biological responses against a target (normally bacteria or viruses) in rational vaccine design, it is imperative to utilize vaccine platforms or adjuvants amenable to modular and customizable composition to raise appropriate responses with minimal adverse effects and inflammation. Moreover, a boon in techniques and prediction algorithms used in the discovery of candidate T cell and B cell epitopes and a growing field of Immunoproteomics [154] suggest that development of future immunotherapies will involve the use of increasingly well-defined components with a more predictable safety profile compared to traditional vaccines based on attenuated pathogens or even whole proteins, in the case of TNF. In this thesis, we demonstrated that modular T and B epitope formulations can result in unique combinations of T cell and B cell responses. In particular, we established that PADRE induces optimal T cell help to B cells at a concentration of 0.05mM (a 1:20 T: B epitope ratio), which surprisingly corresponds to the optimal epitope quantity in a completely different vaccine directed against a *Staphylococcus aureus* B-cell epitope [89]. In contrast, for a different T-cell epitope, VAC, we found that a concentration of

1:1.25 elicited the highest antibody titers. Interestingly, a ratio 25-fold lower of T helper epitope was optimal to elicit maximal T cell responses (1:25 T: B epitope ratio) and thus a concentration of 0.002mM for PADRE and 0.05mM for VAC was sufficient to elicit maximal T effector responses. It is not clear why these two epitopes exhibit optimal efficacy at significantly different doses, but it is plausible that differences in affinity of the peptides for the MHC[142,143] and affinity and avidity of the peptide:MHC for the TCR [155]. Moreover, subtle variations in morphologies or shape/conformation of the peptide assemblies as observed in Chapter 4 by TEM with increasing PADRE or VAC in peptide mixtures could also have biological effects on the presentation of these peptides and the immune response outcomes observed in Chapter 3 that need further assessments for future studies [156]. These observations provide further verification of important design guidelines for other therapeutic applications of immunoactive peptide assemblies. Overall, the disparity with different epitope systems indicates that it is difficult to predict *a priori* what ratios of epitopes may be optimally effective, and so a modular approach such as the one demonstrated here is useful. In supramolecular systems, a range of different formulations can be created with a minimum of synthetic work simply by mixing and co-assembling different quantities of the individual peptides. Covalent systems or those with less surface area for conjugation pose challenges for creating a broad range of different epitope combinations and quantities.

2. Peptide assemblies elicit a neutral or balanced Th1/Th2 phenotype that depends on the peptide epitope composition. For the materials investigated, T-cell phenotypes were Th2-slanted in the case of PADRE-containing assemblies or slightly more Th1/Th2 balanced in the case of VAC-containing assemblies (**Figures 3.6-3.9 and Figures 3.16**), and thus they were compatible with the non-inflammatory goals of the therapeutic strategy. These results further confirm that peptide nanofibers elicit predominantly Th2-slanted responses [34,93] and that they can be modified to be less polarized with addition of Th1-slanting epitopes like VAC. This response phenotype is similar to Alum with the biggest caveat that Alum is a poor adjuvant for peptides and is more suited to larger protein antigens[34]. Peptide assemblies represent a novel adjuvanting platform that is unlike other currently emulsion and TLR-based FDA-approved adjuvants in that it does not elicit a Th1 inflammatory reaction, mediated by inflammasome activation and expression of inflammatory cytokines [157]. Thus, Q11 and other self-adjuvanting supramolecular peptide assemblies represent a novel category of adjuvants with a different mechanism of action and phenotype particularly suited for targeting specific targets with a minimum of inflammation. A particular intriguing influence of peptide dose presented by nanofibers is the finding that in both peptide systems (PADRE and VAC) we observed a dose-dependent decrease in the Th1/Th2 effector response as evidenced by the significant reduction in cytokine ELISPOTs. It is possible that increasing T cell doses expand regulatory phenotypes or promote a T cell hyporesponsive state (anergy

or deletion) [83,158,159]. Our T cell ELISPOT results suggest that peptide assemblies have the potential to tune T cell phenotype via changes in content and concentration of peptide presented in peptide nanofibers. The precise mechanisms behind this reduction should be a topic of further investigation as they could aid in the rational design of these biomaterials towards antigen-specific induction of tolerance, which is highly desirable for the development of active immunotherapies against antigen-specific autoimmune diseases and against environmental or food-based allergens.

3. Th1/Th2 balance can be significantly slanted towards Th1 by the addition of CpG or IFA/CFA adjuvants, and this diminishes the effectiveness of the therapy. One the one hand, we discovered that IFA/CFA-adjuvanted VAC formulations produced 10-fold higher antibody responses (titers $>10^4$-10^5) than unadjuvanted formulations. However, SPR indicated that antibody-TNF interactions from the adjuvanted formulations had higher K_{off} values compared to unadjuvanted formulations. Further, we found that peptide assemblies adjuvanted with CpG also produced higher antibody titers but worse protection compared to unadjuvanted assemblies. This diminished effectiveness was correlated with a Th1-slanted effector responses characterized by a predominant production of IFNγ over IL-4, as shown by ELISPOTs. These results indicate that quantity of antibody alone cannot predict protection and that indeed the quality of the response is critically important for the design of any active immunotherapy.

Future studies should further elucidate the mechanisms by which CpG or IFA leads to this significant shift in the immune response. It is possible that these adjuvants produce damage or inflammation that overrides the otherwise non-inflammatory immunogenicity of the peptide nanofibers. However, the precise mechanism by which this occurs in relation to peptide nanofibers remains to be clearly identified. Components of this full mechanism that have been revealed by previous studies include the importance of the particulate nature and multivalent display [32] the requirement of MyD88 [33]. It would be of interest to understand the limitations in design of this platform toward Th1 and CD8 activation for the benefit of vaccine development against cancers and infectious diseases. Initial studies indicate that CD8 T cell immunity can be engaged with incorporation of CD8 T cell epitopes but have not been tested using therapeutic epitopes and disease models [47,62]. Understanding the limitations/ thresholds of the system in terms of controlled inclusion of CpG or Th1-slanting epitopes would be beneficial toward applications requiring controlled or healthy levels of inflammation to increase immunity to mutating targets or epitopes expressed at very low levels as those encountered in viral or bacterial infections and in cancers, respectively

In sum, a working model can be assembled to partially account for the effects observed using peptide self-assemblies (**Figure 5.1**): First, multivalent display of the peptide assemblies and nanofibrillar (particulate) morphology facilitate uptake, processing and presentation of epitopes by DCs and possibly also by B cells. In B cells,

multivalency and presentation of B peptide at an optimal density results in B-cell receptor clustering, and facilitates the internalization and processing of the nanofibers for B cell activation [67]. After processing, B cells with TNF-specific but immature BCRs (expressing IgM not IgG) present the foreign T cell peptide in the context of MHCII to T cells for T cell help. Upon T cell activation by recognition of high affinity foreign peptide:MHC, CD4 T cells become activated and can produce cytokines (IL4 or IFNγ, possibly others as well) and/or differentiate into T_{FH} cells in response to the dose of T cell epitope delivered by peptide assemblies. Help, presumably from induced T_{FH}, leads to affinity maturation and IgG isotype switching, which in turn increases the affinity of the antibody response for the TNF peptide and protein. Our data also suggests that unadjuvanted assemblies produce polyclonal responses of better quality than assemblies adjuvanted with inflammatory adjuvants. To speculate on a possible mechanism to explain this result, it is possible that adjuvanted assemblies induce polyclonal antibodies against non-neutralizing TNF epitopes or damage-associated epitopes from the host (i.e. epitope spreading to non-therapeutic targets)[160]. Further CpG adjuvants have been shown in other studies to increase uptake by APCs [9,12], and perhaps this process predominates over the multivalent engagement of BCRs on naive B cells, which is important for enhancing the B cell response.

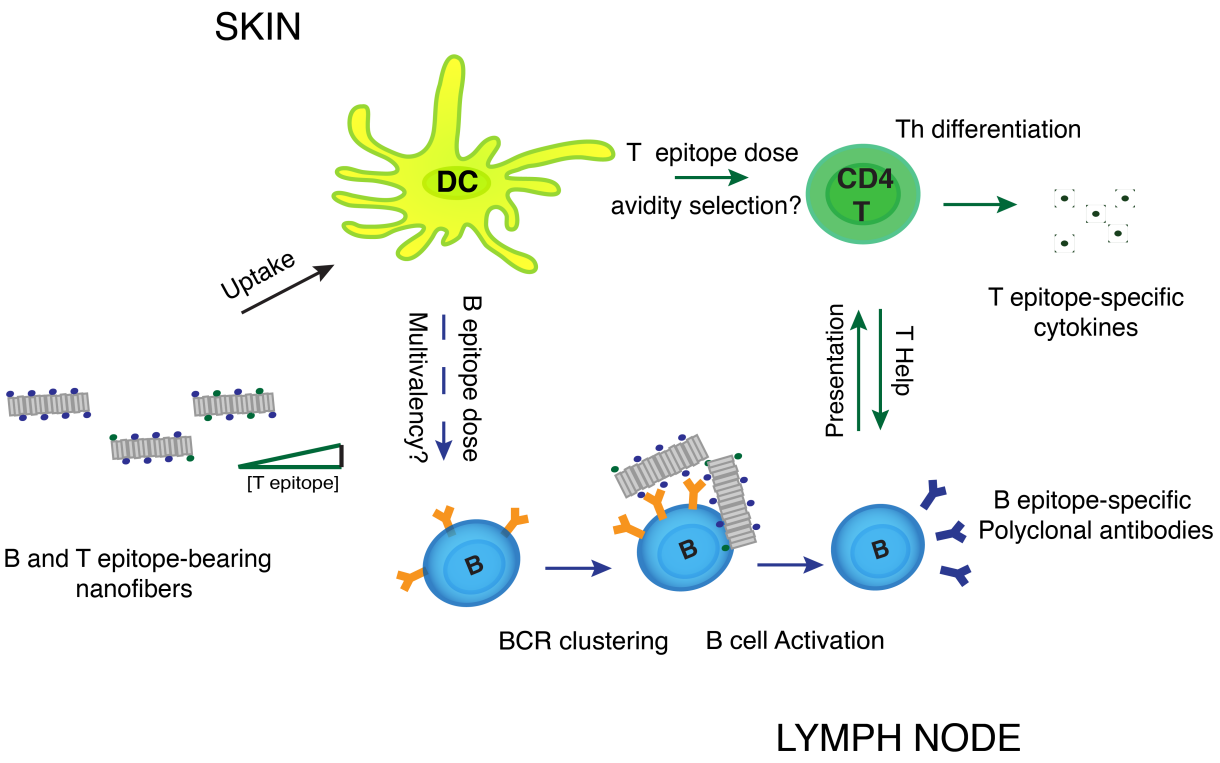


Figure 5.1 Working model of immune recognition of co-assembled T and B epitope-containing nanofibers. The modular nature of peptide nanofibrillar assemblies enables the individual optimization of peptide mixtures resulting in unique combinations of T cell and B cell epitopes into integrated nanofibers. (Top) Uptake and processing of co-assembled peptide nanofibers containing precise amounts of T and B cell epitopes is mediated by DCs in the skin. DCs become activated and migrate to the lymph nodes and present T epitope peptide bound to MHC II to CD4 T cells, which become activated. (Top, right) Upon activation, CD4 T cells expand, differentiate and produce cytokines in response to the level of T peptide dose delivered, presumably through avidity selection of high avidity T cells at low epitope doses and low avidity T cells at high T epitope doses. Activated T cells, predominantly T_{FH} and Th2, provide help to B cells presenting the T epitope via MHC II. (green arrow). Autoreactive B cells recognize TNF-derived B epitope displayed at high density on self-assembled peptide nanofibers (blue arrow), resulting in BCR clustering and activation through multivalent interactions, which presumably do not always depend on T cell help (Bottom). B cells can also work as APCs and process T epitope and present it to activated T cells to receive help (green arrow). Activated B cells undergo affinity maturation and somatic hypermutation in response to the B:T peptide content. In the presence of CpG (not shown), peptide nanofiber uptake is enhanced due to an inflammatory environment, which polarizes the T cell response toward Th1 and induces a B cell antibody response to TNF that is qualitatively different compared to non-adjuvanted nanofibers (presumably through increased reactivity to other TNF epitopes or host proteins, or by changing the effector IgG isotype).

Future Directions

A number of unresolved questions exist that may make for interesting and impactful future studies.

1. How did the inclusion of CpG affect the phenotype?

We observed in chapter 3 that peptide assemblies containing CpG did not protect in the LPS challenge despite the induction of higher anti-TNF titers. This result indicates the CFA and CpG immunization elicits more quantity of antibody but that the quality of the induced antibodies is not effective at blocking TNF-mediated inflammation. This effect could potentially be explored by testing two different hypotheses: 1) The induced antibody phenotype (Ig Fc region/ effector phenotype) is not capable of binding, inactivating, or facilitating the clearance of TNF or 2) CpG enhances epitope spreading to include other TNF non-neutralizing epitopes in TNF or other self-epitopes produced by host damage.

Testing either hypothesis would require immunizing a large number of mice with peptide assemblies with and without CpG and collecting the serum after multiple boosts. The serum could then be tested for IgG isotypes to confirm that there is a different IgG effector phenotype. The serum antibodies could also be purified and tested in vitro by SPR and also in TNF neutralization assays. If CpG promotes epitope spreading it should result in the induction of antibodies with specificities against additional regions in the TNF molecule, which could be ascertained by conducting ELISA against various TNF fragments. As stated above, it is also possible that the presence of CpG promotes

endocytosis of the molecule and overrides the multivalent presentation of the material lending to BCR clustering and promoting B cell activation. How CpG exactly changes the immune responses elicited by self-assembling peptides should be a subject of future exploration.

2. Duration of Anti-TNF Response.

An important hurdle for the potential development of peptide assemblies in the clinic is to accurately predict the longevity of the T cell and the B cell response. In previous studies, we have observed antibody responses that persist for up to a year[32,151]. In the current study, we were able to determine antibody responses against both mouse and human TNF for as long as 6 months by ELISA and these responses were augmented after boosting, indicating that there was memory of the response. Further, the peptide assemblies did not appear to elicit a counteracting neutralizing response in the way that passive immunotherapies can [116,117]. In the case of passive immunotherapy, repeated infusion with large concentration of purified antibodies induces the propagation of ADAs that neutralize the therapy [122]. We expect that peptide assembles would not elicit such responses, but this should be verified explicitly.

3. Application to clinically relevant disease models.

Subsequent research ongoing in the Collier group is studying the extent to which anti-TNF active immunotherapies can be engineered to be protective in different clinical models. At this time, mouse models of rheumatoid arthritis are under study. The

approach may also be applicable to a range of other conditions where TNF is problematic, including psoriasis, autoimmune diseases, Crohn's disease, inflammatory bowel disease, and hereditary inflammatory diseases such as familial Mediterranean fever.

4. Active Immunotherapy against other targets.

We have considered TNF to be an excellent target for a proof-of-concept of the active immunotherapy approach using self-assemble peptides, but many other targets are attractive and would make for impactful follow-on research. Currently in the Collier group, other students are investigating peptide self-assemblies raising antibody responses against IL-17, epitopes significant in Alzheimer's Disease, and epitopes significant in glioblastoma. Other interesting possible immunotherapies include targeting allergens and autoimmune disease antigens through induction of antigen-specific T cell tolerance with formulations containing high dose of T cell epitopes. The work in this thesis has established that therapeutic self-antibodies can be raised with peptide assemblies, and future work will investigate the breadth of applicability of this platform.

Conclusions

The goal of this thesis was to explore a clinically relevant therapeutic target using peptide self-assemblies. In particular, we were interested to understand how T cell and B cell epitope content and dose affected adaptive immune response phenotypes and protection. As a proof-of-principle, we targeted TNF, which is a self-antigen, a cytokine implicated as a critical initiator of inflammation in several chronic inflammatory and autoimmune conditions. In Chapter 3, we developed several peptide nanofiber formulations consisting of a self-derived B cell epitope exposed only in soluble but not membrane-bound TNF and two different foreign T cell epitopes, the pan-HLA DR and mouse MHCII synthetic peptide, PADRE, and a Vaccinia virus-derived antigen, VAC. It was found that formulation of foreign T cell epitopes with TNF-derived B cell epitope elicited unique combinations of B cell (TNF-specific IgG titers and isotypes) and CD4 T cell responses focused against the foreign T cell epitopes (cytokine ELISPOTs), in a dose-dependent manner, some of which protected mice in models of TNF-mediated inflammation. In Chapter 4, we confirmed that nanofiber peptide assemblies are extremely robust at maintaining a fibrillary morphology, despite incorporation of very high doses of T cell and B peptide epitopes displayed by the nanofibers. Overall, the dose of T cell epitope had a significant influence in T cells, whereby high doses nearly completely abolished T cell cytokine production under both T peptide systems and diminished the magnitude of anti-TNF IgG antibody titers with PADRE. These studies highlight an exquisite dose sensitivity of T cells that we can exploit with peptide nanofibers in the future. Moreover, the modularity of this biomaterial enables a very high degree of specificity to the responses elicited, and we were able to separately influence

the magnitude and phenotype of T cell and B cell phenotypes. The finding of reduced T cell output with high T cell peptide doses suggest that this platform could be designed to elicit antigen-specific tolerance or anergy/deletion, which would further expand the breath of clinical application possibilities for this type of materials. The predominant polarization of peptide nanofibers is Th2 and relatively non-inflammatory, which was reproduced in PADRE-containing assemblies. However, incorporation of Th1-slanting epitope VAC elicited more broad B cell and T responses characterized by mixed antibody and T cell cytokine phenotypes. Incorporation of Th1-inflammatory adjuvants (CFA/IFA or CpG) elicited significant Th1 polarization, which resulted in the highest antibody titers that surprisingly were sub-optimal for protection in LPS challenge and had higher K_{off} to TNF by SPR. These results indicate that high antibody titers do not always correlate with protection and that the specific quality of the response is critically important for the development of appropriate immunotherapies. It would important in the future to test whether we observe a similar precise control over B antibody outputs with formulations containing variable doses of B cell epitopes. Ongoing studies in our laboratory will built upon the work from this thesis to better understand the mechanism of innate immune recognition of these materials, the longevity of the induced immune responses, and how they can be developed for targeted therapies against other inflammatory cytokines (IL-1, IL-17), as well as pathogenic self-molecules in Alzheimer's Disease and Glioblastoma.

APPENDIX 1: Detailed Protocols for Peptide Synthesis, Formulation, Immunization, and Immunological Analysis

Adapted from:

Carolina Mora Solano, Yi Wen, Huifang Han, Joel H. Collier “Practical considerations in the design and use of immunologically active fibrillar peptide assemblies” Methods in Molecular Biology, in press (2017).

Summary

The design, formulation, and immunological evaluation of self-assembling peptide materials is relatively straightforward. Indeed, one of the advantages of synthetic self-assembling peptides is that one can progress from initial concept to in vivo testing in a matter of days. However, because these materials are supramolecular, working with them is not without some practical challenges, and subtle changes in design, synthesis, handling, and formulation can affect the materials’ immunogenicity. This paper is intended to communicate some of these practical aspects of working with these materials that are not always enumerated in conventional research papers. Epitope considerations, peptide synthesis, purification, storage, nanofiber formation, immunological evaluation, and the overall phenotypic characteristics of the immune responses to be expected from these materials are discussed.

Introduction

Peptides that self-assemble into nanofibers have been recently developed to elicit therapeutic immune responses, and they are currently being explored for the treatment of a variety of infectious and non-infectious diseases and conditions [7,31,33,34,87,89,161]. In this strategy, a peptide sequence with a high propensity for fibrillization is extended at its N-terminus with a peptide epitope or antigen. Multiple different peptides, when mixed in the proper sequence, molar ratios, and solution conditions, can be formulated into multi-epitope nanofibers. These nanofibers raise immune responses without needing supplemental adjuvants [31], and the phenotype of the responses is advantageously non-inflammatory [34]. Further, the materials' modular nature greatly facilitates the combination and optimization of epitope mixtures, which in turn allows for the independent adjustment of B cell and T cell responses [89]. Although in general these materials are straightforward to design, synthesize, formulate, and test in vivo, working with them requires attention to a number of important practical considerations. These considerations are the focus of this chapter. The self-adjuvanting capacity of these materials is strongly dependent on the organization of the peptides into nanofibers [32], as well as the identity and composition of the various epitope peptides. Failure to produce co-assembled nanofibers with proper epitope mixtures is likely to result in fibers with reduced or absent immunogenicity. Therefore, this chapter will provide in-depth protocols for producing and evaluating reliably immunogenic peptide nanofibers. Our group has focused mainly on the fibrillizing peptide Q11 (QQKFQFQFEQQ) [31-34,89,161], which will be used as an example here, but other

fibrillizing peptides can also function in a similar capacity [32]. Although folded protein antigens can be incorporated into peptide nanofibers and raise specific immune responses [77,78], here we will focus on all-peptide systems for simplicity. Part 1 and its notes will discuss the design, synthesis and preparation of the peptides. Part 2 will focus on immunization procedures, and Part 3 will focus on assessing immune responses.

PART 1: Peptide Design, Synthesis, and Preparation

Materials

1. Rink amide AM resin (Loading ≈ 0.7 mmol/g, 200-400 mesh)
2. 9-fluorenylmethoxycarbonyl (Fmoc) amino acids, appropriately side-chain-protected
3. 2 - (1H - Benzotriazole - 1 - yl) - 1,1,3,3 - tetramethyluronium hexafluorophosphate (HBTU)
4. 6-Chloro-1-hydroxybenzotriazole dehydrate (Cl-HOBt)
5. N,N-dimethylformamide (DMF)
6. Dichloromethane (DCM)
7. Diisopropylethylamine (DIPEA)
8. Piperidine
9. Acetic acid
10. Biotin-ONp
11. 5-(and-6)-Carboxytetramethylrhodamine (5(6) - TAMRA)

12. 1-Ethyl-3-(3-dimethylaminopropyl)carbodiimide (EDC)
13. N-hydroxy succinimidyl ester of fluorescein (NHS-fluorescein)
14. Trifluoroacetic acid (TFA)
15. Triisopropylsilane (TIS)
16. Ethanedithiol (EDT)
17. Diethyl ether

Instrumentation

1. Peptide synthesizer (We use a model CS136XT and CS336XT from CS Bio)
2. Analytical HPLC with C18 column
3. Semipreparative HPLC with C18 column
4. Rotary evaporator
5. Freeze dryer/lyophilizer
6. MALDI-TOF mass spectrometer

Methods

1. Peptide design: Select epitope or epitopes for appending to Q11 (see **Note 1** for important considerations in epitope selection and peptide design). We have found that a Ser-Gly-Ser-Gly linker between the epitope domain and assembling domain is appropriate. Therefore the peptides have the primary structure N-epitope-SGSG-QQKFQFQFEQQ-Am.

2. Synthesize the peptide using standard Fmoc procedures on Rink amide-AM resin. Couple amino acids in DMF with 4 equivalents each of protected amino acid, HBTU, Cl-HOBt, and DIPEA (see **Note 2**) for 45 minutes. Wash the resin with DMF and DCM between couplings. Deprotect with 20% piperidine in DMF. With regards to scale, we usually synthesize 0.25 mmol for in vivo experiments and 0.125 mmol for preliminary in vitro work. For long or difficult peptides, see **Note 3**.
3. Consider N-terminal acetylation, biotinylation, or fluorescent labeling (see **Note 4**).
4. After terminal coupling, wash resin in DCM and dry under vacuum for at least 1 hr in preparation for cleavage. At this point, the resin can be stored at -20 °C if it is to be cleaved within one week or at -80 °C for longer periods.
5. Prepare 20 mL of cleavage cocktail (for a 0.25 mmol scale resin): TFA/Water/TIS (0.95/0.025/0.025 vol %). If the peptide contains Fmoc-Cys(Trt)-OH, the cleavage cocktail should also contain EDT (TFA/Water/TIS/EDT 0.94/0.025/0.025/0.01 vol %).
6. Place the dry resin in a 50 mL Erlenmeyer flask and add enough cleavage solution so it completely covers the resin. Retain about 5-7 mL of cleavage cocktail to wash adhered resin from the flask wall during the cleavage.
7. Swirl the flask gently and regularly for the first 5 minutes. There commonly is a color change from dark yellow to pale yellow (see **Note 5**). Let the reaction proceed for 1.5 to 2 hr, and swirl gently about every 10-15 minutes.

8. Filter the cleavage cocktail using a clean 8 mL polypropylene fritted column, collecting the filtrate in a 100 mL round bottom flask. Discard the resin and crystalline particulate. No particulate should be present in the round bottom flask. If so, filter again using a second fritted column.
9. Prepare rotary evaporator using a dry ice / acetone mixture in the cold trap condenser. Allow the trap to cool for 20-30 minutes before evaporation (see **Note 6**).
10. Remove 75% of the TFA by rotary evaporation. Before applying vacuum, set the rotation to about ½ maximum speed and allow the liquid to stabilize. Lower the flask into an unheated water bath and apply vacuum very slowly. Do not allow bumping. See **Note 7**, which describes critical considerations for this step. Not executing the rotary evaporation correctly will negatively impact the ultimate solubility and self-assembly behavior of the peptide.
11. Continue evaporation to about 25% the original volume. DO NOT ROTOVAP TO DRYNESS. This should take 30-60 seconds. Observe the precipitation of the peptide. The peptide precipitate should form slowly and progressively, and it should be white with the consistency of a fine suspension (not large chunks). Again refer to **Note 7**, as the state of the precipitate significantly affects its subsequent assembly behavior.
12. IMMEDIATELY after partial evaporation, add about 75 mL of cold (4 °C) diethyl ether to the round bottom flask. The peptide should now be a fine, snow-like precipitate in the ether.

13. At this point the peptide is stable, and the following steps can proceed at a more relaxed time scale. Pour precipitated peptide evenly into two 50 mL conical tubes. Use a small amount of ether to wash the round bottom flask. There should not be much peptide adhering to the sides of the flask if the procedures above were followed.
14. Tightly cap the conical tubes and vortex until peptide is in a very fine suspension, without any large chunks.
15. Release the pressure in the tubes and centrifuge tubes for 5 minutes at 3000 RCF. Decant ether into ether waste container and resuspend pellet in about 25 mL of fresh ether. Hazard: see **Note 8**.
16. Add additional ether and repeat the above two steps for a total of 5 washes after the initial precipitation. By the end of 5 washes any remaining small chunks of peptide should disappear into a very fine suspension.
17. Decant the ether and dry the peptide under a stream of nitrogen. Break up the pellet during drying to achieve a fine powder. Desiccate under vacuum for at least two hours to reach complete dryness (see **Note 9**).
18. Dissolve the dry peptide in ultrapure water (we use a Millipore Milli-Q system with >18.1 MΩ resistivity). The final concentration should be about 5-10 mg/mL. We find 50 mL conical tubes to be convenient containers. Sonicate in a bath sonicator if precipitate is visible (see **Note 10**).
19. Lyophilize the peptide to complete dryness. Seal the cap with parafilm. Store at -80 °C or -20 °C.

20. Assess peptide identity using MALDI mass spectrometry and assess peptide purity using analytical HPLC. For HPLC of Q11-based peptides, we typically inject 20 μL of 10 mg/mL peptide dissolved in neat TFA to ensure monomerization (Hazard: see **Note 11**). Linear water/acetonitrile gradients on C18 columns usually resolve the peptide. Analyze fractions with MALDI mass spectrometry.
21. For semipreparative purification of fibrillizing peptides, dissolve peptide in neat TFA at a concentration of about 90 mg/mL. Inject about 1 mL onto a C18 semipreparative column (Hazard: see **Note 11**). Collect fractions and analyze by mass spectrometry.
22. Combine pure fractions, remove acetonitrile with centrifugal evaporation under vacuum, and lyophilize peptide as above.
23. If the peptide does not meet the desired purity, a second round of semipreparative HPLC purification should be applied.
24. Storage: At -20 °C, peptides are stable for at least 2 years as lyophilized powders. When opening stocks, equilibrate at room temperature for 30 min before opening, and use aseptic procedures to minimize moisture accumulation and bacterial contamination.

PART 2: Immunizations: Formulation and Delivery

Formulation

In addition to the epitope considerations described in **Note 1**, we have identified additional design parameters important for inducing robust antigen-specific B cell and T cell immune responses using peptide assemblies. These include:

1. Epitopes must be covalently attached to the nanofibers in order to elicit responses against them. Soluble peptides co-mixed with nanofibers or proteins that cannot assemble into the fibers may not elicit antibody responses [31,32,77,78]
2. If a Q11-based peptide contains a B cell epitope but lacks a CD4 T helper epitope, it must be co-assembled with another Q11-based peptide containing a CD4 T helper epitope in order to raise antibody responses [33,89] [32].
3. If the T cell epitope and a B cell epitope occupy two different peptides (i.e. they are not integrated, as in the $OVA_{323-339}$ epitope), they must be assembled together into the same nanofiber in order to raise antibody responses. If the epitopes are separated into mutually exclusive populations of nanofibers and co-delivered, they may not raise antibody responses [89]. A strategy for generating either co-assembled or separately assembled epitopes has been previously published [139].

Materials

1. Peptides (purified to > 90% purity)

2. Sterile, pyrogen-free, clear microcentrifuge tubes
3. Sterile water
4. Sterile 10X phosphate buffered saline (PBS, Fisher Scientific, Cat#: BP399-500)
5. Instrumentation: balance, vortexer, and sonicator

Methods

1. Determine whether nanofibers will need a single type of epitope peptide or multiple co-assembled types of epitope peptides (see above and **Note 1**).
2. For single peptide preparations:
    a. Prepare 8 mM peptide in sterile water.
    b. Vortex for 1 min and sonicate for 5 min to dissolve fully.
    c. Incubate the solution at 4 °C overnight for a minimum of 12 hours.
    d. Dilute to 2 mM in 1X PBS. Use 10X PBS and water to achieve precisely 1X PBS. Allow complete fibrillization at room temperature for 3 hr before immunization.
3. For co-assembly of two or more peptides:
    a. The total peptide concentration in the aqueous stock solution should be 8 mM, as for single-peptide formulations.
    b. To prepare the stock solution, weigh the peptides and combine the dry powders together into a flip-top microcentrifuge tube. Flick the tube with a finger 3-4 times and vortex the dry powder mixture for at least 30min for complete mixing. Add water to achieve 8 mM total peptide. For very small

amounts of peptide, see **Note 12**. Owing to the importance of producing co-assembled fibrils, we have found that the precision that is sacrificed from not making stock solutions with spectrophotometrically verified peptide concentrations is a necessary trade-off to ensure that the peptides are properly mixed from the earliest point possible.

c. Incubate the solution at 4°C overnight for a minimum of 12 hours.

d. Dilute to 2 mM total peptide in 1X PBS. Use 10X PBS and water to achieve precisely 1X PBS. Allow complete fibrillization at room temperature for 3 hr before immunization.

4. Storage: We have found that some peptide assemblies are extremely stable, with unaltered immunogenicity even when stored at elevated temperatures (e.g. 45 °C for several months) [151]. Indeed, this stability is an advantage of peptide assemblies. However, to reduce the chance of bacterial growth we recommend storage as a dry, lyophilized powder at -20°C. In our experience, self-assembled peptides are generally stable in these storage conditions for at least two years.

Quality Control: Checks prior to immunizations

Materials

1. Limulus Amebocyte Lysate (LAL) chromogenic endpoint assay kit (Lonza).
2. Formvar Carbon film on 400 mesh copper grid (Electron Microscopy Sciences)
3. 1% Uranyl acetate in water

Instruments

1. Transmission electron microscope
2. Circular dichroism spectrometer

Methods

1. **Endotoxin:** In general, peptide self-assemblies contain very low levels of endotoxin. However, given the potential effect of any contaminating endotoxin, all batches of peptide should be tested prior to immunization. Because endotoxin could be inadvertently introduced at any point (synthesis, purification, formulation), it is most useful to measure endotoxin in the final immunization preparation immediately before use in vivo. We use the limulus amebocyte lysate chromogenic endpoint assay (LAL, Lonza). Formulations prepared using the procedures described above typically contain less than 0.5 endotoxin units (EU) per mL of endotoxin, which is within the limit recommended for preclinical studies in rodents (1.5 EU/mL) [121].

2. **Fibrillization:** Whether nanofibers are composed of one peptide or multiple peptides, appropriate fibrillization is critical for raising robust immune responses. Disruption of fibrillization ablates immunogenicity [32]. A simple quality check is to observe nanofiber morphology using Transmission Electron Microscopy (TEM). To prepare TEM samples, dilute immunization formulations (2 mM peptide) to

0.2 mM in PBS and deposit them onto TEM grids. Incubate for 1 minute. Wash 3-5 times with 0.2 μm filtered ultrapure water. Apply 1% w/v uranyl acetate in water for 1 minute for negative staining. Withdraw liquid quickly with a piece of filter paper (see **Note 13**). When the liquid cannot be completely withdrawn owing to thickly deposited nanofibers, further dilute the peptide to 0.1 mM or 0.05 mM, and this may resolve the problem.

3. **Conformation:** Nanofiber formation is based on the organization of the peptides into β-sheet conformations. Circular Dichroism is a simple measure to assess peptide conformation. Dilute peptides to 0.2 mM or 0.1 mM in PBS and scan between 180-260 nm. Owing to scattering and absorbance from nanofibers and buffer constituents, respectively, reliable data below 200 nm may be difficult to obtain.

Immunizations (in mice)

Materials

1. Mice of appropriate haplotype for evaluating the epitope of interest (see **Note 14**).
2. Isoflurane (see **Note 15**).
3. Peptide immunizing formulations
4. Sterile ½ cc insulin syringes with 28G 1/2 needles (Becton Dickinson, 329461)
5. Lancets and microcentrifuge tubes.

Methods

1. Before primary immunization, collect a pre-immune blood draw (<100 µL) to serve as a control for subsequent ELISAs. After immunization, we typically perform blood draws weekly or every other week to evaluate antibody responses.
2. For subcutaneous immunizations:
    a. Using the formulations prepared above and sterile ½ cc insulin syringes with 28G needles, inject 50 µL each into two separate locations on the back.
    b. To boost, inject 25 µL each of the same formulation into two separate locations on the back. The timing of boosting is typically 3-4 weeks after the primary immunization. Subsequent boosting can also be administered at 3-week intervals. In our hands, robust antibody responses of titers of 10^4 or greater are usually observed after one or two boosts. (see **Note 16**).
3. For intraperitoneal immunizations: the prepared formulation is administered using insulin syringes at two intraperitoneal locations (left and right) and with a volume of 50 µL each. Intraperitoneal immunizations are used as a convenient alternative to study antigen uptake and presentation. For peritoneal lavage procedures, see Part 3.

PART 3: Assessment of Immune Response Phenotypes

In general, peptide assemblies tend to elicit immune responses with the following characteristics:

1. Long-lasting antibody titers. After one or two boosts, if the quality control metrics above have been met and the epitopes have been appropriately selected, generally mice produce anti-peptide antibodies for at least a year [32].
2. Variable T cell responses. The magnitude and quality of T cell responses are dependent on the quality of the T cell epitope and the molar ratio with respect to the B cell epitope [89].
3. Minimal inflammation. Peptide assemblies, while able to raise significant antibody responses, do so with negligible inflammation [34].
4. Multiple Ig isotypes [31,89].

To assess the phenotype of immune response raised by peptide self-assemblies, the following methods are useful. These will be described in brief, as they are widely used immunological techniques, but specific practical considerations regarding peptide assemblies will be noted.

1. Enzyme-linked Immunosorbent Assay (ELISA): After drawing blood, allow the blood to clot for 30 min at RT and then centrifuge blood samples at 2000 x g for 15 min to separate the serum. Serum can be stored at -20 °C or -80 °C. For analysis within a

few days, serum can be stored at 4 °C. Practical considerations when performing antibody ELISAs after immunization with peptide nanofibers include:

a. **ELISA coating solutions.** If a protein is the intended target of the antibody response, then make a coating solution of the pure protein in 1X PBS at a concentration of 1 μg/mL protein. If the protein does not coat well, as reflected by low titers of a known positive control, test higher coating densities (up to 20 μg/mL). If peptide is used for coating the ELISA plate, the preferred method is to perform a 2-step coating protocol with streptavidin (SA, 1 μg/mL in 1X PBS), followed by washing off excess SA and coating with biotinylated epitope peptide (without Q11) at 20 μg/mL in 1X PBS. If biotinylated peptide is not available, then use unlabeled epitope peptide or fibrillized peptide (containing Q11) by first making a stock solution of 1 mg/mL peptide in water and then diluting to 20 μg/mL in 1X PBS. The main disadvantage of using unlabeled peptide solutions is that the positioning of the peptide epitope on the ELISA plate cannot be as controlled as for SA + biotinylated peptides. Also, in some cases antibodies may be generated against the SGSG-Q11 fragment of a fibrillizing peptide, especially at early time points. These antibodies may contribute a small amount to the titers measured against epitope-Q11 peptides when such peptides are used as the coating material.

b. **Control sera.** It is important to collect pre-immune serum to detect background antibody binding to ELISA plates. Pooled naive serum serves as a negative

control for the assay and must be included in every ELISA plate that is run. For positive controls, sera from mice with previously determined titers is useful. Control serum samples can be aliquoted and stored at -80 ºC. These controls should maintain consistent titers across different ELISA experiments if they are stored and analyzed properly.

c. **Determination of endpoint titers.** Subtract the absorbance of background wells (those coated only with PBS) from the absorbance of sample wells (controls and experimental samples). Use pooled naive mouse serum as a negative control to determine the signal strength arising from non-specific binding. Create a series of tenfold dilutions for both the control and experimental sera. Run the ELISA with at least triplicate samples, and determine the titer cutoff for each serum dilution by calculating the average absorbance from naive (negative control) serum + 3 standard deviations. The titer for each experimental serum sample is defined as the highest tenfold dilution of serum that gives absorbances larger than the corresponding cutoff values calculated from the negative control sera.

d. **Ig Isotype ELISA.** To identify different antigen-specific Ig isotypes (for example: IgM, IgG1, IgG2b, IgG2c, and IgG3 in C57BL/6 mice), perform ELISA as above but using isotype-specific detection antibodies [89].

2. Enzyme-linked ImmunoSpot (ELISPOT). ELISPOT assays are capable of detecting single cytokine-secreting cells (B or T cells) that are antigen- or peptide epitope-specific. Cell suspensions from organs of interest, for example the spleen, bone marrow, or lymph nodes, are stimulated with peptide ex vivo on an ELISPOT plate that contains a high-protein binding PVDF or nylon membrane. Stimulated cells produce cytokine that binds to the membrane and are subsequently detected using anti-cytokine antibodies. After detection, plates are dried and cytokine spots are counted using ImmunoSpot Analyzer (Cellular Technology, Ltd.). Here, we outline some of the most important practical considerations specific to nanofiber vaccines:

a. **Positive and negative ELISPOT controls.** Negative control wells should be stimulated with complete media alone, while positive control wells should be stimulated with 10 μg/mL phytohemagglutinin (PHA, from Sigma), anti-CD3 antibody, or another appropriate T cell activator. Negative control wells serve as a baseline of actively secreting T cells prior to peptide stimulation, while positive control wells measure the viability of the cells and the successful implementation of the ELISPOT technique. ELISPOTs can be affected by the skill level of the researcher and so these controls are critical. In our experience, wells stimulated with media alone elicit <10 cytokine spots per million cells for both IL-4 and IFNγ. In our hands, for cells isolated from C57BL/6 mice, PHA elicits a higher proportion of IFNγ spots compared to IL-4.

b. **Cell plating density and conditions.** Cell numbers can be adjusted depending on the expected frequency of antigen-specific T cells or on the strength of the immune response. Generally, the more cells plated, the higher the number of activated cells that can be detected. Low cell numbers may prevent detection due to low frequency of antigen-specific T cells, while too high cell numbers may affect cell culture viability. We find that about $5x10^5$ cells per well (in 200 µL volume) is appropriate for detecting responses to peptide nanofibers in previously immunized mice that are boosted one week before the ELISPOT. Also, we recommend re-filtering the cell suspensions just prior to plating. This will reduce smears on the ELISPOT membrane caused by cell clumping.

c. **Stimulation with self-assembling peptides.** Stimulate cells with 1-10 µM peptide in complete media. For non-fibrillized peptides of medium-to-high affinity (for example $OVA_{323-339}$), 5 µM peptide is appropriate. For higher affinity peptides (for example PADRE), 1 µM peptide may provide better results, and for peptide nanofibers (for example OVAQ11), 10 µM peptide is optimal in our experience. For all peptides, prepare stock solutions of 1 mM peptide in PBS by first dissolving peptide in water at slightly greater than 1 mM peptide concentration, then adding 10X PBS and any additional water to achieve 1 mM final peptide concentration in 1X PBS**.** Dilute this peptide stock to 20-200 µM in media and add it to culture wells to achieve the desired concentration of stimulating peptide. The concentrated stock in PBS can be stored at -20 °C for up to 2 years. The

working solution in medium should be used immediately. We typically stimulate cells for 48h at 37 °C (see **Notes 17** and **18**).

3. Analysis of antigen presenting cells using flow cytometry

Peptide internalization by antigen presenting cells (APCs) and the subsequent activation of the APCs can be studied using flow cytometry, using cells isolated from the peritoneal space. Typically, mixed nanofibers containing 0.02 mM of fluorescence-conjugated peptide are prepared by co-assembling labeled and unlabeled peptide (see **Notes 4 and 12**). At predetermined time points after IP immunization (6 h, 18 h, 24 h, or 48 h), inject 2 mL of Hank's balanced salt solution (HBSS) intraperitoneally. Massage the abdomen 40 times and withdraw about 1.2-1.5 mL of fluid from the IP space. Collect the cells by centrifugation and wash them once with flow buffer (PBS containing 2% fetal bovine serum). After blocking the Fc receptor with 2.4G2 antibody (BD Bioscience, Cat#: 553142), stain the cells with fluorescence-conjugated antibodies against F4/80 (Biolegend, Cat#: 123128), MHCII (Biolegend, Cat#: 107606), CD11c (Biolegend, Cat#: 117318), CD11b (BD Bioscience, Cat#: 557657), CD40 (Biolegend, Cat#: 124611), CD80 (Biolegend, Cat#: 104729), and CD86 (BD Bioscience, Cat#:553692). Resuspend cells in flow buffer with 1 μg/mL DAPI, and analyze them using an appropriate flow cytometer. We use an LSRII analyzer (BD Bioscience). Macrophages are gated as $F4/80^{+}$ and dendritic cells are gated as $F4/80^{-}CD11c^{+}CD11b^{+}$. In each cell population, positive fluorescence signals

from nanofibers indicate internalization of the nanofibers. Elevated geometric mean fluorescence intensities of MHCII, CD40, CD80, and CD86 indicate activation.

Notes

1. **Epitope selection:** Generally, self-assembled peptide nanofibers will not raise antibody responses unless B cell epitopes and CD4 T helper epitopes are present together in the same nanofiber. A B cell epitope is the component of an antigen that is specifically recognized by antibodies and by B cells (via B cell receptors). A T cell epitope is the portion of an antigen that is internalized, processed, and presented by antigen-presenting cells in the Class-I or Class-II major histocompatibility complex (MHC-I, MHC-II) for subsequent recognition via T cell receptors. In our hands we have found that it is necessary to incorporate CD4 T cell epitopes along with B cell epitopes in the same peptide nanofibers in order to raise detectable antibody responses [32,33,89]. The presence of CD8 T cell epitopes allows for cytotoxic T cell responses [62]**.** Epitopes can be incorporated into the nanofiber scaffold by appending to the Q11 domain in one continuous peptide [32,33], by co-assembling two or more separate peptides containing either a B cell epitope or a T cell epitope so that the final nanofiber contains both [89,139], via covalent binding of proteins to the fibers [77], or by assembling expressed proteins into the nanofiber via the β-tail system [78]. B cells can recognize linear or discontinuous amino acid sequences as epitopes. In contrast, T cells bind linear peptides that are appropriately presented within MHC

molecules [7]. To predict whether a candidate sequence contains B cell or T cell epitopes, on-line resources such as the Immune Epitope Database are extremely useful (www.iedb.org) [29,30,162-164].

2. A fourfold excess of the amino acid generally results in couplings with > 99% yield in our hands. This is crucial since an accumulated decrease in the coupling efficacy can negatively affect the final yield and purity of even small peptides [165].

3. For long or difficult peptides, Fmoc amino acids may need to be double coupled to the growing resin-bound sequence and require longer coupling time. DMSO can be added to improve resin swelling [166].

4. Additional N-terminal modifications can be considered, including:

a. Acetylation. Removes the positive charge on the N-terminal of peptides, thus mimicking natural proteins. In some cases, it increases peptide stability by preventing N-terminal degradation [167,168]. If an epitope is selected that has been previously described in the literature, in general it is best to keep the N-terminal character originally reported, whether acetylated or not.

b. Biotinylation. Biotin-labeled peptides are commonly used in immunoassays [34,169], histocytochemistry [170], and fluorescence-based flow cytometry [171]. To couple biotin to the N-terminal of completed peptides on-resin, we use 4 equivalents of pre-

activated biotin 4-nitrophenyl ester (Biotin-ONp) in DMF. It is added to the N-terminally deprotected peptide resin and reacted overnight while rocking.

c. Fluorescent labels (e.g. NHS-Fluorescein, TAMRA). N-terminal on-resin conjugation of fluorophores is useful for producing labeled peptides for flow cytometry and localization studies [34,172-174]. Couple NHS-Fluorescein as for biotinylation above, and use EDC coupling to conjugate TAMRA.

5. The cocktail should not turn red. If it does, add more cocktail or more TIS while stirring until the redness disappears. This should be resolved in the first 10 minutes. After about 5-10 minutes commonly there is crystalline precipitation of cleaved protecting groups.

6. Possible Instrument Damage: Be sure that the primary and secondary traps are fully cooled before proceeding with evaporation. TFA can damage the vacuum pump.

7. The peptide should not be evaporated to dryness during this step. Some TFA must remain to keep the peptide in a monomeric state. Rotovapping to dryness can lead to aggregation during work-up and purification that may be difficult to reverse. A rule of thumb is to remove TFA until about 25% of its volume remains. This amount allows subsequent precipitation in diethyl ether but retains the peptide in a low aggregation state.

8. Explosion Hazard: Centrifuging ether is dangerous. This step should be performed in a fume hood using an appropriate centrifuge. Use the smallest quantity of ether possible. Do not centrifuge several tubes at once. Do not centrifuge for longer than the allotted time, and stop the centrifuge immediately if it is unbalanced at all. Discard tube if leaking. Ensure there is no open flame, spark source, or hotplate nearby.

9. It may make the peptide difficult to dissolve in water if it is not completely dry.

10. If the peptide is highly hydrophobic and does not dissolve in water easily, add about ¼ to ½ of total volume of acetonitrile. After dissolution of the peptide, remove the acetonitrile using a centrifugal concentrator under vacuum.

11. HAZARD: TFA is corrosive. When injecting TFA into the HPLC, wear appropriate personal protective gear.

12. If desired peptide quantities are too small to be weighed accurately, dissolve in water an excess amount of peptide that can be accurately weighed, and use this solution to dissolve the other peptides. For example, to prepare a 0.05 mM PADREQ11: 1 mM OVAQ11 : 0.95 mM Q11 mixture, prepare 0.2 mM PADREQ11 in sterile water and add the appropriate volume of this solution to dry OVAQ11 and

Q11 peptides to achieve 8mM total peptide. Add water if final concentration adjustment is needed. Then incubate this solution overnight and dilute to 2 mM for immunizations as described. Work quickly because even in pure water some amount of fibrillization can occur, though the kinetics of assembly are much slower than in buffered salt solutions.

13. Incomplete removal of liquid from the grid may lead to the precipitation of salts, which can compromise the quality of TEM images.

14. For routine work we use C57BL/6 mice purchased from Harlan Laboratories (Envigo). Mice are maintained in a specific pathogen-free (SPF) facility with controlled temperature and light/dark-cycle. The mice are fed water and food ad libitum. All animal work is done under a protocol approved by the Institutional Animal Care and Use Committee. We typically immunize mice that are between 6-12 weeks old.

15. Isoflurane should be administered inside a chemical fume hood, and an isoflurane scavenging device should be employed.

16. If antibody responses are not as high as desired, alterations in the prime/boost regimen should be attempted. These include: additional boosting, larger immunizing doses, different routes of immunization, or adjusting the T:B epitope ratios [89].

17. Do not move the ELISPOT plates during stimulation as this can cause artifacts such as blurred spots and streaks.

18. Low-affinity epitopes require higher concentrations of stimulating peptide to generate spots. We typically limit the concentration of stimulating nanofiber peptides to below 200 μM, as we have not seen any adverse effects on cell viability below this concentration [34]. However, this represents a rather high concentration compared to typical peptide stimulation in ELISPOT. Varying peptide concentrations between 0.1-100 μM peptide should usually reveal the optimal stimulating dose.

REFERENCES

1. Place, E. S., Evans, N. D. & Stevens, M. M. Complexity in biomaterials for tissue engineering. *Nat Mater* **8,** 457–470 (2009).

2. Purcell, A. W., McCluskey, J. & Rossjohn, J. More than one reason to rethink the use of peptides in vaccine design. *Nat Rev Drug Discov* **6,** 404–414 (2007).

3. Pardoll, D. M. Spinning molecular immunology into successful immunotherapy. *Nat. Rev. Immunol.* **2,** 227–238 (2002).

4. Bachmann, M. F. & Jennings, G. T. Vaccine delivery: a matter of size, geometry, kinetics and molecular patterns. *Nat. Rev. Immunol.* **10,** 787–796 (2010).

5. Pape, K. A., Catron, D. M., Itano, A. A. & Jenkins, M. K. The humoral immune response is initiated in lymph nodes by B cells that acquire soluble antigen directly in the follicles. *Immunity* **26,** 491–502 (2007).

6. Crotty, S. Follicular helper CD4 T cells (TFH). *Annu. Rev. Immunol.* **29,** 621–663 (2011).

7. Mora Solano, C. & Collier, J. H. Engaging adaptive immunity with biomaterials. *J Mater Chem B Mater Biol Med* **2,** 2409–2421 (2014).

8. Demento, S. L., Siefert, A. L., Bandyopadhyay, A., Sharp, F. A. & Fahmy, T. M. Pathogen-associated molecular patterns on biomaterials: a paradigm for engineering new vaccines. *Trends Biotechnol.* **29,** 294–306 (2011).

9. Bershteyn, A., Hanson, M. C., Crespo, M. P., Moon, J. J., Li, A. V., Suh, H. & Irvine, D. J. Robust IgG responses to nanograms of antigen using a biomimetic lipid-coated particle vaccine. *et al. J Control Release* **157,** 354–365 (2012).

10. Moon, J. J., Suh, H., Li, A. V., Ockenhouse, C. F., Yadava, A. & Irvine D. J. Enhancing humoral responses to a malaria antigen with nanoparticle vaccines that expand Tfh cells and promote germinal center induction. *Proc. Natl. Acad. Sci. U.S.A.* **109,** 1080–1085 (2012).

11. Molino, N. M., Anderson, A. K. L., Nelson, E. L. & Wang, S.-W. Biomimetic Protein Nanoparticles Facilitate Enhanced Dendritic Cell Activation and Cross-Presentation. *ACS Nano* (2013).

12. de Titta, A., Ballester, M., Julier, Z., Nembrini, C., Jeanbart, L., van der Vlies, A. J., Swartz, M. A. & Hubbell, J. A. Nanoparticle conjugation of CpG enhances

adjuvancy for cellular immunity and memory recall at low dose. *Proc. Natl. Acad. Sci. U.S.A.* (2013).

13. Irvine, D. J., Swartz, M. A. & Szeto, G. L. Engineering synthetic vaccines using cues from natural immunity. *Nat Mater* **12,** 978–990 (2013).

14. Reddy, S. T., van der Vlies, A. J., Simeoni, E., Angeli, V., Randolph, G. J., O'Neil, C. P., Lee, L. K., Swartz, M. A. & Hubbell, J. A. Exploiting lymphatic transport and complement activation in nanoparticle vaccines. *Nat. Biotechnol.* **25,** 1159–1164 (2007).

15. Thomas, S. N., van der Vlies, A. J., O'Neil, C. P., Reddy, S. T., Yu, S. S., Giorgio, T. D., Swartz, M. A. & Hubbell, J.A. Engineering complement activation on polypropylene sulfide vaccine nanoparticles. *Biomaterials* **32,** 2194–2203 (2011).

16. Petersen, L. K., Ramer-Tait, A. E., Broderick, S. R., Kong, C. S., Ulery, B. D., Rajan, K., Wannemuehler, M. J. & Narasimhan, B. Activation of innate immune responses in a pathogen-mimicking manner by amphiphilic polyanhydride nanoparticle adjuvants. *Biomaterials* **32,** 6815–6822 (2011).

17. Ulery, B. D., Petersen, L. K., Phanse, Y., Kong, C.S., Broderick, S. R., Kumar, D., Ramer-Tait, A. E., Carrillo-Conde, B., Rajan, K., Wannemuehler, M.J., Bellaire, B. H., Metzger, D. W. & Narasimhan, B. Rational design of pathogen-mimicking amphiphilic materials as nanoadjuvants. *Sci Rep* **1,** 198 (2011).

18. Pulendran, B. & Ahmed, R. Immunological mechanisms of vaccination. *Nature Immunology* **12,** 509–517 (2011).

19. Iwasaki, A. & Medzhitov, R. Regulation of adaptive immunity by the innate immune system. *Science* **327,** 291–295 (2010).

20. Matzinger, P. The danger model: a renewed sense of self. *Science* **296,** 301–305 (2002).

21. Banchereau, J. & Steinman, R. M. Dendritic cells and the control of immunity. *Nature* **392,** 245–252 (1998).

22. Hubbell, J. A., Thomas, S. N. & Swartz, M. A. Materials engineering for immunomodulation. *Nature* **462,** 449–460 (2009).

23. Trombetta, E. S. & Mellman, I. Cell biology of antigen processing in vitro and in vivo. *Annu. Rev. Immunol.* **23,** 975–1028 (2005).

24. Sun, P., Ju, H., Liu, Z., Ning, Q., Zhang, J., Zhao, X., Huang, Y., Ma, Z. & Li ,Y. Bioinformatics resources and tools for conformational B-cell epitope prediction. *Comput Math Methods Med* **2013,** 943636 (2013).

25. Lundegaard, C., Lund, O., Kesmir, C., Brunak, S. & Nielsen, M. Modeling the adaptive immune system: predictions and simulations. *Bioinformatics* **23,** 3265–3275 (2007).

26. Stranzl, T., Larsen, M. V., Lundegaard, C. & Nielsen, M. NetCTLpan: pan-specific MHC class I pathway epitope predictions. *Immunogenetics* **62,** 357–368 (2010).

27. Nielsen, M., Lundegaard, C., Blicher, T., Peters, B., Sette, A., Justesen, S., Buus, S. & Lund, O. Quantitative Predictions of Peptide Binding to Any HLA-DR Molecule of Known Sequence: NetMHCIIpan. *PLoS Comput Biol* **4,** e1000107 (2008).

28. Nielsen, M., Lund, O., Buus, S. & Lundegaard, C. MHC class II epitope predictive algorithms. *Immunology* **130,** 319–328 (2010).

29. Vita, R., Zarebski, L., Greenbaum, J. A., Emami, H., Hoof, I., Salimi, N., Damle, R., Sette, A. & Peters, B. The immune epitope database 2.0. *Nucleic Acids Res.* **38,** D854–62 (2010).

30. Kim, Y., Ponomarenko, J., Zhu, Z., Tamang, D., Wang, P., Greenbaum, J., Lundegaard, C., Sette, A., Lund, O., Bourne, P. E., Nielsen, M. & Peters, B. Immune epitope database analysis resource. **40,** W525–W530 (2012).

31. Rudra, J. S., Tian, Y. F., Jung, J. P. & Collier, J. H. A self-assembling peptide acting as an immune adjuvant. *Proc. Natl. Acad. Sci. U.S.A.* **107,** 622–627 (2010).

32. Rudra, J. S., Sun, T., Bird, K. C., Daniels, M. D., Gasiorowski, J. Z., Chong, A. S. & Collier, J. H. Modulating adaptive immune responses to peptide self-assemblies. *ACS Nano* **6,** 1557–1564 (2012).

33. Rudra, J. S., Mishra, S., Chong, A. S., Mitchell, R. A., Nardin, E. H., Nussenzweig, V. & Collier, J. H. Self-assembled peptide nanofibers raising durable antibody responses against a malaria epitope. *Biomaterials* **33,** 6476–6484 (2012).

34. Chen, J., Pompano, R. R., Santiago, F. W., Maillat, L., Sciammas, R., Sun, T., Han, H., Topham, D. J., Chong, A. S. & Collier, J. H. The use of self-adjuvanting nanofiber vaccines to elicit high-affinity B cell responses to peptide antigens

without inflammation. *Biomaterials* **34,** 8776–8785 (2013).

35. Mitragotri, S. & Lahann, J. Physical approaches to biomaterial design. *Nat Mater* **8,** 15–23 (2009).

36. Ahsan, F., Rivas, I. P., Khan, M. A. & Torres Suarez, A. I. Targeting to macrophages: role of physicochemical properties of particulate carriers--liposomes and microspheres--on the phagocytosis by macrophages. *J Control Release* **79,** 29–40 (2002).

37. Choi, H. S., Liu, W., Liu, F., Nasr, K., Misra, P., Bawendi, M. G. & Frangioni, J. V. Design considerations for tumour-targeted nanoparticles. *Nat Nanotechnol* **5,** 42–47 (2009).

38. Reddy, S. T., Rehor, A., Schmoekel, H. G., Hubbell, J. A. & Swartz, M. A. In vivo targeting of dendritic cells in lymph nodes with poly(propylene sulfide) nanoparticles. *J Control Release* **112,** 26–34 (2006).

39. Manolova, V., Flace, A., Bauer, M., Schwarz, K., Saudan, P. & Bachmann, M. F. Nanoparticles target distinct dendritic cell populations according to their size. *Eur. J. Immunol.* **38,** 1404–1413 (2008).

40. Tran, K. K. & Shen, H. The role of phagosomal pH on the size-dependent efficiency of cross-presentation by dendritic cells. *Biomaterials* **30,** 1356–1362 (2009).

41. Sexton, A., Whitney, P. G., Chong S. F., Zelikin, A. N., Johnston, A. P., De Rose, R., Brooks, A. G., Caruso, F. & Kent, S. J. A protective vaccine delivery system for in vivo T cell stimulation using nanoengineered polymer hydrogel capsules. *ACS Nano* **3,** 3391–3400 (2009).

42. Kaba, S. A., Brando, C., Guo, Q., Mittelholzer, C., Raman, S., Tropel, D., Aebi, U., Burkhard, P. & Lanar, D. E. A nonadjuvanted polypeptide nanoparticle vaccine confers long-lasting protection against rodent malaria. *J. Immunol.* **183,** 7268–7277 (2009).

43. Moon, J. J., Suh, H., Bershteyn, A., Stephan, M. T., Liu, H., Huang, B., Sohail, M., Luo, S., Um, S. H., Khant, H., Goodwin, J. T., Ramos, J., Chiu, W. & Irvine D. J. Interbilayer-crosslinked multilamellar vesicles as synthetic vaccines for potent humoral and cellular immune responses. *Nat Mater* **10,** 243–251 (2011).

44. Kaba, S. A., McCoy, M. E., Doll, T. A., Brando, C., Guo, Q., Dasgupta, D., Yang, Y., Mittelholzer, C., Spaccapelo, R., Crisanti, A., Burkhard, P. & Lanar, D. E. Protective antibody and CD8+ T-cell responses to the Plasmodium falciparum

circumsporozoite protein induced by a nanoparticle vaccine. *PLoS ONE* **7,** e48304 (2012).

45. Wahome, N., Pfeiffer, T., Ambiel, I., Yang, Y., Keppler, O. T., Bosch, V. & Burkhard, P. Conformation-specific display of 4E10 and 2F5 epitopes on self-assembling protein nanoparticles as a potential HIV vaccine. *Chem Biol Drug Des* **80,** 349–357 (2012).

46. De Geest, B. G., Willart, M. A., Hammad, H., Lambrecht, B. N., Pollard, C., Bogaert, P., De Filette, M., Saelens, X., Vervaet, C., Remon, J. P., Grooten, J. & De Koker, S. Polymeric Multilayer Capsule-Mediated Vaccination Induces Protective Immunity Against Cancer and Viral Infection. *ACS Nano* **6,** 2136–2149 (2012).

47. Black, M., Trent, A., Kostenko, Y., Lee, J. S., Olive, C. & Tirrell, M. Self-assembled peptide amphiphile micelles containing a cytotoxic T-cell epitope promote a protective immune response in vivo. *Adv. Mater. Weinheim* **24,** 3845–3849 (2012).

48. Stano, A., Nembrini, C., Swartz, M. A., Hubbell, J. A. & Simeoni, E. Nanoparticle size influences the magnitude and quality of mucosal immune responses after intranasal immunization. *Vaccine* **30,** 7541–7546 (2012).

49. Stano, A., Scott, E. A., Dane, K. Y., Swartz, M. A. & Hubbell, J. A. Tunable T cell immunity towards a protein antigen using polymersomes vs. solid-core nanoparticles. *Biomaterials* **34,** 4339–4346 (2013).

50. Smith, D. M., Simon, J. K. & Baker, J. R. Applications of nanotechnology for immunology. *Nat. Rev. Immunol.* **13,** 592–605 (2013).

51. Jardine, J., Julien, J. P., Menis, S., Ota, T., Kalyuzhniy, O., McGuire, A., Sok, D., Huang, P. S., MacPherson, S., Jones, M., Nieusma, T., Mathison, J., Baker, D, Ward, A. B., Burton, D. R., Stamatatos, L., Nemazee, D., Wilson, I. A. & Schief W. R. Rational HIV immunogen design to target specific germline B cell receptors. *Science* **340,** 711–716 (2013).

52. Swartz, M. A., Hubbell, J. A. & Reddy, S. T. Lymphatic drainage function and its immunological implications: from dendritic cell homing to vaccine design. *Semin. Immunol.* **20,** 147–156 (2008).

53. Roozendaal, R., Mempel, T. R., Pitcher, L. A., Gonzalez, S. F., Verschoor, A., Mebius, R. E., von Andrian, U. H. & Carroll, M. C. Conduits mediate transport of low-molecular-weight antigen to lymph node follicles. *Immunity* **30,** 264–276 (2009).

54. Swartz, M. A., Hirosue, S. & Hubbell, J. A. Engineering approaches to immunotherapy. *Sci Transl Med* **4,** 148rv9 (2012).

55. Gonzalez, S. F., Degn, S. E., Pitcher, L. A., Woodruff, M., Heesters, B. A. & Carroll M. C. Trafficking of B cell antigen in lymph nodes. *Annu. Rev. Immunol.* **29,** 215–233 (2011).

56. CLARK, S. L. The reticulum of lymph nodes in mice studied with the electron microscope. *Am. J. Anat.* **110,** 217–257 (1962).

57. Gretz, J. E., Norbury, C. C., Anderson, A. O., Proudfoot, A. E. & Shaw, S. Lymph-borne chemokines and other low molecular weight molecules reach high endothelial venules via specialized conduits while a functional barrier limits access to the lymphocyte microenvironments in lymph node cortex. *J. Exp. Med.* **192,** 1425–1440 (2000).

58. Itano, A. A. & Jenkins, M. K. Antigen presentation to naive CD4 T cells in the lymph node. *Nature Immunology* **4,** 733–739 (2003).

59. Sixt, M., Kanazawa, N., Selg, M., Samson, T., Roos, G., Reinhardt, D. P., Pabst, R., Lutz, M. B. & Sorokin, L. The conduit system transports soluble antigens from the afferent lymph to resident dendritic cells in the T cell area of the lymph node. *Immunity* **22,** 19–29 (2005).

60. Jewell, C. M., López, S. C. B. & Irvine, D. J. In situ engineering of the lymph node microenvironment via intranodal injection of adjuvant-releasing polymer particles. *Proc. Natl. Acad. Sci. U.S.A.* **108,** 15745–15750 (2011).

61. Kasturi, S. P., Skountzou, I., Albrecht, R. A., Koutsonanos, D., Hua, T., Nakaya, H. I., Ravindran, R., Stewart, S., Alam, M., Kwissa, M., Villinger, F., Murthy, N., Steel, J., Jacob, J., Hogan, R. J., García-Sastre, A., Compans, R. & Pulendran B. Programming the magnitude and persistence of antibody responses with innate immunity. *Nature* **470,** 543–547 (2011).

62. Chesson, C. B., Huelsmann, E.J., Lacek, A. T., Kohlhapp, F. J., Webb, M. F., Nabatiyan, A., Zloza, A. & Rudra, J.S. Antigenic peptide nanofibers elicit adjuvant-free CD8(+) T cell responses. *Vaccine* (2013). doi:10.1016/j.vaccine.2013.11.047

63. Puffer, E. B., Pontrello, J. K., Hollenbeck, J. J., Kink, J. A. & Kiessling, L. L. Activating B cell signaling with defined multivalent ligands. *ACS Chem. Biol.* **2,** 252–262 (2007).

64. Hinton, H. J., Jegerlehner, A. & Bachmann, M. F. Pattern recognition by B cells: the role of antigen repetitiveness versus Toll-like receptors. *Curr. Top. Microbiol. Immunol.* **319,** 1–15 (2008).

65. Tam, J. P. Synthetic peptide vaccine design: synthesis and properties of a high-density multiple antigenic peptide system. *Proc. Natl. Acad. Sci. U.S.A.* **85,** 5409–5413 (1988).

66. Tam, J. P., Clavijo, P., Lu, Y. A., Nussenzweig, V., Nussenzweig, R. & Zavala, F. Incorporation of T and B epitopes of the circumsporozoite protein in a chemically defined synthetic vaccine against malaria. *J. Exp. Med.* **171,** 299–306 (1990).

67. Bachmann, M. F., Rohrer, U. H., Kündig, T. M., Bürki, K., Hengartner, H. & Zinkernagel, R. M. The influence of antigen organization on B cell responsiveness. *Science* **262,** 1448–1451 (1993).

68. Liu, W. & Chen, Y. H. High epitope density in a single protein molecule significantly enhances antigenicity as well as immunogenicity: a novel strategy for modern vaccine development and a preliminary investigation about B cell discrimination of monomeric proteins. *Eur. J. Immunol.* **35,** 505–514 (2005).

69. Zhang, S., Yong, L. K., Li, D., Cubas, R., Chen, C. & Yao, Q. Mesothelin Virus-Like Particle Immunization Controls Pancreatic Cancer Growth through CD8(+) T Cell Induction and Reduction in the Frequency of CD4(+)foxp3(+)ICOS(-) Regulatory T Cells. *PLoS ONE* **8,** e68303 (2013).

70. Chackerian, B., Durfee, M. R. & Schiller, J. T. Virus-like display of a neo-self antigen reverses B cell anergy in a B cell receptor transgenic mouse model. *J. Immunol.* **180,** 5816–5825 (2008).

71. Wilkinson, B. L., Day, S., Chapman, R., Perrier, S., Apostolopoulos, V. & Payne, R. J. Synthesis and immunological evaluation of self-assembling and self-adjuvanting tricomponent glycopeptide cancer-vaccine candidates. *Chemistry* **18,** 16540–16548 (2012).

72. Webber, M. J., Appel, E. A., Meijer, E. W. & Langer, R. Supramolecular biomaterials. *Nat Mater* **15,** 13–26 (2016).

73. Ghosh, A., Haverick, M., Stump, K., Yang, X., Tweedle, M. F. & Goldberger, J. E. Fine-tuning the pH trigger of self-assembly. *J. Am. Chem. Soc.* **134,** 3647–3650 (2012).

74. Dong, H., Paramonov, S. E., Aulisa, L., Bakota, E. L. & Hartgerink, J. D. Self-

assembly of multidomain peptides: balancing molecular frustration controls conformation and nanostructure. *J. Am. Chem. Soc.* **129,** 12468–12472 (2007).

75. Ulijn, R. V. & Smith, A. M. Designing peptide based nanomaterials. *Chem Soc Rev* **37,** 664–675 (2008).

76. Hauser, C. A. E. & Zhang, S. Designer self-assembling peptide nanofiber biological materials. *Chem Soc Rev* **39,** 2780–2790 (2010).

77. Hudalla, G. A., Modica, J. A., Tian, Y. F., Rudra, J. S., Chong, A. S., Sun, T., Mrksich, M. & Collier, J. H. A self-adjuvanting supramolecular vaccine carrying a folded protein antigen. *Adv Healthc Mater* **2,** 1114–1119 (2013).

78. Hudalla, G.A., Sun, T., Gasiorowski, J. Z., Han, H., Tian, Y. F., Chong, A. S. & Collier, J. H.Gradated assembly of multiple proteins into supramolecular nanomaterials. *Nat Mater* **13,** 829–836 (2014).

79. Spohn, R., Buwitt-Beckmann, U., Brock, R., Jung, G., Ulmer, A. J. & Wiesmüller, K. H. Synthetic lipopeptide adjuvants and Toll-like receptor 2--structure-activity relationships. *Vaccine* **22,** 2494–2499 (2004).

80. Rathinam, V. A. K., Vanaja, S. K. & Fitzgerald, K. A. Regulation of inflammasome signaling. *Nature Immunology* **13,** 333–342 (2012).

81. Hogquist, K. A., Jameson, S. C., Heath, W. R., Howard, J. L., Bevan, M.J. & Carbone, F. R. T cell receptor antagonist peptides induce positive selection. *Cell* **76,** 17–27 (1994).

82. Hailemichael, Y., Dai, Z., Jaffarzad, N., Ye, Y., Medina, M. A., Huang, X. F., Dorta-Estremera, S. M., Greeley, N. R., Nitti, G., Peng, W., Liu, C., Lou, Y., Wang, Z., Ma, W., Rabinovich, B., Sowell, R. T., Schluns, K. S., Davis, R. E., Hwu, P. & Overwijk, W. W. Persistent antigen at vaccination sites induces tumor-specific CD8+ T cell sequestration, dysfunction and deletion. *Nat. Med.* – (2013).

83. Wherry, E. J., Ha, S. J., Kaech, S. M., Haining, W. N., Sarkar, S., Kalia, V., Subramaniam, S., Blattman, J. N., Barber, D. L. & Ahmed, R. Molecular signature of CD8+ T cell exhaustion during chronic viral infection. *Immunity* **27,** 670–684 (2007).

84. Kim, P. S. & Ahmed, R. Features of responding T cells in cancer and chronic infection. *Curr. Opin. Immunol.* **22,** 223–230 (2010).

85. Eisenbarth, S. C., Colegio, O. R., O'Connor, W., Sutterwala, F. S. & Flavell, R.

A. Crucial role for the Nalp3 inflammasome in the immunostimulatory properties of aluminium adjuvants. *Nature* **453,** 1122–1126 (2008).

86. Rudra, J. S., Ding, Y., Neelakantan, H., Ding, C., Appavu, R., Stutz, S., Snook, J. D., Chen, H., Cunningham, K. A. & Zhou, J. Suppression of Cocaine-Evoked Hyperactivity by Self-Adjuvanting and Multivalent Peptide Nanofiber Vaccines. *ACS Chem Neurosci* **7,** 546–552 (2016).

87. Huang, Z. H., Shi, L., Ma, J. W., Sun, Z.Y., Cai, H., Chen, Y. X., Zhao, Y. F. & Li, Y. M. A totally synthetic, self-assembling, adjuvant-free MUC1 glycopeptide vaccine for cancer therapy. *J. Am. Chem. Soc.* **134,** 8730–8733 (2012).

88. Rad-Malekshahi, M., Fransen, M. F., Krawczyk, M., Mansourian, M., Bourajjaj, M., Chen, J., Ossendorp, F., Hennink, W. E., Mastrobattista, E. & Amidi, M. Self-Assembling Peptide Epitopes as Novel Platform for Anticancer Vaccination. *Mol. Pharm.* **14,** 1482–1493 (2017).

89. Pompano, R. R., Chen, J., Verbus, E. A., Han, H., Fridman, A., McNeely, T., Collier, J. H. & Chong, A. S. Titrating T-cell epitopes within self-assembled vaccines optimizes CD4+ helper T cell and antibody outputs. *Adv Healthc Mater* **3,** 1898–1908 (2014).

90. Friedrich, B. M., Beasley, D. W. C. & Rudra, J. S. Supramolecular peptide hydrogel adjuvanted subunit vaccine elicits protective antibody responses against West Nile virus. *Vaccine* **34,** 5479–5482 (2016).

91. Ding, Y., Liu, J., Lu, S., Igweze, J., Xu, W., Kuang, D., Zealey, C., Liu, D., Gregor, A., Bozorgzad, A., Zhang, L., Yue, E., Mujib, S., Ostrowsk,i M. & Chen, P. Self-assembling peptide for co-delivery of HIV-1 CD8+ T cells epitope and Toll-like receptor 7/8 agonists R848 to induce maturation of monocyte derived dendritic cell and augment polyfunctional cytotoxic T lymphocyte (CTL) response. *J Control Release* **236,** 22–30 (2016).

92. Grenfell, R. F. Q., Shollenberger, L. M., Samli, E. F. & Harn, D. A. Vaccine self-assembling immune matrix is a new delivery platform that enhances immune responses to recombinant HBsAg in mice. *Clin. Vaccine Immunol.* **22,** 336–343 (2015).

93. Vigneswaran, Y., Han, H., De Loera, R., Wen, Y., Zhang, X, Sun, T., Mora-Solano, C & Collier, J. H. Peptide biomaterials raising adaptive immune responses in wound healing contexts. *J Biomed Mater Res A* **104,** 1853–1862 (2016).

94. Ansaloni, L., Cambrini, P., Catena, F., Di Saverio, S., Gagliardi, S., Gazzotti, F.,

Hodde, J. P., Metzger, D. W., D'Alessandro, L & Pinna, A. D. Immune response to small intestinal submucosa (surgisis) implant in humans: preliminary observations. *J Invest Surg* **20,** 237–241 (2007).

95. Allman, A. J., McPherson, T. B., Badylak, S. F., Merrill, L. C., Kallakury, B., Sheehan, C., Raeder, R. H. & Metzger, D. W. Xenogeneic extracellular matrix grafts elicit a TH2-restricted immune response. *Transplantation* **71,** 1631–1640 (2001).

96. Eck, M. J., Beutler, B., Kuo, G., Merryweather, J. P. & Sprang, S. R. Crystallization of trimeric recombinant human tumor necrosis factor (cachectin). *J. Biol. Chem.* **263,** 12816–12819 (1988).

97. Eck, M. J. & Sprang, S. R. The structure of tumor necrosis factor-alpha at 2.6 A resolution. Implications for receptor binding. *J. Biol. Chem.* **264,** 17595–17605 (1989).

98. Baeyens, K. J., De Bondt, H. L., Raeymaekers, A., Fiers, W. & De Ranter, C. J. The structure of mouse tumour-necrosis factor at 1.4 A resolution: towards modulation of its selectivity and trimerization. *Acta Crystallogr. D Biol. Crystallogr.* **55,** 772–778 (1999).

99. Mukai Y1, Shibata H, Nakamura T, Yoshioka Y, Abe Y, Nomura T, Taniai M, Ohta T, Ikemizu S, Nakagawa S, Tsunoda S, Kamada H, Yamagata Y, Tsutsumi Y.Structure-function relationship of tumor necrosis factor (TNF) and its receptor interaction based on 3D structural analysis of a fully active TNFR1-selective TNF mutant. *J. Mol. Biol.* **385,** 1221–1229 (2009).

100. Mukai, Y., Nakamura, T., Yoshikawa, M., Yoshioka, Y., Tsunoda, S., Nakagawa, S., Yamagata, Y. & Tsutsumi, Y. Solution of the structure of the TNF-TNFR2 complex. *Sci Signal* **3,** ra83 (2010).

101. Ware, C. F. Protein therapeutics targeted at the TNF superfamily. *Adv. Pharmacol.* **66,** 51–80 (2013).

102. Parry, S. L., Sebbag, M., Feldmann, M. & Brennan, F. M. Contact with T cells modulates monocyte IL-10 production: role of T cell membrane TNF-alpha. *J. Immunol.* **158,** 3673–3681 (1997).

103. Alexopoulou, L., Kranidioti, K., Xanthoulea, S., Denis, M., Kotanidou, A., Douni, E., Blackshear, P. J., Kontoyiannis, D. L. & Kollias G. Transmembrane TNF protects mutant mice against intracellular bacterial infections, chronic inflammation and autoimmunity. *Eur. J. Immunol.* **36,** 2768–2780 (2006).

104. Winsauer, C., Kruglov, A. A., Chashchina, A. A., Drutskaya, M. S. & Nedospasov, S. A. Cellular sources of pathogenic and protective TNF and experimental strategies based on utilization of TNF humanized mice. *Cytokine Growth Factor Rev.* **25,** 115–123 (2014).

105. Horiuchi, T., Mitoma, H., Harashima, S.-I., Tsukamoto, H. & Shimoda, T. Transmembrane TNF-alpha: structure, function and interaction with anti-TNF agents. *Rheumatology (Oxford)* **49,** 1215–1228 (2010).

106. Olsen, T., Goll, R., Cui, G., Husebekk, A., Vonen, B., Birketvedt, G. S. & Florholmen, J. Tissue levels of tumor necrosis factor-alpha correlates with grade of inflammation in untreated ulcerative colitis. *Scand. J. Gastroenterol.* **42,** 1312–1320 (2007).

107. Bamias G1, Dahman MI, Arseneau KO, Guanzon M, Gruska D, Pizarro TT, Cominelli F. Intestinal-Specific TNFα Overexpression Induces Crohn's-Like Ileitis in Mice. *PLoS ONE* **8,** e72594 (2013).

108. Kollias, G., Douni, E., Kassiotis, G. & Kontoyiannis, D. On the role of tumor necrosis factor and receptors in models of multiorgan failure, rheumatoid arthritis, multiple sclerosis and inflammatory bowel disease. *Immunol. Rev.* **169,** 175–194 (1999).

109. Kaymakcalan, Z., Sakorafas, P., Bose, S., Scesney, S., Xiong, L., Hanzatian, D.K., Salfeld, J. & Sasso, E. H. Comparisons of affinities, avidities, and complement activation of adalimumab, infliximab, and etanercept in binding to soluble and membrane tumor necrosis factor. *Clin. Immunol.* **131,** 308–316 (2009).

110. Shealy, D. J., Cai, A., Staquet, K., Baker, A., Lacy, E. R., Johns, L., Vafa, O., Gunn, G., Tam, S., Sague, S., Wang, D., Brigham-Burke, M., Dalmonte, P., Emmell, E., Pikounis, B., Bugelski, P. J., Zhou, H., Scallon, B. J. & Giles-Komar J. Characterization of golimumab, a human monoclonal antibody specific for human tumor necrosis factor α. *MAbs* **2,** 428–439 (2010).

111. Mitoma, H., Horiuchi, T., Tsukamoto, H., Tamimoto, Y., Kimoto, Y., Uchino, A., To, K., Harashima, S., Hatta, N. & Harada, M. Mechanisms for cytotoxic effects of anti-tumor necrosis factor agents on transmembrane tumor necrosis factor alpha-expressing cells: comparison among infliximab, etanercept, and adalimumab. *Arthritis Rheum.* **58,** 1248–1257 (2008).

112. Nesbitt, A., Fossati, G., Bergin, M., Stephens, P., Stephens, S., Foulkes, R., Brown, D., Robinson, M. & Bourne, T. Mechanism of action of certolizumab pegol (CDP870): in vitro comparison with other anti-tumor necrosis factor alpha

agents. *Inflamm. Bowel Dis.* **13,** 1323–1332 (2007).

113. Liang, S., Dai, J., Hou, S., Su, L., Zhang, D., Guo, H., Hu, S., Wang, H., Rao, Z., Guo, Y. & Lou, Z. Structural Basis for Treating Tumor Necrosis Factor (TNF)-associated Diseases with the Therapeutic Antibody Infliximab. *Journal of Biological Chemistry* **288,** 13799–13807 (2013).

114. Goel, N. & Stephens, S. Certolizumab pegol. *MAbs* **2,** 137–147 (2010).

115. Murdaca, G., Spanò, F., Contatore, M., Guastalla, A., Penza, E., Magnani, O. & Puppo, F. Immunogenicity of infliximab and adalimumab: what is its role in hypersensitivity and modulation of therapeutic efficacy and safety? *Expert Opin Drug Saf* **15,** 43–52 (2016).

116. Thomas, S.S., Borazan, N., Barroso, N., Duan, L., Taroumian, S., Kretzmann, B., Bardales, R., Elashoff, D., Vangala, S. & Furst, D. E. Comparative Immunogenicity of TNF Inhibitors: Impact on Clinical Efficacy and Tolerability in the Management of Autoimmune Diseases. A Systematic Review and Meta-Analysis. *BioDrugs* **29,** 241–258 (2015).

117. Atzeni, F., Talotta, R., Salaffi, F., Cassinotti, A., Varisco, V., Battellino, M., Ardizzone, S., Pace, F. & Sarzi-Puttini, P. Immunogenicity and autoimmunity during anti-TNF therapy. *Autoimmun Rev* **12,** 703–708 (2013).

118. Banerjee, S., Biehl, A., Gadina, M., Hasni, S. & Schwartz, D. M. JAK-STAT Signaling as a Target for Inflammatory and Autoimmune Diseases: Current and Future Prospects. *Drugs* **77,** 521–546 (2017).

119. Jung, J. P., Nagaraj, A. K., Fox, E. K., Rudra, J. S., Devgun, J. M. & Collier, J. H. Co-assembling peptides as defined matrices for endothelial cells. *Biomaterials* **30,** 2400–2410 (2009).

120. Wen, Y., Waltman, A., Han, H. & Collier, J. H. Switching the Immunogenicity of Peptide Assemblies Using Surface Properties. *ACS Nano* (2016).

121. Malyala, P. & Singh, M. Endotoxin limits in formulations for preclinical research. *J Pharm Sci* **97,** 2041–2044 (2008).

122. Hansel, T. T., Kropshofer, H., Singer, T., Mitchell, J. A. & George, A. J. T. The safety and side effects of monoclonal antibodies. *Nat Rev Drug Discov* **9,** 325–338 (2010).

123. Zagury, D., Le Buanec, H., Bizzini, B., Burny, A., Lewis, G. & Gallo, R. C. Active versus passive anti-cytokine antibody therapy against cytokine-associated

chronic diseases. *Cytokine Growth Factor Rev.* **14,** 123–137 (2003).

124. Jia, T., Pan, Y., Li, J. & Wang, L. Strategies for active TNF-α vaccination in rheumatoid arthritis treatment. *Vaccine* **31,** 4063–4068 (2013).

125. Dalum, I., Butler, D.M., Jensen, M.R., Hindersson, P., Steinaa, L., Waterston, A. M., Grell, S.N., Feldmann, M., Elsner, H.I. & Mouritsen, S. Therapeutic antibodies elicited by immunization against TNF-alpha. *Nat. Biotechnol.* **17,** 666–669 (1999).

126. Wan, Y., Xue, X., Li, M., Zhang, X., Qin, X., Zhang, C., You, Y., Wang, W., Jiang, C., Wu, S., Liu, Y., Zhu, W., Ran, Y., Zhang, Z., Han, W. & Zhang, Y. Prepared and screened a modified TNF-alpha molecule as TNF-alpha autovaccine to treat LPS induced endotoxic shock and TNF-alpha induced cachexia in mouse. *Cell. Immunol.* **246,** 55–64 (2007).

127. Grünewald, J., Hunt, G. S., Dong, L., Niessen, F., Wen, B. G., Tsao, M. L., Perera, R., Kang, M., Laffitte, B. A., Azarian, S., Ruf, W., Nasoff, M., Lerner, R. A., Schultz, P. G. & Smider, V. V. Mechanistic studies of the immunochemical termination of self-tolerance with unnatural amino acids. *Proc. Natl. Acad. Sci. U.S.A.* **106,** 4337–4342 (2009).

128. Chackerian, B., Lowy, D. R. & Schiller, J. T. Conjugation of a self-antigen to papillomavirus-like particles allows for efficient induction of protective autoantibodies. *J. Clin. Invest.* **108,** 415–423 (2001).

129. Delavallée, L., Le Buanec, H., Bessis, N., Assier, E., Denys, A., Bizzini, B., Zagury, D. & Boissier, M. C. Early and long-lasting protection from arthritis in tumour necrosis factor alpha (TNFalpha) transgenic mice vaccinated against TNFalpha. *Ann. Rheum. Dis.* **67,** 1332–1338 (2008).

130. Delavallée, L., Semerano, L., Assier, E., Vogel, G., Vuagniaux, G., Laborie, M., Zagury, D., Bessis, N. & Boissier, M. C. Active immunization to tumor necrosis factor-alpha is effective in treating chronic established inflammatory disease: a long-term study in a transgenic model of arthritis. *Arthritis Res. Ther.* **11,** R195 (2009).

131. Assier, E., Semerano, L., Duvallet, E., Delavallée, L., Bernier, E., Laborie, M., Grouard-Vogel, G., Larcier, P., Bessis, N. & Boissier, M. C. Modulation of Anti-Tumor Necrosis Factor Alpha (TNF-α) Antibody Secretion in Mice Immunized with TNF-α Kinoid. *Clin. Vaccine Immunol.* **19,** 699–703 (2012).

132. Spohn, G., Guler, R., Johansen, P., Keller, I., Jacobs, M., Beck, M., Rohner, F., Bauer, M., Dietmeier, K., Kündig, T. M., Jennings, G. T., Brombacher, F &

Bachmann, M. F. A virus-like particle-based vaccine selectively targeting soluble TNF-alpha protects from arthritis without inducing reactivation of latent tuberculosis. *J. Immunol.* **178,** 7450–7457 (2007).

133. Le Buanec H., Delavallée, L., Bessis, N., Paturance, S., Bizzini, B., Gallo. R., Zagury, D., & Boissier, M. C. TNFalpha kinoid vaccination-induced neutralizing antibodies to TNFalpha protect mice from autologous TNFalpha-driven chronic and acute inflammation. *Proc. Natl. Acad. Sci. U.S.A.* **103,** 19442–19447 (2006).

134. Capini ,C. J., Bertin-Maghit, S. M., Bessis, N., Haumont, P. M., Bernier, E. M., Muel, E. G., Laborie, M. A., Autin, L., Paturance, S., Chomilier, J., Boissier, M. C., Briand, J. P., Muller, S., Cavaillon, J. M., Therwath, A. & Zagury, J. F. Active immunization against murine TNFα peptides in mice: generation of endogenous antibodies cross-reacting with the native cytokine and in vivo protection. *Vaccine* **22,** 3144–3153 (2004).

135. Wildbaum, G., Youssef, S. & Karin, N. A targeted DNA vaccine augments the natural immune response to self TNF-alpha and suppresses ongoing adjuvant arthritis. *J. Immunol.* **165,** 5860–5866 (2000).

136. Durez, P., Vandepapeliere, P., Miranda, P., Toncheva, A., Berman, A., Kehler, T., Mociran, E., Fautrel, B., Mariette, X., Dhellin, O., Fanget, B., Ouary, S., Grouard-Vogel, G., Boissier, M. C. Therapeutic vaccination with TNF-Kinoid in TNF antagonist-resistant rheumatoid arthritis: a phase II randomized, controlled clinical trial. *PLoS ONE* **9,** e113465 (2014).

137. Goodnow, C. C., Vinuesa, C. G., Randall, K. L., Mackay, F. & Brink, R. Control systems and decision making for antibody production. *Nature Immunology* **11,** 681–688 (2010).

138. Coffman, R. L., Sher, A. & Seder, R. A. Vaccine adjuvants: putting innate immunity to work. *Immunity* **33,** 492–503 (2010).

139. Gasiorowski, J. Z. & Collier, J. H. Directed intermixing in multicomponent self-assembling biomaterials. *Biomacromolecules* **12,** 3549–3558 (2011).

140. Jung, J. P., Moyano, J. V. & Collier, J. H. Multifactorial optimization of endothelial cell growth using modular synthetic extracellular matrices. *Integr Biol (Camb)* **3,** 185–196 (2011).

141. Collier, J. H. & Messersmith, P. B. Enzymatic modification of self-assembled peptide structures with tissue transglutaminase. *Bioconjug. Chem.* **14,** 748–755 (2003).

142. Alexander, J., Sidney, J., Southwood, S., Ruppert, J., Oseroff, C., Maewal, A., Snoke, K., Serra, H. M., Kubo, R. T., Sette, A. & Grey, H. M. Development of high potency universal DR-restricted helper epitopes by modification of high affinity DR-blocking peptides. *Immunity* **1,** 751–761 (1994).

143. Moutaftsi, M., Bui, H. H., Peters, B., Sidney, J., Salek-Ardakani, S., Oseroff, C., Pasquetto, V., Crotty, S., Croft, M., Lefkowitz, E. J., Grey, H. & Sette, A. Vaccinia virus-specific CD4+ T cell responses target a set of antigens largely distinct from those targeted by CD8+ T cell responses. *J. Immunol.* **178,** 6814–6820 (2007).

144. Blanqué, R., Meakin, C., Millet, S. & Gardner, C. R. Hypothermia as an indicator of the acute effects of lipopolysaccharides: comparison with serum levels of IL1 beta, IL6 and TNF alpha. *Gen. Pharmacol.* **27,** 973–977 (1996).

145. Krarup, A., Chattopadhyay, P., Bhattacharjee, A. K., Burge, J. R. & Ruble, G. R. Evaluation of surrogate markers of impending death in the galactosamine-sensitized murine model of bacterial endotoxemia. *Lab. Anim. Sci.* **49,** 545–550 (1999).

146. Saia, R. S. & Carnio, E. C. Thermoregulatory role of inducible nitric oxide synthase in lipopolysaccharide-induced hypothermia. *Life Sci.* **79,** 1473–1478 (2006).

147. Acar, H., Srivastava, S., Chung, E. J., Schnorenberg, M. R., Barrett, J. C., LaBelle J. L. & Tirrell, M. Self-assembling peptide-based building blocks in medical applications. *Adv. Drug Deliv. Rev.* (2016). doi:10.1016/j.addr.2016.08.006

148. Trent, A., Ulery, B. D., Black, M. J., Barrett, J. C., Liang, S., Kostenko, Y., David, N. A. & Tirrell M. V. Peptide amphiphile micelles self-adjuvant group A streptococcal vaccination. *AAPS J* **17,** 380–388 (2015).

149. Fazilleau, N., McHeyzer-Williams, L. J., Rosen, H. & McHeyzer-Williams, M. G. The function of follicular helper T cells is regulated by the strength of T cell antigen receptor binding. *Nature Immunology* **10,** 375–384 (2009).

150. Tubo, N. J. & Jenkins, M. K. TCR signal quantity and quality in CD4+ T cell differentiation. *Trends Immunol.* (2014).

151. Sun, T., Han, H., Hudalla, G. A., Wen, Y., Pompano, R. R. & Collier, J. H. Thermal stability of self-assembled peptide vaccine materials. *Acta Biomater* (2015). doi:10.1016/j.actbio.2015.11.019

152. Biancalana, M. & Koide, S. Molecular mechanism of Thioflavin-T binding to amyloid fibrils. *Biochim. Biophys. Acta* **1804,** 1405–1412 (2010).

153. Tostanoski, L. H. & Jewell, C. M. Engineering self-assembled materials to study and direct immune function. *Adv. Drug Deliv. Rev.* (2017). doi:10.1016/j.addr.2017.03.005

154. Fulton, K. M. & Twine, S. M. Immunoproteomics: current technology and applications. *Methods Mol. Biol.* **1061,** 21–57 (2013).

155. Billeskov, R., Wang, Y., Solaymani-Mohammadi, S., Frey, B., Kulkarni, S., Andersen, P., Agger, E. M., Sui, Y. & Berzofsky, J. A. Low Antigen Dose in Adjuvant-Based Vaccination Selectively Induces CD4 T Cells with Enhanced Functional Avidity and Protective Efficacy. *The Journal of Immunology* **198,** 3494–3506 (2017).

156. Sunshine, J. C., Perica, K., Schneck, J. P. & Green, J. J. Particle shape dependence of CD8+ T cell activation by artificial antigen presenting cells. *Biomaterials* **35,** 269–277 (2014).

157. De Gregorio, E., D'Oro, U. & Wack, A. Immunology of TLR-independent vaccine adjuvants. *Curr. Opin. Immunol.* **21,** 339–345 (2009).

158. Loo, E. W., Krantz, M. J. & Agrawal, B. High dose antigen treatment with a peptide epitope of myelin basic protein modulates T cells in multiple sclerosis patients. *Cell. Immunol.* **280,** 10–15 (2012).

159. Bercovici, N., Delon, J., Cambouris, C., Escriou, N., Debré, P. & Liblau, R. S. Chronic intravenous injections of antigen induce and maintain tolerance in T cell receptor-transgenic mice. *Eur. J. Immunol.* **29,** 345–354 (1999).

160. Tuohy, V. K., Yu, M., Yin, L., Kawczak, J. A. & Kinkel, P. R. Regression and spreading of self-recognition during the development of autoimmune demyelinating disease. *J. Autoimmun.* **13,** 11–20 (1999).

161. Wen, Y. & Collier, J. H. Supramolecular peptide vaccines: tuning adaptive immunity. *Curr. Opin. Immunol.* **35,** 73–79 (2015).

162. Nielsen, M. & Marcatili, P. Prediction of Antibody Epitopes. *Methods Mol. Biol.* **1348,** 23–32 (2015).

163. Liu, J. & Zhang, W. Databases for B-cell epitopes. *Methods Mol. Biol.* **1184,** 135–148 (2014).

164. Tung, C. W. Databases for T-cell epitopes. *Methods Mol. Biol.* **1184,** 123–134 (2014).

165. Nagarkar, R. P. & Schneider, J. P. Synthesis and primary characterization of self-assembled peptide-based hydrogels. *Methods Mol. Biol.* **474,** 61–77 (2008).

166. Hyde, C., Johnson, T. & Sheppard, R. C. Internal aggregation during solid phase peptide synthesis. Dimethyl sulfoxide as a powerful dissociating solvent. *J. Chem. Soc., Chem. Commun.* 1573 (1992). doi:10.1039/c39920001573

167. Arnesen, T. Towards a functional understanding of protein N-terminal acetylation. *PLoS Biol.* **9,** e1001074 (2011).

168. Wallace, R. J. Acetylation of peptides inhibits their degradation by rumen micro-organisms. *Br. J. Nutr.* **68,** 365–372 (1992).

169. Sélo, I., Négroni, L., Créminon, C., Grassi, J. & Wal, J. M. Preferential labeling of α-amino N-terminal groups in peptides by biotin: application to the detection of specific anti-peptide antibodies by enzyme immunoassays. *Journal of Immunological Methods* **199,** 127–138 (1996).

170. Howl, J., Wang, X., Kirk, C. J. & Wheatley, M. Fluorescent and biotinylated linear peptides as selective bifunctional ligands for the V1a vasopressin receptor. *Eur J Biochem* **213,** 711–719 (1993).

171. Buranda, T., Lopez, G. P., Keij, J., Harris, R. & Sklar, L. A. Peptides, antibodies, and FRET on beads in flow cytometry: A model system using fluoresceinated and biotinylated beta-endorphin. *Cytometry* **37,** 21–31 (1999).

172. Farley, R. A., Tran, C. M., Carilli, C. T., Hawke, D. & Shively, J. E. The amino acid sequence of a fluorescein-labeled peptide from the active site of (Na,K)-ATPase. *J. Biol. Chem.* **259,** 9532–9535 (1984).

173. Richard, J. P., Melikov, K., Vives, E., Ramos, C., Verbeure, B., Gait, M. J, Chernomordik, L. V. & Lebleu, B. Cell-penetrating peptides. A reevaluation of the mechanism of cellular uptake. *J. Biol. Chem.* **278,** 585–590 (2003).

174. Futaki, S., Suzuki, T., Ohashi, W., Yagami, T., Tanaka, S., Ueda, K. & Sugiura, Y. Arginine-rich peptides. An abundant source of membrane-permeable peptides having potential as carriers for intracellular protein delivery. *J. Biol. Chem.* **276,** 5836–5840 (2001).